ESPOO 2008 VTT PUBLICATIONS 677

Antti Hanhijärvi & Ari Kevarinmäki

Timber failure mechanisms in high-capacity dowelled connections of timber to steel

Experimental results and design

PUBLICATIONS 677

Timber failure mechanisms in high-capacity dowelled connections of timber to steel

Experimental results and design

Antti Hanhijärvi & Ari Kevarinmäki

ISBN 978-951-38-7090-4 (URL: http://www.vtt.fi/publications/index.jsp)
ISSN 1455-0849 (URL: http://www.vtt.fi/publications/index.jsp)

JULKAISIJA – UTGIVARE – PUBLISHER

VTT, Vuorimiehentie 3, PL 1000, 02044 VTT
puh. vaihde 020 722 111, faksi 020 722 4374

VTT, Bergsmansvägen 3, PB 1000, 02044 VTT
tel. växel 020 722 111, fax 020 722 4374

VTT Technical Research Centre of Finland, Vuorimiehentie 3, P.O.Box 1000, FI-02044 VTT, Finland
phone internat. +358 20 722 111, fax + 358 20 722 4374

VTT, Kemistintie 3, PL 1000, 02044 VTT
puh. vaihde 020 722 111, faksi 020 722 7007

VTT, Kemistvägen 3, PB 1000, 02044 VTT
tel. växel 020 722 111, fax 020 722 7007

VTT Technical Research Centre of Finland, Kemistintie 3, P.O. Box 1000, FI-02044 VTT, Finland
phone internat. +358 20 722 111, fax +358 20 722 7006

Technical editing Maini Manninen

Hanhijärvi, Antti & Kevarinmäki, Ari. Timber failure mechanisms in high-capacity dowelled connections of timber to steel. Experimental results and design. [Puurakenteiden tappivaarnaliitosten murtomekanismit]. Espoo 2008. VTT Publications 677. 53 p. + app. 37 p.

Keywords timber, gluelam, LVL, dowelled connections, high capacity, design methods, steel-to-timber connections, block shear, plug shear, row shear

Abstract

The timber failure mechanisms at the connection area (block shear, plug shear, row shear, tension at the joint area) of high capacity dowelled steel-to-timber connections were explored by arranging a large experimental program to investigate the strength of both double shear and multiple shear connections. All tested connections were steel-to-timber connections using large diameter and consequently fairly rigid dowels. The experiments consisted altogether of more than 150 tension tests by which different and versatile dowel configurations were tested. Based on the experimental results, a new design method against timber failure mechanisms at the connection area was developed. The new method is suitable especially for high capacity steel-to-timber connections.

Hanhijärvi, Antti & Kevarinmäki, Ari. Timber failure mechanisms in high-capacity dowelled connections of timber to steel. Experimental results and design. [Puurakenteiden tappivaarnaliitosten murtomekanismit]. Espoo 2008. VTT Publications 677. 53 s. + liitt. 37 s.

Avainsanat timber, gluelam, LVL, dowelled connections, high capacity, design methods, steel-to-timber connections, block shear, plug shear, row shear

Tiivistelmä

Suuren kapasiteetin omaavien tappivaarnaliitosten puustamurtomekanismeja (lohkeamismurtotavat: läpilohkeaminen, palalohkeaminen, rivilohkeaminen ja vetomurto liitosalueella) tutkittiin laajalla koeohjelmalla. Kokeissa tutkittiin sekä kaksileikkeisiä että monileikkeisiä liitoksia vedossa. Kaikki testatut liitokset olivat teräs-puuliitoksia, joissa käytettiin halkaisijaltaan melko suuria tappeja, jotka ovat siten myös jäykkiä. Koeohjelmaan kuului järjestää yli 150 vetokoetta, joissa käytettiin erilaisia ja monipuolisia tappiasetelmia. Koetuloksiin perustuen kehitettiin uusi mitoitusmenetelmä puustamurtomekanismikapasiteetin laskemiseen nimenomaan korkean kapasiteetin teräs-puuliitoksille.

Preface

The present report documents research performed in a subtask of the joint Swedish-Finnish project "Innovative design, a new strength paradigm for joints, QA and reliability for long-span wood construction (InnoLongSpan)", conducted 2004–2007. The project dealt with two main issues: (1) design and performance of joints used in long span timber structures and (2) documenting reliability and developing quality assurance of large and demanding timber structures. This publication documents the results of the Finnish subtask to deal with joint design, where the objective has been to improve the design methods against timber failure mechanisms in the joint area.

The project was part of the Wood Material Science and Engineering Research Programme (Wood Wisdom), and has been supported by the following organisations and companies

In Finland
- Tekes – Finnish Funding Agency for Technology and Innovation
- VTT
- SPU Systems Oy
- Finnforest (Metsäliitto Cooperative)
- Versowood Oyj
- Late-Rakenteet Oy
- Exel Oyj

In Sweden
- Vinnova (Swedish Governmental Agency for Innovation Systems)
- Skogsindustrierna
- Casco Products AB
- SFS-Intec AB
- Limträteknik i Falun AB
- Svenskt Limträ AB
- Skanska Teknik AB

The contributions and funding from the above mentioned parties are gratefully acknowledged.

The authors

Contents

List of symbols

a_1	dowel spacing parallel to grain
a_2	dowel spacing perpendicular to grain
a_3	dowel end distance
a_4	dowel edge distance
B	specimen height
b	block shear failure mechanism
b-r	block shear failure mechanism with calculational shear failure capacity > tension failure capacity
b-t	block shear failure mechanism with calculational tension failure capacity > shear failure capacity
CoV	coefficient of variation
d	dowel diameter
DF	design failure mode (critical failure mechanism according to design)
F_{max}	failure load in tests
F_{Bk}	calculated characteristic load-carrying capacity of connection according to EC5 Annex A (block/plug shear)
F_{Bm}	calculated load-carrying capacity of connection according to EC5 Annex A (block/plug shear) and using mean properties
F_{Rk}	calculated characteristic load-carrying capacity of connection according to EC5 assuming $n_{ef} = n$
F_{Rm}	calculated load-carrying capacity according to EC5 assuming $n_{ef} = n$ and using mean properties of the test material

F_{Sk}	calculated characteristic load-carrying capacity according to EC5 assuming splitting etc. ($n_{ef} \neq n$) but not block/plug shear
F_{Sm}	calculated load-carrying capacity according to EC5 assuming splitting etc. ($n_{ef} \neq n$) but not block/plug shear and using mean properties of the test material
F_{Tm}	calculated capacity according to the EC5 assuming only tension failure and using mean properties of the test material and cross-section reduction due to dowel holes
N	number of specimens
n	number of dowels in a row
n_{ef}	effective number of dowels in a row
m	number of dowel rows
p	plug shear failure
row	row shear failure
s/r	splitting or row shear failure
T	tension failure mechanism (of cross-section)
TF	test failure mode (prevailing failure mechanism in test)
t_1	thickness of outer timber member
t_2	thickness of inner timber member
t_S	thickness of steel plate
v_{max}	connection slip at maximum load
ρ_m	mean density of the test material

1. Introduction

1.1 Timber in long span constructions

Timber is an excellent material for the load-bearing components for large buildings and for their challenging roof structures with long spans. It is naturally strong but at the same time it is very light, so that the gravitational loads caused by own weight of the long structure does not substantially hinder the design. As timber is also a highly oriented material, it is naturally fit for beam and truss constructions of all types.

The challenge in the use of timber in large structures is mainly set by the capability to join timber members with sufficiently high capacity connections. In long-span structures this is necessary, since the components themselves are naturally available only in practical sizes, which are limited – if nothing else by transportation requirements. The forces that need to be transmitted by the connections are high, so that truly heavy duty connections are needed. The need for the use of long and longer spans in timber structures can be expected to grow as the demand for higher flexibility of buildings is increasing. Flexibility of building means for the construction engineer the demand for minimizing of the number of load-bearing inside walls, which in turn inevitably leads to long span lengths.

1.2 Present design situation

The design of dowel type connections (nailed, screwed, dowelled and bolted connections) of timber is well established in the Eurocode 5 by the use of the Johansen theory (Johansen 1949), as long as the fasteners are sufficiently slender. The Johansen theory considers the failure mechanism of dowel yield and embedment failure in timber and it has shown to perform well, when the fastener diameters are small and consequently the fasteners slender (see e.g. Hilson 1995). If small diameter and slender dowels are used for very high capacity connections, the implementation usually requires a very high number of dowels. Consequently, the high capacity dowelled connections are often implemented with large diameter dowels or bolts and slotted-in steel plates are used as intermediate components in the connection rather than directly connecting timber to timber.

With the increase of the dowel or bolt diameter, the rigidity of the dowel increases more than the embedment capacity. Therefore with large diameter rigid dowels, also the failure of timber at the joint area becomes more easily critical for the capacity of the connection – not only as embedment failure but through failure of the whole joint area by tension or shear. The failure mechanisms in this manner at the connection area are known as row shear, block shear, plug shear and tension failure at farthest dowel column, Figs 1 and 2. In addition, embedment failure can also be seen as one of the timber failure mechanisms. It is characterized as ductile failure mode as it is caused by compressive crushing of wood, whereas all the other timber failure mechanisms are brittle in nature.

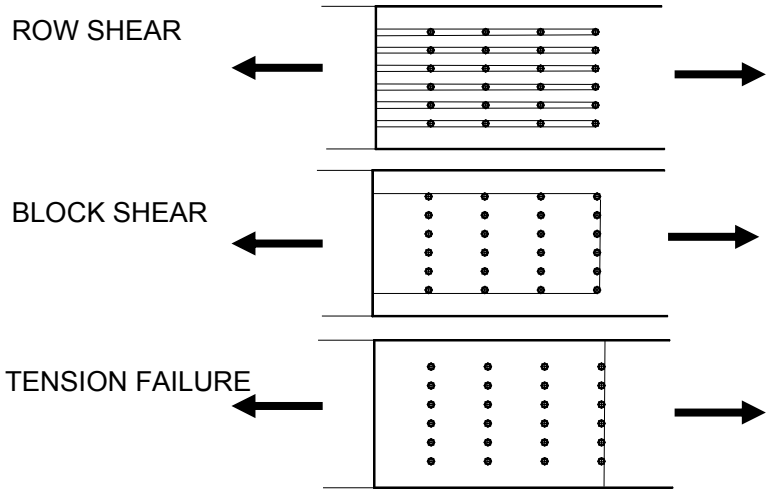

Figure 1. Shematic of (top) row shear failure (middle) block shear failure and (bottom) tension failure at farthest dowel column of a dowelled connection.

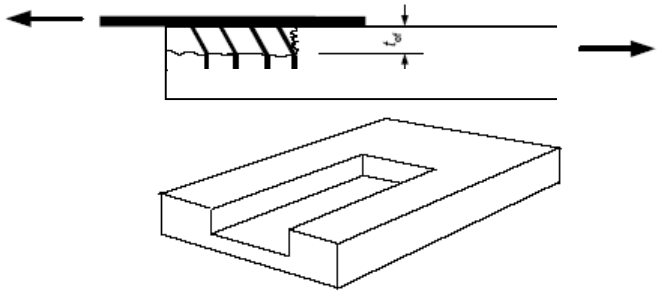

Figure 2. Schematic of the plug shear failure of a dowelled connection.

The brittle timber failure mechanisms are not considered in the Johanssen theory. However, a design method against the block shear and plug shear mechanisms is presented in the informative Annex A of Eurocode 5 (EC5). Annex A does not consider row shear. The basis for the design of dowelled steel-to-timber connections with slotted in steel plates against timber failure mechanisms as instructed by the formulas of EC5 and Annex A (EC5, EN 1995-1-1:2004) is presented briefly in the following.

The reduction of the load-carrying capacity in case of splitting or rowshear (compared to Johanssen theory) is calculated by a reduction of the number of dowels n and capacity given by Johansen theory (EC5, Eqs. 8.1, 8.34):

$$F_{Sk} = \frac{n_{\mathrm{ef}}}{n} F_{\mathrm{Rk}}, \quad where \;\; n_{ef} = \min\left(n, n^{0.9} \left(\frac{a_1}{13d} \right)^{0.25} \right) \tag{1}$$

where F_{Rk} is the capacity by the Johansen theory. The reduction of the number of dowels in this manner basically should take care also of the effect of uneven load distrubution between the dowels in the row, for which it was in the first place intended for.

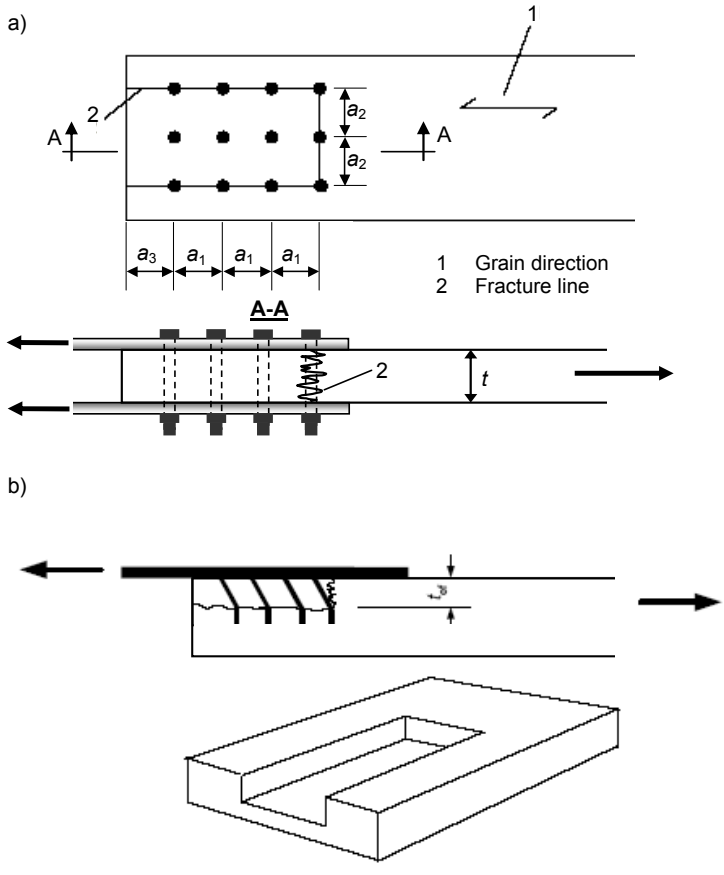

Figure 3. (Top) Block shear failure and (Bottom) plug shear failure of a dowelled connection with notation of the dowel distances according to the EC5 design equations.

The load-carrying capacity in case of block or plug shear failure is calculated by the formula (A.1) in the Annex A:

$$F_{bs,Rk} = F_{Bk} = \max\begin{cases} 1.5 A_{net,t} f_{t,0,k} \\ 0.7 A_{net,v} f_{v,k} \end{cases} \tag{2}$$

where $f_{t,0,k}$ and $f_{v,k}$ are the tensile and shear strengths of the material, respectively, and $A_{net,t}$ and $A_{net,v}$ are the areas along the assumed failure surface that are under tension and shear stress, respectively. The areas are calculated as (Annex A Eq. A.2, A.3):

$$A_{\text{net,t}} = L_{\text{net,t}} t_1 \tag{3}$$

$$A_{\text{net,v}} = \begin{cases} L_{\text{net,v}} t_1 & \text{embedm. fail. or steel - timber - steel connect.} \\ \frac{L_{\text{net,v}}}{2}\left(L_{\text{net,t}} + 2t_{ef}\right) & \text{other cases} \end{cases} \tag{4}$$

where t_{ef} is the calculational distance from the surface to the dowel plastic hinge according to the Johansen theory. The magnitudes of $L_{\text{net,t}} = (m\text{-}1)*(a_2\text{-}d)$ and $L_{\text{net,v}} = (n\text{-}1)*(a_1\text{-}d)+(a3–d)$ (see Fig. 3).

1.3 Background and aim of the work

The lack of design against timber failure as consequence of shear and tension at the connection area (block shear) was found to be the partial reason for a recent failure of a large roof structure in Finland (Anon. 2004, Ranta-Maunus and Kevarinmäki 2003). Although the primary reason for the failure was a manufacturing fault in one connection (missing dowels) of a large glulam truss, the failure would not have proceeded to a catastrophic one, unless the true capacity of the properly manufactured joint had not been much lower than the capacity assumed in the design, which did not include any consideration of brittle timber failure at the joint area. The true capacity of the failed connection type was tested later after the collapse in a full-scale test, in which it was found that the true capacity was only appr. 50% of the design value (Ranta-Maunus and Kevarinmäki 2003). The tests showed also clearly the importance of the block shear failure mechanism as the critical one. At the time of the design of the roof, the ENV-version of the Eurocode 5 did not contain Annex A or other mention of this type of failure mechanisms.

The aim of the present work is to improve the grounds for design of heavy-duty dowelled connections by experimental investigation of the timber failure at the connection area. The work focuses on connections implemented by steel plates and loaded in tension. These types of connections in the high capacity range have not been investigated much in the past and the experimental data is very limited in the literature available. In the experimental program of this work, altogether more than 150 tension tests parallel to grain were made with glulam

and Kerto-LVL specimens with heavy-duty dowelled connections of timber to steel plates. The experimental program contained tests of both double-shear and multiple shear (4- and 6-shear) plane connections. In double shear, both timber-steel-timber and steel-timber-steel specimens were tested. In multiple shear the outermost parts were always timber.

2. Experimental program

2.1 Material

All glulam for the tests was manufactured in an industrial process at Laterakenteet Oy, Turku, or Versowood Oy, Vierumäki, from spruce (*Picea abies*) wood. To get more homogenious properties, the lamellas were specially selected. The selection was made using a commercial strength grading machine (Dynagrader), which measures the natural frequency of the lamellae. First, a sufficiently large batch of lamellas was graded with settings of grade MT30 (= C30). Second, the pieces which had passed the requirements of this grade were re-graded using the settings of MT40 (= C40) and only those pieces with failed this higher criterion were taken for the production of the test glulam. Thus the lamellas had properties exceeding the requirements for MT30 but not MT40. The glulam can be considered to correspond to strength class GL28h. The LVL for the tests was produced at the Kerto-LVL factory of Finnforest Oyj in Lohja, Finland.

Dowels were produced by cutting and machining from cold drawn steel bars. The binder bolts were produced from the same material as the dowels and the smooth length was at least a few mm's longer than the width of the joint. This was to insure that in no case did the threaded part touch the wood or the steel plates. The dimensional accuracy of the diameter of the dowels and bolts was very high.

The steel plates were manufactured by laser cutting from steel quality S355 using an NC-machine tool. The dowel holes were cut to diameters Ø13 mm and Ø8.7 mm for the dowel diameters 12 and 8 mm, respectively.

All test specimens were manufactured so that a similar dowelled connection was manufactured at both ends of the specimen. Thus, actually, twice as many connections were tested than the number of specimens shows. However, the actual strength of only the weaker one of the pair of joints in one specimen was obtained – and it can be only said that the other one was at least as strong.

2.2 Double shear connection specimens

The double-shear test series are listed in Table 1 for glulam and Tables 2 and 3 for Kerto-S and Kerto-Q LVL, respectively. Kerto-S is standard LVL, where all veneers are oriented in the longitudinal direction. Kerto-Q is cross veneered, i.e. it has few veneers in the perpendicular direction. The double shear test series of the timber-steel-timber type were made with unattached timber parts: For glulam the two halves were obtained by splitting a glulam beam into two and manufacturing the specimen using the two halves but leaving them unattached in the middle part. For LVL specimens the two halves were obtained from two pieces of LVL coming from the same manufacturing batch.

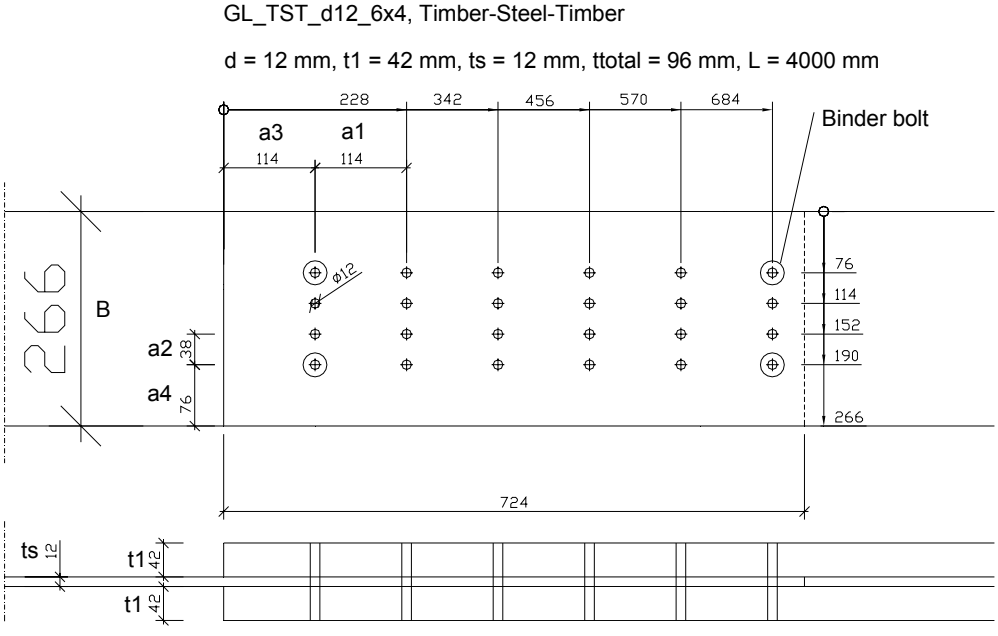

Figure 4. Example of a double shear dowelled timber-steel-timber connection used in the tests (GL_TST_d12_6x4).

Table 1. Glulam series with double-shear dowelled connections.

Series name	Dowel pattern n x m	dowel diam. d mm	thick-ness t_1 or t_2 mm	width B mm	steel plate t_s mm	spacing parall. a_1 mm	spacing, perp. a_2 mm	end dist. a_3 mm	edge dist. a_4 mm	N
Timber-Steel-Timber, Dowel diameter 12 mm										
GL28h, t_1 = 42 mm, d = 12 mm, dowel strength.cl. 8.8, a_2 = 38 mm, a_3 = a_1										
GL_TST_d12_12x2	12 x 2	12	42	220	12	93	38	93	91	3
GL_TST_d12_8x3	8 x 3	12	42	244	12	105	38	105	84	3
GL_TST_d12_6x4	6 x 4	12	42	266	12	114	38	114	76	5
GL_TST_d12_4x6	4 x 6	12	42	296	12	114	38	114	53	3
Steel-Timber-Steel, Dowel diameter 12 mm										
GL28h, t_2 = 90 mm, d = 12 mm, dowel strength cl. 8.8, a_3 = max(a_1; 84 mm), t_s = 6 mm										
GL_STS_d12_12x2	12 x 2	12	90	250	6	84	48	84	101	3
GL_STS_d12_8x3	8 x 3	12	90	262	6	120	48	120	83	3
GL_STS_d12_6x4	6 x 4	12	90	276	6	60	58	84	51	5
GL_STS_d12_4x6	4 x 6	12	90	304	6	60	40	84	52	3
GL_STS_d12_3x8	3 x 8	12	90	372	6	84	36	84	60	3
Timber-Steel-Timber, Dowel diameter 8 mm										
GL28h, t_1 = 28 mm, d = 8 mm, dowel strength cl. 10.9, a_2 = 26 mm, a_3 = 80 mm										
GL_TST_d8_12x2	12 x 2	8	28	158	8	64	26	80	66	3
GL_TST_d8_6x4	6 x 4	8	28	192	8	80	26	80	57	3
Steel-Timber-Steel, Dowel diameter 8 mm										
GL28h, t_2 = 60 mm, d = 8 mm, dowel strength cl. 10.9, a_3 = 80 mm, t_s = 4 mm										
GL_STS_d8_12x2	12 x 2	8	60	174	4	56	32	80	71	3
GL_STS_d8_6x4	6 x 4	8	60	190	4	40	40	80	35	3

Table 2. Kerto-S LVL series with double-shear dowelled connections. Kerto-S is standard LVL.

Series name	Dowel pattern n x m	dowel diam. d mm	thick-ness t_1 or t_2 mm	width B mm	steel plate t_s mm	spacing parall. a_1 mm	spacing, perp. a_2 mm	end dist. a_3 mm	edge dist. a_4 mm	N
Timber-Steel-Timber, Dowel diameter 12 mm										
Kerto-S, t_1 = 39 mm, d = 12 mm, dowel strength cl 8.8, a_2 = 38 mm, a_3 = max(a_1; 105mm)										
KS_TST_d12_12x2	12x2	12	39	162	12	84	38	105	62	3
KS_TST_d12_8x3	8x3	12	39	180	12	93	38	105	52	3
KS_TST_d12_6x4	6x4	12	39	204	12	105	38	105	45	5
KS_TST_d12_4x6	4x6	12	39	266	12	105	38	105	38	3
Steel-Timber-Steel, Dowel diameter 12 mm										
Kerto-S, t_2 = 75 mm, d = 12 mm, dowel strength cl. 8.8, a_3 = 105 mm, t_s = 6 mm, F_{Rk} = 624 kN										
KS_STS_d12_12x2	12x2	12	75	228	6	84	48	105	90	3
KS_STS_d12_8x3	8x3	12	75	224	6	105	48	105	64	3
KS_STS_d12_6x4	6x4	12	75	252	6	84	60	105	36	5
KS_STS_d12_4x6	4x6	12	75	272	6	84	40	105	36	3
KS_STS_d12_3x8	3x8	12	75	324	6	84	36	105	36	3
Timber-Steel-Timber, Dowel diameter 8 mm										
Kerto-S, t_1 = 27 mm, d = 8 mm, dowel strength cl. 10.9, a_2 = 26 mm, a_3 = 105 mm										
KS_TST_d8_12x2	12x2	8	27	116	8	56	26	105	45	3
KS_TST_d8_6x4	6x4	8	27	138	8	64	26	105	30	3
Steel-Timber-Steel, Dowel diameter 8 mm										
Kerto-S, t = 51 mm, d = 8 mm, dowel strength cl. 10.9, a_3 = 105 mm, t_s = 4 mm										
KS_STS_d8_12x2	12x2	8	51	160	4	56	32	105	64	3
KS_STS_d8_6x4	6x4	8	51	174	4	56	42	105	24	3
Edgewise Kerto-S, t = 51 mm, d = 8 mm, dowel strength cl. 10.9, a_3 = 105 mm, t_s = 4 mm										
KE_STS_d8_6x4	6x4	8	51	174	4	56	42	105	24	3

Table 3. Kerto-Q LVL series with double-shear dowelled connections. Kerto-Q is cross veneered LVL.

Series name	Dowel pattern n x m	dowel diam. d mm	thick-ness t_1 or t_2 mm	width B mm	steel plate t_s mm	spacing parall. a_1 mm	spacing, perp. a_2 mm	end dist. a_3 mm	edge dist. a_4 mm	N
Timber-Steel-Timber, Dowel diameter 12 mm										
Kerto-Q, t_1 = 39 mm, d = 12 mm, dowel strength cl. 8.8, a_2 = 38 mm, a_3 = 105mm										
KQ_TST_d12_6x4	6x4	12	39	258	12	105	38	105	72	3
Steel-Timber-Steel, Dowel diameter 8mm										
Kerto-Q, t = 51 mm, d = 8 mm, dowel strength cl. 10.9, a_3 = 60 mm, t_s = 4 mm										
KQ_STS_d8_12x2	12x2	8	51	210	4	56	32	60	89	3
KQ_STS_d8_6x4	6x4	8	51	224	4	56	42	60	49	3

2.3 Multiple shear connection specimens

The multiple shear tests series are shown in Table 4, 5 and 6 for glulam, Kerto-S LVL and Kerto-Q LVL, respectively.

The two parallel series – GL_4Sh_d8_6x4A and GL_4Sh_d8_6x4AZ – were made as first 4-shear tests for comparison between cases with and without connected timber members. The results showed that there is not much difference in their capacity. However, since the series with the connected timber members showed slightly smaller value, it was decided to make the rest of the series as connected. So all multiple shear test series were made with connected members except the one mentioned series (GL-4Sh_d8_AZ). The glulam specimens were manufactured from split glulam, but the split parts were glued together using two battens of either 14 mm thickness or 10 mm thickness depending on the steel plate thickness 12 mm or 8 mm, respectively. Similarly, LVL-specimens were manufactured by gluing the parts together. The gluing was made as screw-gluing with polyurethane glue.

Table 4. Glulam series with multiple shear dowelled connections.

Series name	Dowel pattern n x m	dowel diam. d mm	thick-ness t_1/t_2 mm	width B mm	steel plate t_s mm	spacing parall. a_1 mm	spacing perp. a_2 mm	end dist. a_3 mm	edge dist. a_4 mm	N
4-Shear, Timber-Steel-Timber-Steel-Timber, Dowel diameter 12 mm										
GL28h, d = 12 mm, dowel strength cl. 8.8, a_2 = 38 mm, $a_3 = a_1$, t_s = 12 mm										
GL_4Sh_d12_12x2A	12x2	12	42/90	250	12	93	38	93	106	3
GL_4Sh_d12_12x2B	12x2	12	35/104	250	12	93	38	93	106	3
GL_4Sh_d12_6x4A	6x4	12	42/90	276	12	114	38	114	81	3
GL_4Sh_d12_6x4B	6x4	12	35/104	276	12	114	38	114	81	3
4-Shear, Timber-Steel-Timber-Steel-Timber, Dowel diameter 8 mm										
GL28h, d = 8 mm, dowel strength class10.9, a_2 = 26 mm, a_3 = 80 mm, t_s = 8 mm										
GL_4Sh_d8_12x2A	12x2	8	28/60	174	8	64	26	80	74	3
GL_4Sh_d8_12x2B	12x2	8	22/72	174	8	64	26	80	74	3
GL_4Sh_d8_6x4AZ(*	6x4	8	28/60	192	8	80	26	80	57	3
GL_4Sh_d8_6x4B	6x4	8	22/72	192	8	80	26	80	57	3
GL_4Sh_d8_6x4A(*	6x4	8	28/60	192	8	80	26	80	57	3
6-Shear, Timber-Steel-Timber-Steel-Timber-Steel-Timber, Dowel diameter 8 mm										
GL28h, d = 8 mm, dowel strength class10.9, a_2 = 26 mm, a_3 = 80 mm, t_s = 8 mm										
GL_6Sh_d8_12x2	12x2	8	28 / 60	174	8	64	26	80	74	3

Table 5. Kerto-S LVL series with multiple shear dowelled connections.

Series name	Dowel pattern n x m	dowel diam. d mm	thick-ness t_1/t_2 mm	width B mm	steel plate t_s mm	spacing parall. a_1 mm	spacing perp. a_2 mm	end dist. a_3 mm	edge dist. a_4 mm	N
4-Shear, Timber-Steel-Timber-Steel-Timber, Dowel diameter 12 mm										
Kerto-S, d = 12 mm, Dowel strength class 8.8, a_2 = 48 mm, a_3 = 105 mm, t_s = 8 mm										
KS_4Sh_d12_12x2	12 x 2	12	38/72	228	8	84	48	105	90	3
KS_4Sh_d12_6x4	6 x 4	12	38/72	252	8	105	48	105	54	3
4-Shear, Timber-Steel-Timber-Steel-Timber, Dowel diameter 8 mm										
Kerto-S, d = 8 mm, Dowel strength class 10.9, a_2 = 32 mm, a_3 = 105 mm, t_s = 8 mm										
KS_4Sh_d8_12x2A	12 x 2	8	26/49	160	8	56	32	105	64	3
KS_4Sh_d8_12x2B	12 x 2	8	20/61	160	8	56	32	105	64	3
KS_4Sh_d8_6x4A	6 x 4	8	26/49	176	8	56	32	105	40	3
KS_4Sh_d8_6x4B	6 x 4	8	20/61	176	8	56	32	105	40	3
6-Shear, Timber-Steel-Timber-Steel-Timber-Steel-Timber, Dowel diameter 8 mm										
Kerto-S, d = 8 mm, Dowel strength class 10.9, a_2 = 32 mm, a_3 = 105 mm, t_s = 8 mm										
KS_6Sh_d8_6x4	6 x 4	8	26/49	176	8	56	32	105	40	3

Table 6. Kerto-Q LVL series with multiple shear dowelled connections.

Series name	Dowel pattern n x m	dowel diam. d mm	thick-ness t_1/t_2 mm	width B mm	steel plate t_s mm	spacing parall. a_1 mm	spacing perp. a_2 mm	end dist. a_3 mm	edge dist. a_4 mm	N
4-Shear, Timber-Steel-Timber-Steel-Timber, Dowel diameter 12 mm										
Kerto-Q, d = 12 mm, Dowel strength class 8.8, a_2 = 48 mm, a_3 = 105 mm, t_s = 8 mm										
KQ_4Sh_d12_5x4	5 x 4	12	38/72	322	8	105	48	105	89	3
4-Shear, Timber-Steel-Timber-Steel-Timber, Dowel diameter 8 mm										
Kerto-Q, d = 8 mm, Dowel strength class 10.9, a_2 = 32 mm, a_3 = 60 mm, t_s = 8 mm										
KQ_4Sh_d8_6x4	6 x 4	8	26/49	226	8	56	32	60	65	3

2.4 Test methods

The dowel holes for glulam were drilled using a numerical control (NC) machine tool. The glulam specimens were first allowed to reach equilibrium moisture content in a climate chamber with relative humidity of 65% and temperature 20°C (corresponding to equilibrium moisture content 12%) and drilled within 12h from taking outside the chamber. Then the specimens were taken back to the climate chamber. After that, the steel plates were put in place, dowels inserted as well as the binderbolts and nuts assembled. The LVL specimens were also drilled using a numerical control machine tool, at the Kerto-LVL factory.

All series were kept in a climate chamber (20 °C, 65%RH) long enough that they reached the equilibrium moisture content before manufacturing of joints and testing.

The loading was made according to EN26891:1991 using a specially made test bench, Fig. 5. The slip was measured between the steel plate(s) and timber members(s) near the steel plate end at both top and bottom sides of the specimen and at both ends (altogether four locations of each specimen, Figs. 5 and 6. The slip of each connection was calculated as the average of the values measured on the top and the bottom.

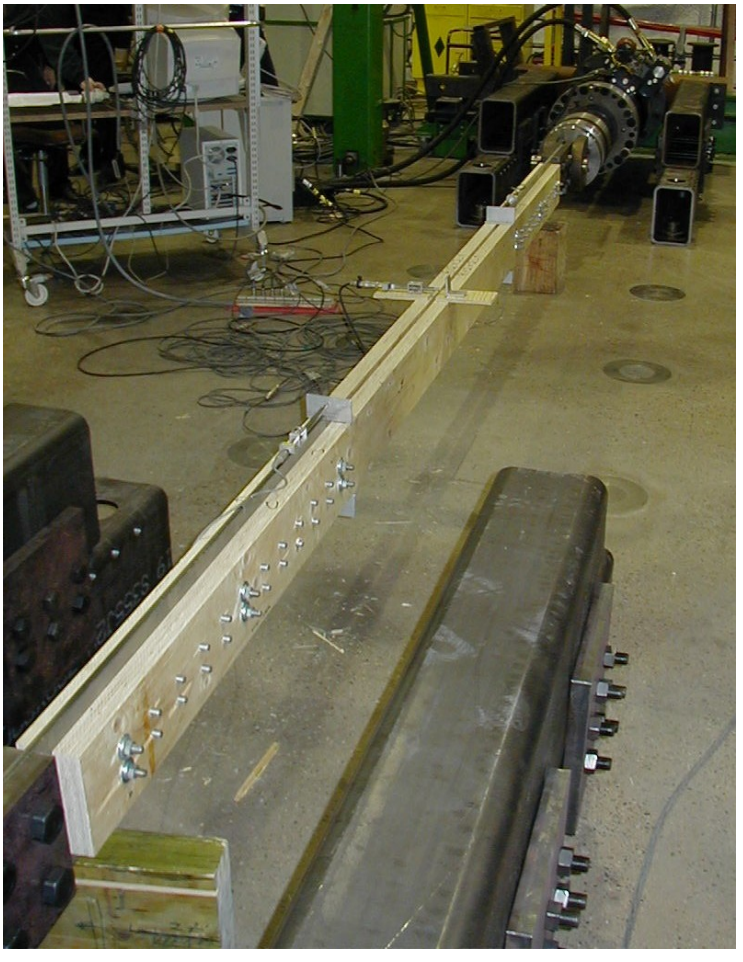

Figure 5. Load bench for the tests. Note the connection slip measurements at four locations of the specimen, two for each connection. The transverse measurement in the middle of the specimen between the timber members was not normally used.

Figure 6. Slip measurement by LVDT's at top and bottom of each connection.

3. Experimental results and discussion

3.1 Results and analysis

The results of the double shear tests are presented in Tables 7, 8 and 9 and the multiple shear tests in Tables 10, 11 and 12 for glulam, Kerto-S LVL and Kerto-Q LVL, respectively. The presented test results contain the measured mean density, mean maximum slip (v_{max}) and mean maximum load (F_{max}) and its coefficient of variation. The observed failure mechanism is also reported. The load-displacement curves of all specimens are given in Appendix A. The prevailing failure mechanism was block shear (Fig. 7), but also tensile failures (Fig. 8) occurred as well as their combination (Fig. 9) and a few rowshear failures (Fig. 10). However, no plug shear failures were detected. It could also happen that the failure occurred on different sides of the specimen (Fig. 11).

Figure 7. Typical failure by the block shear failure mechanism.

Figure 8. Failure by tension at the farthest column of dowels.

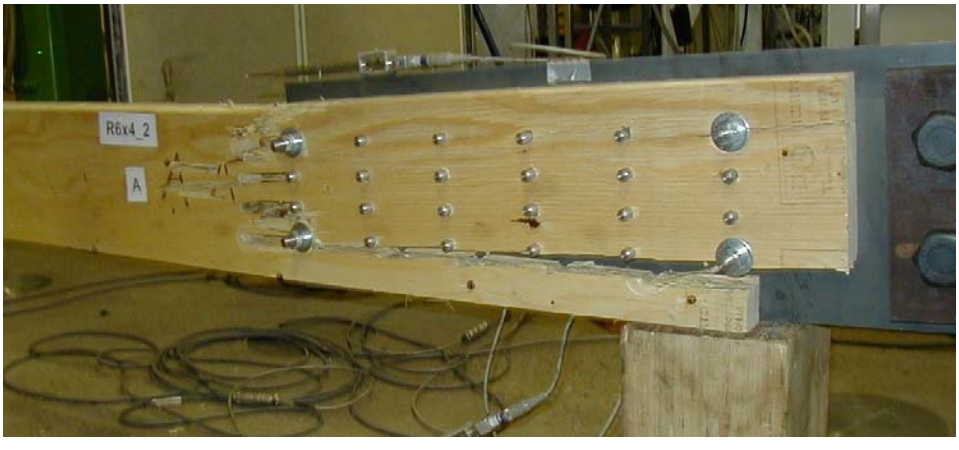

Figure 9. Combination of block shear and tension failure.

Figure 10. Partial row shear failure, only very few row shear occurred.

Figure 11. Failure, which has occurred across the specimen.

For better comparison of the test results to the design formulas of Eurocode 5 (EC5, EN 1995-1-1:2004) some calculated values based on EC5 equations are also added to Tables 7–12. The calculated values represent either characteristic values (subscript k) or mean values (subscript m) and are explained in the list of symbols above. The characteristic values have been calculated based on characteristic material properties as obtained from standards. The mean values

are based on the measured values of density of timber and tensile strength of dowels. The mean values of non-measured properties have been assumed the following values:

- Glulam: $f_{tm} = 1.3 * f_{tk} = 29$ N/mm^2, $f_{vm} = 1.3 * f_{vk} = 4.9$ N/mm^2
- Kerto-S: $f_{tm} = 43$ N/mm^2, $f_{vm,edge} = 4.9$ N/mm^2, $f_{vm,flat} = 3.0$ N/mm^2
- Kerto-Q: $f_{tm} = 33$ N/mm^2, $f_{vm,edge} = 5.4$ N/mm^2, $f_{vm,flat} = 1.7$ N/mm^2.

The above values for Kerto-LVL are estimated based on initial tests made at VTT according to the product standard EN14374. The values for glulam are an estimation based on experience.

The load-carrying capacity in case of splitting or rowshear has been calculated by Eq. (1) corresponding to formulas 8.1, 8.34 in EC5 as a reduction of the number of dowels n and capacity given by Johansen theory. The load-carrying capacity in case of block or plug shear failure has been calculated by Eq. (2) above corresponding to the formula (A.1) in the Annex A of EC5.

Table 7. The calculated capacities and test results of the glulam series with double-shear dowelled connections. Symbols: see List of Symbols.

Series name	F_{Sk} kN	F_{Bk} kN	DF	F_{Rm} kN	F_{Sm} kN	F_{Bm} kN	F_{Tm} kN	ρ_m kg/m^3	v_{max} mean mm	F_{max} mean kN	F_{max} CoV %	TF	F_{max} / F_{Sm}	F_{max} / F_{Bm}
Timber-Steel-Timber, Dowel diameter 12 mm														
GL28h, t_1 = 42 mm, d = 12 mm, Dowel strength cl. 8.8, F_{Rk} = 520 kN														
GL_TST_d12_12x2	356	297	p	579	397	385	459	466	1.9	424	8.3	b	1.07	1.10
GL_TST_d12_8x3	382	315	p	574	422	409	487	460	2.0	504	11.6	b	1.19	1.23
GL_TST_d12_6x4	402	332	p	585	452	430	511	474	2.3	529	4.4	b	1.17	1.23
GL_TST_d12_4x6	418	319	p	577	464	415	525	464	2.8	571	6.2	b	1.23	1.38
Steel-Timber-Steel, Dowel diameter 12 mm														
GL28h, t_2 = 90 mm, d = 12 mm, dowel strength cl. 8.8, F_{Rk} = 576 kN														
GL_STS_d12_12x2	385	353	b-r	635	424	459	567	462	2.4	537	2.8	b	1.27	1.17
GL_STS_d12_8x3	438	353	b-r	644	490	459	567	475	3.7	646	7.4	b	1.32	1.41
GL_STS_d12_6x4	379	363	b-t	625	411	472	572	447	3.0	606	10.1	b	1.47	1.28
GL_STS_d12_4x6	395	369	b-t	638	438	479	582	467	2.6	552	6.0	b	1.26	1.15
GL_STS_d12_3x8	442	442	b-t	638	490	575	693	466	4.0	671	1.5	row	1.37	1.17
Timber-Steel-Timber, Dowel diameter 8 mm														
GL28h, t_1 = 28 mm, d = 8 mm, dowel strength cl. 10.9, F_{Rk} = 279 kN														
GL_TST_d8_12x2	193	148	p	314	217	191	222	472	1.9	266	5.6	b	1.23	1.39
GL_TST_d8_6x4	218	164	p	296	232	214	250	425	1.6	238	17.7	b	1.03	1.11
Steel-Timber-Steel, Dowel diameter 8 mm														
GL28h, t_2 = 60 mm, d = 8 mm, dowel strength cl. 10.9, F_{Rk} = 318 kN														
GL_STS_d8_12x2	212	163	b-r	355	237	212	264	468	2.6	295	21.6	b	1.24	1.39
GL_STS_d8_6x4	209	168	b-t	353	232	219	264	462	2.0	299	4.8	(*	1.29	1.37

*) the dominating failure mode is unclear

Table 8. The calculated capacities and results of the Kerto-S LVL series with double-shear dowelled connections. Symbols: see List of symbols.

Series name	F_{Sk} kN	F_{Bk} kN	DF	F_{Rm} kN	F_{Sm} kN	F_{Bm} kN	F_{Tm} kN	ρ_m kg/m^3	v_{max} mean mm	F_{max} mean kN	F_{max} CoV %	TF	F_{max} / F_{Sm}	F_{max} / F_{Bm}
Timber-Steel-Timber, Dowel diameter 12 mm														
Kerto-S, t_1 = 39 mm, d = 12 mm, Dowel strength cl. 8.8, F_{Rk} = 563 kN														
KS_TST_d12_12x2	376	331	p	594	397	395	506	499	2.6	400	7.9	b	1.01	1.01
KS_TST_d12_8x3	402	347	p	588	420	414	528	492	2.3	460	6.8	b	1.10	1.11
KS_TST_d12_6x4	426	378	p	603	456	449	572	512	2.6	507	6.1	b	1.11	1.13
KS_TST_d12_4x6	444	532	s/r	586	462	649	711	488	3.1	598	0.8	b	1.29	0.92
Steel-Timber-Steel, Dowel diameter 12 mm														
Kerto-S, t_2 = 75 mm, d = 12 mm, Dowel strength cl. 8.8, F_{Rk} = 665 kN														
KS_STS_d12_12x2	444	386	b-r	722	483	459	719	523	2.7	500	5.2	b	1.04	1.09
KS_STS_d12_8x3	489	325	b-r	726	534	387	662	527	3.2	568	0.8	b	1.06	1.47
KS_STS_d12_6x4	476	567	s/r	736	527	692	719	537	3.7	591	7.1	b	1.12	0.85
KS_STS_d12_4x6	496	551	s/r	753	562	673	705	556	2.8	570	4.9	b	1.01	0.85
KS_STS_d12_3x8	510	662	s/r	717	551	807	803	518	2.8	561	7.3	b	1.02	0.70
Timber-Steel-Timber, Dowel diameter 8 mm														
Kerto-S, t_1 = 27 mm, d = 8 mm, Dowel strength cl. 10.9, F_{Rk} = 303 kN														
KS_TST_d8_12x2	203	167	p	324	216	199	254	502	1.8	200	7.6	b	0.93	1.01
KS_TST_d8_6x4	224	180	p	328	243	214	269	514	1.7	241	13.0	b	0.99	1.13
Steel-Timber-Steel, Dowel diameter 8 mm														
Kerto-S, t_2 = 51 mm, d = 8 mm, Dowel strength cl. 10.9, F_{Rk} = 344 kN														
KS_STS_d8_12x2	230	185	b-r	374	250	220	345	524	2.8	296	2.0	b	1.18	1.35
KS_STS_d8_6x4	246	273	s/r	380	272	333	340	518	3.8	336	2.3	b	1.25	1.01
Edgewise Kerto-S, t_2 = 51 mm, d = 8 mm, Dowel strength cl. 10.9, F_{Rk} = 344 kN														
KE_STS_d8_6x4	246	273	s/r	380	272	333	340	513	2.6	206	7.5	row	0.76	0.62

Table 9. The calculated capacities and results of the Kerto-Q LVL series with double-shear dowelled connections. Symbols: see List of symbols.

Series name	F_{Sk} kN	F_{Bk} kN	DF	F_{Rm} kN	F_{Sm} kN	F_{Bm} kN	F_{Tm} kN	ρ_m kg/m^3	v_{max} mean mm	F_{max} mean kN	F_{max} CoV %	TF	F_{max} / F_{Sm}	F_{max} / F_{Bm}
Timber-Steel-Timber, Dowel diameter 12 mm														
Kerto-Q, t_1 = 39 mm, d = 12 mm, Dowel strength cl. 8.8, F_{Rk} = 542 kN														
KQ_TST_d12_6x4	411	237	p	561	425	297	586	482	2.6	447	2.1	T	1.05	1.51
Steel-Timber-Steel, Dowel diameter 8 mm														
Kerto-Q, t_2 = 51 mm, d = 8 mm, Dowel strength cl. 10.9, F_{Rk} = 333 kN														
KQ_STS_d8_12x2	223	188	b-r	341	228	226	354	492	3.7	308	7.0	T	1.35	1.36
KQ_STS_d8_6x4	239	203	b-t	348	249	254	350	501	3.9	335	7.3	b,T	1.35	1.32

Table 10. The calculated capacities and test results of the Glulam series with multiple-shear dowelled connections. Symbols: see List of Symbols.

Series name	F_{Sk} kN	F_{Bk} kN	DF	F_{Rm} kN	F_{Sm} kN	F_{Bm} kN	F_{Tm} kN	ρ_m kg/m^3	v_{max} mm	F_{max} mean kN	F_{max} CoV %	TF	F_{max} / F_{Sm}	F_{max} / F_{Bm}
4-Shear, Dowel diameter 12 mm														
GL28h, d = 12 mm, dowel str. cl. 10.9, t_s = 12 mm, F_{Rk} = 1040 kN (A), 1122 kN (12x2B), 1447 (6x4B)														
GL_4Sh_d12_12x2A	781	702	p,b-r	1216	833	910	1096	447	2.0	968	6.9	b,b	1.16	1.06
GL_4Sh_d12_12x2B	769	744	p,b-r	1196	820	965	1096	449	2.1	1084	5.7	b,b	1.32	1.12
GL_4Sh_d12_6x4A	881	589	p,b-r	1240	958	762	1106	463	1.4	856	5.9	b,b	0.89	1.12
GL_4Sh_d12_6x4B	1118	616	p,b-r	1592	1230	798	1106	462	1.8	1069	6.3	b,b	0.87	1.34
4-Shear, Dowel diameter 8 mm														
GL28h, d = 8 mm, dowel strength class10.9, t_s = 8 mm, F_{Rk} = 558 kN (A), 689 kN (B)														
GL_4Sh_d8_12x2A	385	335	p,b-r	598	413	435	511	447	2.0	501	20.3	b,b	1.21	1.15
GL_4Sh_d8_12x2B	476	363	b-r,b-r	791	546	468	511	471	1.9	530	4.3	b,b	0.97	1.13
GL_4Sh_d8_6x4AZ	437	282	p,b-r	606	474	366	518	458	2.0	586	6.1	b,b	1.24	1.60
GL_4Sh_d8_6x4B	539	299	b-r,b-r	765	599	388	517	455	1.8	478	15.9	b,b	0.80	1.23
GL_4Sh_d8_6x4A	437	282	p,b-r	596	467	366	518	444	1.8	546	4.5	b,b	1.17	1.49
6-Shear, Dowel diameter 8 mm														
GL28h, d = 8 mm, dowel strength class10.9, t_s = 8 mm, F_{Rk} = 837 kN														
GL_6Sh_d8_12x2	655	400	p,b-r	879	688	521	786	431	1.7	765	11.7	b,b	1.11	1.47

Table 11. The calculated capacities and test results of the Kerto-S LVL series with multiple-shear dowelled connections. Symbols: see List of Symbols.

Series name	F_{Sk} kN	F_{Bk} kN	DF	F_{Rm} kN	F_{Sm} kN	F_{Bm} kN	F_{Tm} kN	ρ_m kg/m^3	v_{max} mm	F_{max} mean kN	F_{max} CoV %	TF	F_{max} / F_{Sm}	F_{max} / F_{Bm}
4-Shear, Dowel diameter 12 mm														
Kerto-S, d = 12 mm, Dowel strength class 10.9, F_{Rk} = 1226kN														
KS_4Sh_d12_12x2	819	758	p,b-r	1314	878	898	1418	525	2.3	898	7.6	b,b	1.02	1.00
KS_4Sh_d12_6x4	928	886	b-t,b-t	1312	993	1065	1418	523	2.2	1157	1.2	b,b	1.17	1.09
4-Shear, Dowel diameter 8 mm														
Kerto-S, d = 8 mm, Dowel strength class 10.9, F_{Rk} =604kN (A), F_{Rk} = 702 kN (B)														
KS_4Sh_d8_12x2A	404	364	p,b-r	658	440	431	683	538	1.8	460	8.8	b,b	1.05	1.07
KS_4Sh_d8_12x2B	469	396	b-r,b-r	790	528	468	684	540	2.0	511	2.5	b,b	0.97	1.09
KS_4Sh_d8_6x4A	433	382	b-t,b-t	660	473	466	683	541	1.5	492	1.1	b,b	1.04	1.06
KS_4Sh_d8_6x4B	503	419	b-t,b-t	772	553	504	684	528	1.7	528	2.8	b,b	0.95	1.05
6-Shear, Dowel diameter 8 mm														
Kerto-S, d = 8 mm, Dowel strength class 10.9, F_{Rk} = 906 kN														
KS_6Sh_d8_12x2	649	567	b-t,b-t	876	627	462	670	550	1.7	729	8.8	b,b	1.16	1.58

Table 12. The calculated capacities and test results of the Kerto-Q LVL series with multiple-shear dowelled connections. Symbols: see List of Symbols.

Series name	F_{Sk} kN	F_{Bk} kN	DF	F_{Rm} kN	F_{Sm} kN	F_{Bm} kN	F_{Tm} kN	ρ_m kg/m^3	v_{max} mm	F_{max} mean kN	F_{max} CoV %	TF	F_{max} / F_{Sm}	F_{max} / F_{Bm}
4-Shear, Dowel diameter 12 mm														
Kerto-Q, d = 12 mm, Dowel strength class 10.9, F_{Rk} = 1188kN														
KQ_4Sh_d12_5x4	900	623	b-t,b-r	1272	963	779	1449	527	4.3	1196	3.1	b,b	1.24	1.53
4-Shear, Dowel diameter 8 mm														
Kerto-Q, d = 8 mm, Dowel strength class 10.9, F_{Rk} = 584 kN														
KQ_4Sh_d12_6x4	418	324	b-t,b-t	618	443	396	701	518	2.3	584	4.9	b,b	1.31	1.47

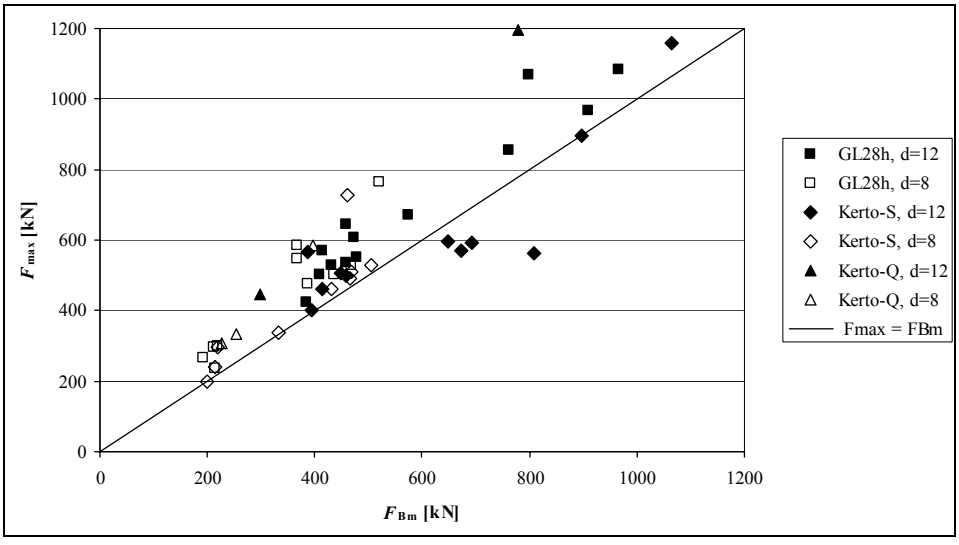

Figure 12. F_{max} plotted against F_{Bm}. Each point is the mean result of one series. Note that in all four series which are under the $F_{max} = F_{Bm}$ line, the critical design is not due to block shear but splitting or rowshear, represented by F_S, and in all four cases $F_{max} > F_{Sm}$.

3.2 Discussion and conclusions on test results

One striking feature in the results is that the observed failure mode is in a large proportion different than what the calculation of the capacity value is based on (EN1995-1-1:2004). Especially this concerns the double-shear timber-steel-timber series and the outer timber members of the multiple-shear series. In a large part of the series of these kinds, the calculation of the capacity is based on the plug-shear failure mechanisms, whereas the observed failure was block shear. In fact, in no cases was plug shear observed. For the Kerto-Q LVL the plug shear failure design value is in some cases very low, due to the low shear strength of the cross-veneers (rolling shear). However, in no cases was the plug shear observed for the Kerto-Q specimens, either. The plug shear failure does not occur, because the dowels remain straight or bend only very little before failure and failure occurs as block shear.

Another general observation is that, even if according to the design equations the failure load due to block or plug shear and splitting (F_{Bm} and F_{Sm}) are very close

to each other, and F_{Sm} is even lower than F_{Bm}, there were very few rowshear failures detected, which should be represented by F_{Sm}. This indicates that the equation by which F_{Sm} is calculated is too conservative for these types of connections, although the dowels were rather rigid.

Kerto-Q behaves differently from what could be anticipated from design equations. The low value of flatwise shear strength leads calculationally to very low capacity, if the critical failure mechanism is plug shear. However, in practice the plug shear does not occur due to rigid dowels and the capacity is much higher than expected by design calculations.

4. Design method against timber failure mechanisms

4.1 Principles of the method

The ultimate goal of the project was to improve the design of heavy duty dowelled connections. As pointed out in the Introduction, the next necessary step with these connections is the design against timber failure mechanisms, which are observed, when the connections are loaded in tension parallel-to-grain. So the experimental program was designed to give these kind of results, which well realized in tests. Based on the experience and observations of the test results, a design method was derived for prediction of the capacity of dowel type steel-to-timber connections against timber failure mechanisms. As mentioned, the method deals with timber failure mechanisms and – in the way it is presented here – is restricted to steel-to-timber connections and connections in which the fasteners extend through the whole thickness of all timber members and parallel-to-grain tension loading. (It can be noted that compression parallel to grain poses no further problem, since it can be easily considered otherwise).

The proposed design method is based on the following principles:

- The method concerns only the timber failure mechanisms, the dowel yielding is assumed to be taken care by the Johansen theory as instructed in EC5. The timber failure mechanisms contain: (1) embedment failure, (2) tension failure at the connection area, (3) block shear and (4) row shear. (Note: embedment failure is also covered in the Johansen theory.)
- Plug shear failure mechanism is assumed not to be relevant, if the dowels extend through the whole thickness of all timber members. However, effect of dowel deformation (elastic or plastic bending) on timber failure mechanisms is considered through a slenderness ratio based reduction of timber thickness, when shear and splitting failure modes are considered.
- The different failure modes are considered separately, i.e. the method pursues to make the design against the different stress components (tension, shear, splitting, embedment) transparent, and so that no parameter is assigned to cover more than one failure type. However, the interaction between the stress components is considered.

The design calculation procedure goes as follows:

1) The connection area is divided into parts according to the possible failure surfaces. (In the end, the capacity of the connection is assumed to be calculable as a sum.)
2) The effect of load distribution between dowels is calculated in terms of effective number of dowels, which is applied when calculating the capacities of individual parts.
3) The effect of dowel slenderness on capacity is calculated in terms of reduced thickness which is applied when calculating the capacities of individual parts.
4) Each part is assigned with possible failure modes and the capacity against all modes is calculated (effect of load distribution and dowel slenderness are taken into account).
5) Interaction effects between different failure modes (stress components) are considered.
6) The smallest obtained capacity (strength) determines the capacity of each part.
7) The total capacity of the connection against tension is obtained as the sum of the capacities of the parts.

The capacities against different failure modes at the part level are derived below by combination of theoretically and empirically based reasoning.

4.2 Division of connection area to parts

As a first step, the connection area is divided into parts according to the possible failure surfaces. The failure surfaces pass along the dowel rows on both sides of the dowels (shear and splitting failure) and along the line that passes through the dowel column that is farthest from the end of timber (tension failure), an example is shown in Fig. 2. (Besides these surfaces, the compressed areas of the dowel holes must be understood as the failure surface for the embedment failure capacity.) The parts are indexes as j = 0…m, so that parts 0 and m are located by the edge and are named as *outer parts*, where as the parts from 1 to m-1 are called the *inner parts*.

(It can be noted that splitting failure in most cases passes along a slightly different surface as instructed above, namely not along the sides of the dowel holes but through the middle lines of the dowel row. Due to pursuit for simplicity, however, the same surface is used for it as for the shear failure.)

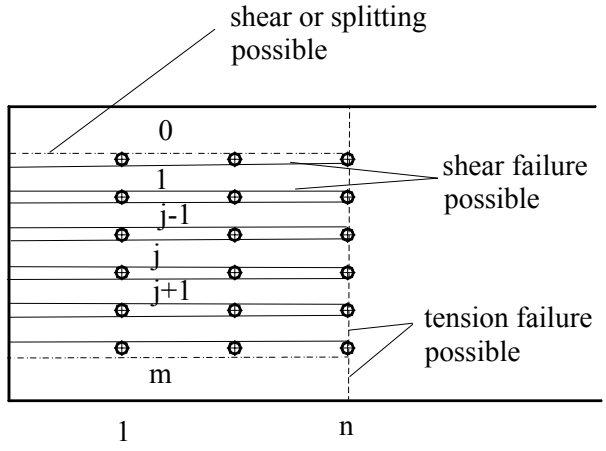

Figure 13. Division of connection area to parts by determining the possible failure surfaces.

4.3 Effect of load distribution between dowels

When there are several dowels in a row, the load per fastener cannot exceed the strength of a single fastener connection, and can reach it only if plasticity type ductile phenomena with large deformations occur. The large deformations are possible when embedment failure occurs with strong crushing of timber under the compression of the dowels. However, the other timber failure mechanisms show brittle failure and do not permit large deformations. In the case of brittle failure modes, the need for reduction of capacity due to several dowels in a row is quite obvious even as consequence of the different stress level and thus different deformation along the areas between the dowels. (Jorissen 1998)

In EC 5 this kind of reduction is applied by the definition of effective number of fasteners in a row n_{ef}, which is dependent on the number of dowels, spacing and dowel diameter. Here a similar approach is adopted, but for simplicity dependent on only the number of dowels in a row:

$$n_{\text{ef}} = n^{0.9} \tag{5}$$

The reduction is applied to all brittle failure modes: tension, shear and splitting, but *not* to embedment failure.

4.4 Effect of dowel deformations (slenderness)

As stated above, the plug shear failure was not observed in the experimental test program. The conclusion was made that it is not relevant, if the dowels extend through the whole thickness of all timber members, because the plug shear failure would require the plastic hinges to develop to high degree. However, some dowels were observed to be bent slightly and all dowels do bend a least a little due to elastic deformation. It was found that, if the slenderness of the dowels is taken into account, the model fit is improved. The conclusion was therefore that even the slight bending of the dowels has an effect on the load carrying capacity. The slenderness of the dowels is taken into account by reducing the timber thickness, but only when considering shear and splitting, not parallel-to-grain tension:

$$t_{1,\text{red}} = \min\left(1, \frac{d}{0.6\,d_{\text{gr},1}}\right) \cdot t_1 \text{ , where } d_{\text{gr},1} = 2.45\sqrt{\frac{f_{\text{h,m}}}{f_{\text{y,m}}}}\,t_1 \text{ (side members)} \tag{6, 7}$$

$$t_{2,\text{red}} = \min\left(1, \frac{d}{0.5\,d_{\text{gr},2}}\right) \cdot t_2 \text{ , where } d_{\text{gr},2} = 1.23\sqrt{\frac{f_{\text{h,m}}}{f_{\text{y,m}}}}\,t_2 \text{ (middle members)}$$

d_{gr} is the limit above which the dowel is rigid according to the Johansen theory.

4.5 Principle of interaction effect between stress components

The stress state in the connection area is complex and all directions and components of stresses are present. Above all, the timber failure mechanisms are dependent on the parallel-to-grain tension, parallel-to-grain shear and perpendicular-to-grain tension stress components. Sjödin and Serrano (2006) and

Sjödin et al. (2006) studied the distributions of these stresses both computationally and by contact free measurements. The calculations and measurements both show that highly stressed areas under the different stress components overlap. It can be assumed that in such a complex stress state the different stresses affect the strength in a combined way, which was also indirectly concluded based on the experimental results of this project. Therefore, it is reasonable to assume an interaction effect for the stress components in the design.

In many design applications, interaction of stress components is modelled by assuming that the sum of the utilisation rates of the different components must not exceed 1 = 100%. Here, a slightly different parameterized approach is taken. It is assumed that, because the maxima of the stress components do not act in exactly the same location, the above mentioned condition is relaxed and parameterized as follows:

$$F_{1+2} = \begin{cases} F_1\left(1 - k_{\text{interaction}}\frac{F_1}{F_2}\right), \textit{if } F_1 \le F_2 \\ F_2\left(1 - k_{\text{interaction}}\frac{F_2}{F_1}\right), \textit{if } F_2 < F_1 \end{cases}, \textit{with } k_{\text{interaction}} = 0.3 \tag{8}$$

Eq. (8) essentially states that when two stress components affect the capacity of a part, the interaction is taken into account by reducing the lower capacity by subtracting an amount which is proportional to the ratio of the lower capacity to the higher. $k_{\text{interaction}}$ is a parameter, which could be varied depending on interaction type, but is here given value 0.3 for all cases. Eq. (8) is illustrated graphically in Fig. 3a.

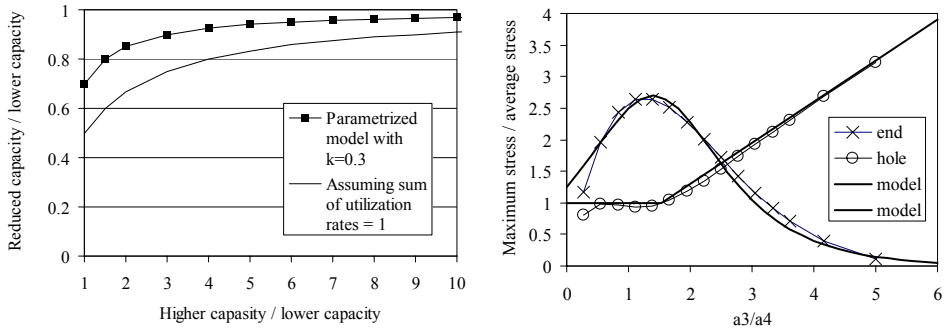

Figure 14. a) Left – Reduction of capacity due to the interaction of two stress components. Comparison of the effect of a classical model which assumes the sum of utilization rates to be 100% and relaxed parameterized model Eq. (8), which does not cause so strong reduction (interaction parameter = 0.3). b) Right – The ratio between maximum and average splitting stress (perpendicular to grain) vs. geometry parameter a_3/a_4.

4.6 Calculation of capacity of inner parts

When calculating the capacity of the inner parts ($j = 1 \ldots m\text{-}1$), the failure phenomena to be considered include:

- embedment strength at the area $A_{\mathrm{h,j}} = d\ t$
- tension failure at the area $A_{\mathrm{t,j}} = (a_2 - d)\ t$
- shear failure at the area $A_{\mathrm{v,j}} = 2\ [(n-1)a_1 + a_3]\ t$
- interaction effect of tension and shear.

4.6.1 Embedment failure

The embedment capacity is calculated in harmony with the rigid dowel case in the Johansen theory [EC 5 Equations (8.10e), (8.11f), (8.12j) and (8.13l), however, without effect of n_{ef}]:

$$F_{\mathrm{h,j,k}} = A_{\mathrm{h,j}} f_{\mathrm{h,k}} = d\ t\ f_{\mathrm{h,k}} \tag{9}$$

4.6.2 Tension failure

The tension capacity is calculated simply as tension strength times tensioned area multiplied by a stress concentration factor $k_{\mathrm{t,cnctr}}$. and the effect of load distribution taken into account (n_{ef}). $k_{\mathrm{t,cnctr}}$ has in fact higher value than 1, which can be justified by arguing that the tension stress acts on a small volume only and due to the high size effect of tension strength allows tension strength to have a higher value than in general (A similar factor has the value of 1.5 in EC 5 Annex A).

$$F_{\mathrm{t,j,k}} = k_{t,cnctr}\,(n_{\mathrm{ef}} / n) A_{\mathrm{t,i}} f_{t,0,k} = k_{t,cnctr}\,(n_{\mathrm{ef}} / n)(a_2 - d)\, t\, f_{t,0,k} \qquad (10)$$

4.6.3 Shear failure

The shear capacity is calculated also in a similar simple manner. Now, both load distribution effect (n_{ef}) and dowel deformation effect (t_{red}) are taken into account. The stress concentration factor $k_{\mathrm{v,cnctr}}$ has a value lower than 1 in order take into account the unevenness of the shear stress distribution. (A corresponding factor has a value of 0.7 in EC 5 Annex A):

$$F_{\mathrm{v,j,k}} = k_{v,cnctr}\,(n_{\mathrm{ef}} / n) A_{\mathrm{v,j}} f_{\mathrm{v,k}} = k_{v,cnctr}\,(n_{\mathrm{ef}} / n) \cdot 2((n-1)\, a_1 + a_3)\, t_{red}\, f_{\mathrm{v,k}} \qquad (11)$$

4.6.4 Interaction of tension and shear

The tension stresses and shear stresses are assumed to have an interaction effect on capacity, which is taken into account in the way described above [Eq. (8), subscripts 1 => t, 2 => v].

4.6.5 Capacity of the inner part

The capacity of the j'th inner part is obtained as the smaller of the embedment strength and the combined effect of tension and shear:

$$F_{j,k} = \min\left(F_{h,j,k}, F_{t+v,j,k}\right) \tag{12}$$

4.7 Calculation of capacity of outer parts

When calculating the capacity of the outer parts (j = 0 or m), the failure phenomena to be considered include:

- embedment strength at the area $A_{h,j} = 0.5\, d\, t$
- tension failure at the area $A_{t,j} = (a_4 - d/2)\, t$
- shear failure at the area $A_{v,j} = [(n-1)a_1 + a_3]\, t$
- interaction effect of tension and shear
- splitting failure originating either at the end of timber or at the hole nearest to the end
- interaction effect of shear and splitting originating at the hole nearest to the end.

4.7.1 Embedment failure

The embedment capacity is again calculated in accordance with the case of rigid dowel of the Johansen theory (without effect of n_{ef}).

$$F_{h,j,k} = A_{h,j} f_{h,k} = 0.5\, d\, t\, f_{h,k} \tag{13}$$

4.7.2 Tension failure

The tension capacity is obtained in a similar manner as for the inner parts (Eq. 10 above), except that a reduction factor $k_{t,outer} = 1/(1+A_{t,j}/A_{v,j})$ is used to take into account the asymmetry of the tensile stress distribution:

$$F_{t,j,k} = k_{t,cnctr}\,(n_{ef}/n) A_{t,i} f_{t,0,k} k_{t,outer} = k_{t,cnctr}\,(n_{ef}/n)(a_2 - d)\, t\, f_{t,0,k} k_{t,outer} \tag{14}$$

4.7.3 Shear failure

The shear capacity is also obtained in a similar manner as for the inner parts (Eq. 11 above, however, the area under shear is only half of that of the inner parts):

$$F_{\mathrm{v,j,k}} = k_{v,cnctr}\,(n_{\mathrm{ef}} / n) A_{\mathrm{v,j}} f_{\mathrm{v,k}} = k_{v,cnctr}\,(n_{\mathrm{ef}} / n) \cdot ((n-1)\,a_1 + a_3)\,t_{red}\, f_{\mathrm{v,k}} \qquad (15)$$

4.7.4 Interaction of tension and shear

The interaction of tension and shear stresses are taken into account exactly as for the inner parts Eq. (8).

4.7.5 Splitting failure

For consideration of the splitting of the outer parts, two different ways of splitting are considered:

– splitting originating at the end of the timber
– splitting originating at the dowel hole nearest to the end of the timber.

This is based on the work of Jorissen (1998) who derived a model for the perpendicular-to-grain stresses on a plane parallel to the dowel row. The model is based on the analytical solution of a beam on an elastic foundation. His model is used here to develop an approximate mathematical expression between the splitting (maximum perpendicular-to-grain) stress and the geometry of the joint. It was applied assuming only one dowel and used to calculate the ratio between the maximum and average perpendicular-to-grain stress in the area between the dowel and the timber end. The average perpendicular to grain stress was calculated as the wedging force divided by $a_3 \cdot t$. (The peak stress in the very vicinity of the hole as well as the effect of timber thickness were not considered here.)

To study the effect of the geometry of the connection, the ratio a_3/a_4 was varied in calculations, and it was found that – for practical purposes – either the stress at the timber end or the stress at the hole corresponds to the maximum, so that it

is enough to consider only these two locations. The results of the geometry effect, viz., the ratio between maximum and average perpendicular-to-grain stress at the end and at the hole as function of a_3/a_4 is plotted in Fig. 3b. By curve fitting, the ratio between the maximum and average perpendicular to grain stress is approximately expressed by at hole and at end, respectively, by the following equations:

$$s_{\mathrm{t90,hole}} = \max\left(1\,,\, 0.65\, a_3 / a_4\right) \qquad (16, 17)$$
$$s_{\mathrm{t90,end}} = 2.7 / \cosh\left(a_3 / a_4 - 1.4\right)$$

Jorissen (1998) estimated that the wedging force is of the order of 0.1 times the axial force transmitted by the dowel. A stress concentration factor $k_{\mathrm{t90,cnctr}}$ is assumed also for the splitting failure. With these two further facts taken into account, the splitting capacity can be expressed as (effect of load distribution and dowel deformation also taken into account by n_{ef} and t_{red}):

$$F_{\mathrm{splhole,j,k}} = k_{t90,cnctr}\, n_{\mathrm{ef}}\, 10\, f_{\mathrm{t,90,k}}\, t_{red}\, a_3 / s_{\mathrm{t90,hole}} \qquad (18, 19)$$
$$F_{\mathrm{splend,j,k}} = k_{t90,cnctr}\, n_{\mathrm{ef}}\, 10\, f_{\mathrm{t,90,k}}\, t_{red}\, a_3 / s_{\mathrm{t90,end}}$$

4.7.6 Interaction of shear and splitting at the dowel hole

The shear stress and splitting stress at the dowel hole are assumed to have an interaction effect on capacity, which is taken into account in the way described above in Eq. (8) [subscripts 1 => v, 2 => splithole].

The splitting failure originating at the end of the timber is not assumed to interact with shear, because the shear stress must vanish at the end.

4.7.7 Capacity of the outer part

The capacity of the outer part (j = 0, m) is obtained as the smallest capacity value:

$$F_{\mathrm{j,k}} = \min\left(F_{\mathrm{h,j,k}}\,,\, F_{\mathrm{t+v,j,k}}\,,\, F_{\mathrm{v+splhole,j,k}}\,,\, F_{\mathrm{splend,j,k}}\right) \qquad (20)$$

4.8 Capacity of whole connection against timber failure

Finally, the capacity of the connection against timber failure is obtained in case of double shear connections simply as the sum of the capacities of the parts:

$$F_{\mathrm{TFMk}} = \sum_{\mathrm{j}} F_{\mathrm{j,k}} \tag{21}$$

In case of 4-shear connections of the timber-steel-timber-steel-timber type, the capacity is first calculated as for two double shear connections and the total capacity is then obtained as the sum.

$$F_{\mathrm{TFMk}}^{4-shear} = F_{\mathrm{TFMk}}^{Timber-steel-timber} + F_{\mathrm{TFMk}}^{Steel-timber-steel} \tag{22}$$

4.9 Verification to test results

The design method was developed based on the observations and experience obtained in the experimental program reported. Simultaneously, it was verified against the results of the approximately 150 tension tests carried out in the test program. The verification results are presented in Tables 1–3 for double shear tests and multiple shear tests in Tables 4–6 for glulam and Kerto-S LVL, respectively. For better comparison of the results to the design formulas of Eurocode 5 some calculated values taken from the previous tables based on EC5 equations are also added to Tables 13–17. The observed failure mechanism as well as the critical failure mechanism of design are also given. The calculated values represent mean values (subscript m) and are explained in the list of symbols. The mean values are based on the measured values of density of timber and tensile yield strength of dowels.

All calculations have been made using mean properties. If the properties have been measured, then the mean measured values are used in calculations (reported in the corresponding Tables). The mean values of properties that were not measured have been assumed the following values:

– Glulam: $f_{\mathrm{tm}} = 1.3\, f_{\mathrm{tk}} = 29$ N/mm^2, $f_{\mathrm{vm}} = 1.3\, f_{\mathrm{vk}} = 4.9$ N/mm^2 , $f_{\mathrm{t90m}} = 1.0$ N/mm^2

– Kerto-S: f_{tm} = 43 N/mm^2, $f_{vm,edge}$ = 4.9 N/mm^2, $f_{vm,flat}$ = 3.0 N/mm^2 , f_{t90m} = 1.4 N/mm^2

– Kerto-Q: f_{tm} = 32 N/mm^2, $f_{vm,edge}$ = 5.3 N/mm^2, f_{t90m} = 10.5 N/mm^2.

The following values have been used for the stress concentration factors:

– Glulam: $k_{t,cnctr}$ = 2.0, $k_{v,cnctr}$ = 1.0 , $k_{t90,cnctr}$ = 0.7

– Kerto-S: $k_{t,cnctr}$ = 1.7, $k_{v,cnctr}$ = 0.7 , $k_{t90,cnctr}$ = 0.7

– Kerto-Q: $k_{t,cnctr}$ = 1.7, $k_{v,cnctr}$ = 1.0 , $k_{t90,cnctr}$ = 0.7.

Table 13. The calculated capacities and test results of the glulam series with double-shear dowelled connections. Symbols: see List of Symbols.

Series name	ρ_m kg/m^3	DF EC5	F_{Rm} kN	F_{Sm} kN	F_{Bm} kN	F_{Tm} kN	$\boldsymbol{F_{NEW,m}}$ kN	DF New	F_{max} mean kN	F_{max} CoV %	TF	$\boldsymbol{F_{max}}$ / $\boldsymbol{F_{NEWm}}$	F_{max} / F_{Bm}
Timber-Steel-Timber, Dowel diameter 12 mm													
GL28h, t_1 = 42 mm, d = 12 mm, Dowel strength cl. 8.8, measured f_{ym} = 720 MPa, F_{Rk} = 520 kN													
GL_TST_d12_12x2	466	p	579	397	385	459	**393**	sple,t	424	8.3	b	**1.08**	1.10
GL_TST_d12_8x3	460	p	574	422	409	487	**414**	sple,t	504	11.6	b	**1.22**	1.23
GL_TST_d12_6x4	474	p	585	452	430	511	**473**	sple,t	529	4.4	b	**1.12**	1.23
GL_TST_d12_4x6	464	p	577	464	415	525	**610**	sh,t	571	6.2	b	**0.94**	1.38
Steel-Timber-Steel, Dowel diameter 12 mm													
GL28h, t_2 = 90 mm, d = 12 mm, dowel strength cl. 8.8, measured f_{ym} = 720 MPa, F_{Rk} = 576 kN													
GL_STS_d12_12x2	462	b-r	635	424	459	567	**490**	spe,t	537	2.8	b	**1.10**	1.17
GL_STS_d12_8x3	475	b-r	644	490	459	567	**579**	spe,t	646	7.4	b	**1.11**	1.41
GL_STS_d12_6x4	447	b-t	625	411	472	572	**609**	sh,t	606	10.1	b	**0.99**	1.28
GL_STS_d12_4x6	467	b-t	638	438	479	582	**602**	sh,t	552	6.0	b	**0.92**	1.15
GL_STS_d12_3x8	466	b-t	638	490	575	693	**716**	sple,t	660	1.5	row	**0.92**	1.17
Timber-Steel-Timber, Dowel diameter 8 mm													
GL28h, t_1 = 28 mm, d = 8 mm, dowel strength cl. 10.9, measured f_{ym} = 1010 MPa, F_{Rk} = 279 kN													
GL_TST_d8_12x2	472	p	314	217	191	222	**243**	sh,t	266	5.6	b	**1.09**	1.39
GL_TST_d8_6x4	425	p	296	232	214	250	**248**	spe,t	238	17.7	b	**0.96**	1.11
Steel-Timber-Steel, Dowel diameter 8 mm													
GL28h, t_2 = 60 mm, d = 8 mm, dowel strength cl. 10.9, measured f_{ym} = 1010 MPa, F_{Rk} = 318 kN													
GL_STS_d8_12x2	468	b-r	355	237	212	264	**273**	sh,t	295	21.6	b	**1.08**	1.39
GL_STS_d8_6x4	462	b-t	353	232	219	264	**307**	sh,t	299	4.8	(*	**0.97**	1.37

*) the dominating failure mode is unclear

Table 14. The calculated capacities and test results of the Kerto-S LVL series with double-shear dowelled connections. Symbols: see List of Symbols.

Series name	ρ_m kg/m^3	DF EC5	F_{Rm} kN	F_{Sm} kN	F_{Bm} kN	F_{Tm} kN	$\boldsymbol{F_{NEWm}}$ kN	DF NEW	F_{max} mean kN	F_{max} CoV %	TF	F_{max} / F_{NEW}	F_{max} / F_{Bm}
Timber-Steel-Timber, Dowel diameter 12 mm													
Kerto-S, t_1 = 39 mm, d = 12 mm, Dowel strength cl. 8.8, measured f_{ym} = 720 MPa, F_{Rk} = 563 kN													
KS_TST_d12_12x2	499	p	594	397	395	506	**361**	sh,t	400	7.9	b	**1.11**	1.01
KS_TST_d12_8x3	492	p	588	420	414	528	**408**	sh,t	460	6.8	b	**1.13**	1.11
KS_TST_d12_6x4	512	p	603	456	449	572	**467**	sh,t	507	6.1	b	**1.09**	1.13
KS_TST_d12_4x6	488	s/r	586	462	649	711	**586**	sh,t	598	0.8	b	**1.02**	0.92
Steel-Timber-Steel, Dowel diameter 12 mm													
Kerto-S, t_2 = 75 mm, d = 12 mm, Dowel strength cl. 8.8, measured f_{ym} = 720 MPa, F_{Rk} = 665 kN													
KS_STS_d12_12x2	523	b-r	722	483	459	719	**450**	sh,t	500	5.2	b	**1.11**	1.09
KS_STS_d12_8x3	527	b-r	726	534	387	662	**530**	sh,t	568	0.8	b	**1.07**	1.47
KS_STS_d12_6x4	537	s/r	736	527	692	719	**600**	sh,t	591	7.1	b	**0.98**	0.85
KS_STS_d12_4x6	556	s/r	753	562	673	705	**588**	sh,t	570	4.9	b	**0.97**	0.85
KS_STS_d12_3x8	518	s/r	717	551	807	803	**661**	sh,t	561	7.3	b	**0.85**	0.70
Timber-Steel-Timber, Dowel diameter 8 mm													
Kerto-S, t_1 = 27 mm, d = 8 mm, Dowel strength cl. 10.9, measured f_{ym} = 1010 MPa, F_{Rk} = 303 kN													
KS_TST_d8_12x2	502	p	324	216	199	254	**187**	sh,t	200	7.6	b	**1.07**	1.01
KS_TST_d8_6x4	514	p	328	243	214	269	**232**	sh,t	241	13.0	b	**1.04**	1.13
Steel-Timber-Steel, Dowel diameter 8 mm													
Kerto-S, t_2 = 51 mm, d = 8 mm, Dowel strength cl. 10.9, measured f_{ym} = 1010 MPa, F_{Rk} = 344 kN													
KS_STS_d8_12x2	524	b-r	374	250	220	345	**223**	sh,t	296	2.0	b	**1.34**	1.35
KS_STS_d8_6x4	518	s/r	380	272	333	340	**306**	sh,t	336	2.3	b	**1.10**	1.01

Table 15. The calculated capacities and test results of the Kerto-Q LVL series with double-shear dowelled connections. Symbols: see List of Symbols.

Series name	ρ_m kg/m^3	DF EC5	F_{Rm} kN	F_{Sm} kN	F_{Bm} kN	F_{Tm} kN	$\boldsymbol{F_{NEWm}}$ kN	DF NEW	F_{max} mean kN	F_{max} CoV %	TF	F_{max} / F_{NEW}	F_{max} / F_{Bm}
Timber-Steel-Timber, Dowel diameter 12 mm													
Kerto-Q, t_1 = 39 mm, d = 12 mm, Dowel strength cl. 8.8, F_{Rk} = 542 kN													
KQ_TST_d12_6x4	482	p	561	425	297	586	**504**	b	447	2.1	T	**0.89**	1.51
Steel-Timber-Steel, Dowel diameter 8 mm													
Kerto-Q, t_2 = 51 mm, d = 8 mm, Dowel strength cl. 10.9, F_{Rk} = 333 kN													
KS_STS_d8_12x2	492	b-r	341	228	226	354	**260**	b,T	308	7.0	T	**1.19**	1.36
KS_STS_d8_6x4	501	b-t	348	249	254	350	**315**	b	335	7.3	b,T	**1.07**	1.32

Table 16. The calculated capacities and test results of the Glulam series with multiple-shear dowelled connections. Symbols: see List of Symbols.

Series name	ρ_m kg/m^3	DF EC5	F_{Rm} kN	F_{Sm} kN	F_{Bm} kN	F_{Tm} kN	$\boldsymbol{F}_{NEWm}$ kg/m^3	DF NEW mm	F_{max} mean kN	F_{max} CoV %	TF	$\boldsymbol{F}_{max}$ / $\boldsymbol{F}_{NEWm}$	F_{max} / F_{Bm}
4-Shear, Dowel diameter 12 mm													
GL28h, d = 12 mm, dowel str. cl. 10.9, measured f_{ym} = 933 MPa, t_s = 12 mm, F_{Rk} = 1040 kN (A), 1122 kN (12x2B) 1447 (6x4B)													
GL_4Sh_d12_12x2A	447	p,b-r	1216	833	910	1096	**1008**	spe,t	968	6.9	b,b	**0.96**	1.06
GL_4Sh_d12_12x2B	449	p,b-r	1196	820	965	1096	**999**	spe,t	1084	5.7	b,b	**1.09**	1.12
GL_4Sh_d12_6x4A	463	p,b-r	1240	958	762	1106	**1073**	spe,t	856	5.9	b,b	**0.80**	1.12
GL_4Sh_d12_6x4B	462	p,b-r	1592	1230	798	1106	**1071**	spe,t	1069	6.3	b,b	**1.00**	1.34
4-Shear, Dowel diameter 8 mm													
GL28h, d = 8 mm, dowel strength class10.9, measured f_{ym} = 950 MPa, t_s = 8 mm, F_{Rk} = 558 kN (A), 689 kN (B)													
GL_4Sh_d8_12x2A	447	p,b-r	598	413	435	511	**510**	sh,t	501	20.3	b,b	**0.98**	1.15
GL_4Sh_d8_12x2B	471	b-r,b-r	791	546	468	511	**491**	sh,t	530	4.3	b,b	**1.08**	1.13
GL_4Sh_d8_6x4AZ	458	p,b-r	606	474	366	518	**497**	spe,t	586	6.1	b,b	**1.18**	1.60
GL_4Sh_d8_6x4B	455	b-r,b-r	765	599	388	517	**491**	spe,t	478	15.9	b,b	**0.97**	1.23
GL_4Sh_d8_6x4A	444	p,b-r	596	467	366	518	**500**	spe,t	546	4.5	b,b	**1.09**	1.49
6-Shear, Dowel diameter 8 mm													
GL28h, d = 8 mm, dowel strength class10.9, measured f_{ym} = 950 MPa, t_s = 8 mm, F_{Rk} = 837 kN													
GL_6Sh_d8_12x2	431	p,b-r	879	688	521	786	**798**	sh,t	765	11.7	b,b	**0.96**	1.47

Table 17. The calculated capacities and test results of the Kerto-S LVL series with multiple-shear dowelled connections. Symbols: see List of Symbols.

Series name	ρ_m kg/m^3	DF EC5	F_{Rm} kN	F_{Sm} kN	F_{Bm} kN	F_{Tm} kN	$\boldsymbol{F}_{NEWm}$ kg/m^3	DF NEW mm	F_{max} mean kN	F_{max} CoV %	TF	$\boldsymbol{F}_{max}$ / $\boldsymbol{F}_{NEWm}$	F_{max} / F_{Bm}
4-Shear, Dowel diameter 12 mm													
Kerto-S, d = 12 mm, Dowel strength class 10.9, measured f_{ym} = 933 MPa, F_{Rk} = 1226kN													
KS_4Sh_d12_12x2	525	p,b-r	1314	878	898	1418	**890**	sh,t	898	7.6	b,b	**1.01**	1.00
KS_4Sh_d12_6x4	523	b-t,b-t	1312	993	1065	1418	**1180**	sh,t	1157	1.2	b,b	**0.98**	1.09
4-Shear, Dowel diameter 8 mm													
Kerto-S, d = 8 mm, Dowel strength class 10.9, measured f_{ym} = 950 MPa, F_{Rk} =604kN (A), F_{Rk} = 702 kN (B)													
KS_4Sh_d8_12x2A	538	p,b-r	658	440	431	683	**415**	sh,t	460	8.8	b,b	**1.11**	1.07
KS_4Sh_d8_12x2B	540	b-r,b-r	790	528	468	684	**413**	sh,t	511	2.5	b,b	**1.24**	1.09
KS_4Sh_d8_6x4A	541	b-t,b-t	660	473	466	683	**511**	sh,t	492	1.1	b,b	**0.96**	1.06
KS_4Sh_d8_6x4B	528	b-t,b-t	772	553	504	684	**511**	sh,t	528	2.8	b,b	**1.03**	1.05
6-Shear, Dowel diameter 8 mm													
Kerto-S, d = 8 mm, Dowel strength class 10.9, measured f_{ym} = 950 MPa, F_{Rk} = 906 kN													
KS_6Sh_d8_12x2	550	b-t,b-t	876	627	462	670	**623**	sh,t	729	8.8	b,b	**1.17**	1.58

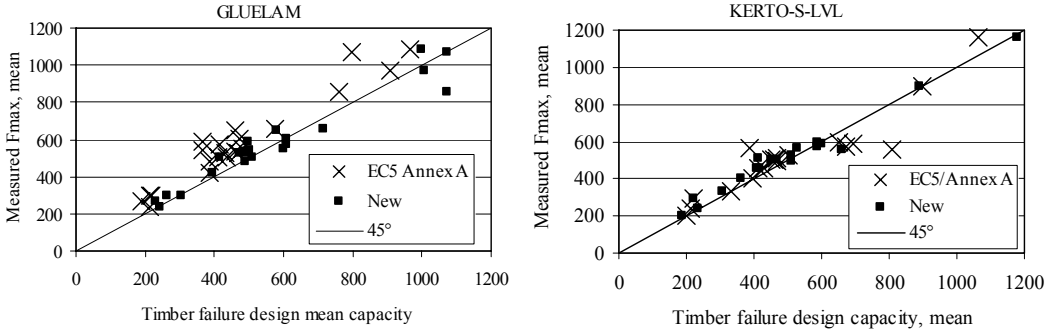

Figure 15. F_{max} plotted against block shear design capacity for Gluelam (left) and LVL (right). Each point is the mean result of one series. (Note that in all four LVL series which are under 45 degree line for the EC5 value, the critical design is not due to block shear but splitting or rowshear.)

4.10 Discussion and conclusions on design method

The proposed design procedure presents a method to design dowelled timber-to-steel connections under tension parallel-to-grain against timber failure mechanisms. The method pursues to distinguish all failure modes and present a sufficiently accurate equation for each one. This methodology chops up the complex failure phenomenon to many rather simple equations which all have reasonable purpose and derivation. Although the method is suitable for hand calculation, the best way to apply it is through a calculation spreadsheet or a small computer program, for which it is extremely suitable, since the method does not require iteration or interpolation.

The method has so far been verified only against the test results of this project for which is fits surprisingly well. More verification calculations would be advantageous but are limited by the small amount of experimental data available. However, the model should be verified properly against situations with only one row of dowels (not included in this project), which would give more insight to its performance in regard to the splitting behaviour. Also experimental results should be used to verify whether the omission of n_{ef} in case of embedment failure is justified, since the present study did not contains this failure either.

5. Conclusions and recommendation

Based on the large experimental data that has been gathered by the loading of more than 150 specimens and 300 connections, the following recommendations can be given for the improvement of the design of dowelled timber-to-steel connections:

- The plug shear failure mechanism does not occur in the connection area contrarily to what the design equations in EC5 (EN 1995-1-1:2004; Annex A) suggest, if the dowels extend through the whole timber thickness. This is due to the fact that the relatively rigid dowels remain straight or bend very little before failure, which is then mostly due to the block shear mechanism. Failure by plug shear would probably require the development of plastic hinges to a high degree, which does not occur at the failure level of block shear. The present design equations in EC5 Annex A assume the fully developed plastic hinges in order to determine the failure mechanism based on the Johansen theory.

- If the mean material property values are substituted in the design equations of EC5, the value of F_{Sm} and F_{Bm}, representing splitting or rowshear failure and block shear or plug shear failure, respectively, are often very close to each other. In many cases the value of F_{Sm} is lower that F_{Bm}. However, in these experimental tests rowshear was observed in only few series. This indicates that the equation for the reduction effect of the number of dowels in a row is too conservative for these connections, because it does not take into account the slenderness of the dowels.

- Connections with cross-veneered Kerto-Q-LVL showed much higher experimental capacities than could be anticipated from the design calculations using the characteristic values in EC5. This is due to the fact that the plug shear failure does not occur because of rigid dowels and because the low flatwise shear strength reduces the calculational capacity dramatically in case of plug shear.

- When the calculational failure mode of EC5 is block shear (b-r, b-t) it can be concluded that the formulas result usually in clearly conservative design for glulam, but they are approximately on the right level for Kerto-

S-LVL. Higher coefficients (instead of 1.5 and 0.7) could therefore be used for glulam in Eq. (2). However, the following additional condition should be given for the failure mode b-r (block-shear with shear capacity higher than tension): it works only if the edge distance a_3 is sufficiently large so that the tensile capacity of the outermost timber strips is enough to carry the whole failure load. It is apparent that, in most block shear failure cases, a simultaneous combination of tensile and shear stress is acting.

- The proposed design procedure presents a method to design dowelled timber-to-steel connections under tension parallel-to-grain against timber failure mechanisms in a way that takes into account the above.

- The method distinguish all failure modes and present a sufficiently accurate equation for each one. This methodology chops up the complex failure phenomenon to many but simple equations which all have reasonable purpose and derivation. The method is suitable for hand calculation, but the best way to apply it is through a calculation spreadsheet or program.

Acknowledgements

This work was financed by The Technology Agency of Finland, Finnforest Oyj, Versowood Oyj, SPU-Systems Oy, LATE-Rakenteet Oy, Exel Oyj and VTT which is gratefully acknowledged.

References

Anon. 2004. Tutkintaselostus. Messuhallin katon romahtaminen Jyväskylässä 1.2.2003. (Fair centre roof collapsing in Jyväskylä, Finland, on 1 Feb 2003.) Accident Investigation Report. Accident Investigation Board of Finland Report B 2/2003 Y.

Hilson, B.O. 1995. Joints with dowel type fasteners – Theory. STEP Lecture C3. In: Blass, H.J., Aune, P., Choo, B.S., Görlacher, R., Griffiths, D.R., Hilson, B.O., Racher P. and Steck G. (Eds.): Timber Engineering STEP 1. Basis of design, material properties, structural components and joints. Centrum Hout, The Netherlands.

Johansen, K.W. 1949. Theory of timber connections. International Association of Bridge and Structural Engineering. Bern. Publication No. 9. Pp. 249–262.

Jorissen, A. 1998. Double shear timber connection with dowel type fasteners. Ph.D. Thesis, Delft University Press, Delft, Netherlands.

Ranta-Maunus, A. and Keverinmäki, A. 2003. Reliability of timber structures, theory and dowel-type connection failures. CIB-W18/36-7-11, Colorado, USA, August 2003.

Sjödin, J. and Serrano, E. 2006. A numerical study of the effects of stresses induced by moisture gradients in steel-to-timber dowel joint. Holzforschung, Vol. 62, Issue 2.

Appendix A: Calculation example Gluelam

Example of calculation (GL_TST_d12_6x4 series)

As an example of the calculation method, the capacity against timber failure mechanisms of series GL_TST_d12_6x4 is shown below. The connection parameters are listed in Table B1. The glulam class is GL28h, with ρ_k = 410 kg/m^3, $f_{t,k}$ = 19.5 MPa, $f_{v,k}$ = 3.2 MPa, f_{t90k} = 0.45 MPa. (The capacities according to current design methods can be seen in Table 7.)

Table A1. The listed connection parameters.

nxm	d	t1	B	ts	a1	a2	a3	a4
	mm	mm	mm	mm	mm	mm	mm	mm
6x4	12	42	266	12	114	38	114	76

Division of connection area to parts

As a first step, the connection area is divided into parts j = 0…4 according to the possible failure surfaces as shown in Fig. A1.

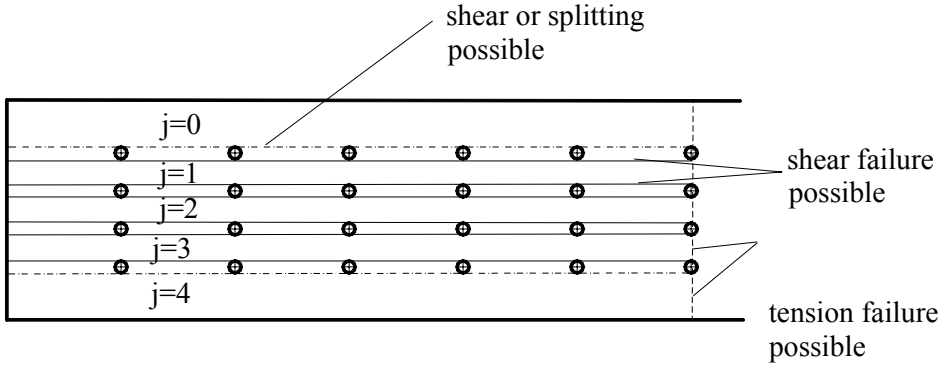

Figure A1. Division of connection area to parts.

Effect of load distribution between dowels

Effect of load distribution between dowels is taken into account by n_{ef}

$$n_{ef} = n^{0.9} = 6^{0.9} = 5{,}02 \tag{A1}$$

The reduction is applied to all brittle failure modes: tension, shear and splitting, but *not* to embedment failure.

Effect of dowel deformations (slenderness)

The slenderness of the dowels is taken into account by reducing the timber thickness, but only when considering shear and splitting, not parallel-to-grain tension. d_{gr} is calculated first and then t_{red}. (It is the limit above which the dowel is rigid according to the Johansen theory.) When calculating d_{gr}, the mean embedment strength $f_{h,k}$ should be taken as 1.5 times the characteristic value $f_{h,k}$ and the mean yield strength of $f_{y,m}$ of dowels as the nominal yield strength (here: $f_{h,m}$ = 1.5 · 29.6 MPa = 44.4 MPa and $f_{y,m}$ = 0.8 · 800 MPa = 640 MPa for dowel strength class 8.8).

$$d_{gr,1} = 2.45\sqrt{\frac{f_{h,m}}{f_{y,m}}}\,t_1 = 2.45\sqrt{\frac{1.5 f_{h,k}}{f_{y,nominal}}}\,t_1 = 2.45\sqrt{\frac{44.4\ \text{MPa}}{640\ \text{MPa}}}\,42\ \text{mm} = 27.1\ \text{mm} \tag{A2, 3, 4}$$

$$t_{1,red} = \min\left(1, \frac{d}{0.6\, d_{gr,1}}\right) t_1 = \min\left(1, \frac{12\ \text{mm}}{0.6\ \ 27.1\ \text{mm}}\right) 42\text{mm} = 31.0\text{mm}$$

$$t_{red} = 2t_1 = 62.0\text{mm}, \ \text{(two side members)}$$

Calculation of capacity of inner parts

When calculating the capacity of the inner parts (in the example case j = 1…m-1 = 1…3), the following areas are calculated first:

– embedment failure area $A_{h,j} = n\ d\ t$ = 6 · 12 mm · 84 mm = 6048 mm^2

– tension failure area $A_{t,j} = (a_2 - d)\ t$ = (38 mm - 12 mm) · 84 mm = 2184 mm^2

– shear failure area $A_{v,j} = 2\,[(n–1)a_1 + a_3]\,t_{red} = 2 \cdot [(6\text{-}1)\ 114\text{mm} + 114\ \text{mm}\ ] \cdot 62\ \text{mm} = 84800\ \text{mm}^2$.

Embedment failure

The embedment capacity of the inner parts:

$$F_{h,j,k} = A_{h,j} f_{h,k} = 6048\ mm^2\ 29.6\ N/mm^2 = 178900\ N \qquad \text{(A5)}$$

Tension failure

The tension capacity:

$$F_{t,j,k} = k_{t,cnctr}\ (n_{ef}/n) A_{t,i} f_{t,0,k} = 2.0(5.02/6)\ 2184\ mm \cdot 19.5 N/mm^2 = 71200 N \qquad \text{(A6)}$$

Shear failure

The shear capacity:

$$F_{v,j,k} = k_{v,cnctr}\ (n_{ef}/n) A_{v,j} f_{v,k} = 1.0(5.02/6) \cdot 84800 mm^2 \cdot 3.2 N/mm^2 = 226900 N \qquad \text{(A7)}$$

Interaction of tension and shear

The tension stress and shear stress interaction effect on capacity is taken into account in the [subscripts 1 => t, 2 => v and $F_{t,j,k} < F_{v,j,k}$].

$$F_{t+v,jk} = F_{t,j,k}\left(1 - k_{interaction}\frac{F_{t,j,k}}{F_{v,j,k}}\right) = 71200 N/mm^2\left(1 - 0.3\frac{71200}{226900}\right) = 64500 N/mm^2 \qquad \text{(A8)}$$

Capacity of the inner part

The capacity of all inner parts is obtained as the smaller of the embedment strength and the combined effect of tension and shear:

$$F_{j,k} = \min\left(F_{h,j,k}, F_{t+v,j,k}\right) = 64500 N/mm^2 \qquad \text{(A9)}$$

Calculation of capacity of outer parts

When calculating the capacity of the outer parts (in the example case $j = 0$ and $j = m = 4$), the following areas are calculated first:

- embedment failure area $A_{h,j} = n\ 0.5\ d\ t = 6 \cdot 0{,}5 \cdot 12\ \text{mm} \cdot 2 \cdot 42\ \text{mm} = 3024\ \text{mm}^2$
- tension failure area $A_{t,j} = (a_4 - d/2)\ t = (76\text{mm-}12/2\ \text{mm}) \cdot 2 \cdot 42\ \text{mm} = 5880\ \text{mm}^2$
- shear failure area $A_{v,j} = [(n-1)a_1 + a_3]\ t_{red} = [(6\text{-}1)\ 114\text{mm} + 114\ \text{mm}\ ] \cdot 62\ \text{mm} = 42400\ \text{mm}^2$.

Embedment failure

The embedment capacity of the outer parts:

$$F_{h,j,k} = A_{h,j} f_{h,k} = 3024\ mm^2\ 29.6\ N/mm^2 = 89500\ N \qquad \text{(A10)}$$

Tension failure

The tension capacity is calculated (factor $k_{t,outer} = 1/(1+A_{t,j}/A_{v,j}) = 0.88$):

$$F_{t,j,k} = k_{t,cnctr} k_{t,outer}\ (n_{ef}/n) A_{t,i} f_{t,0,k} = 2.0 \cdot 0.88 \cdot (5.02/6)\ \ 5880\ mm \cdot 19.5 N/mm^2 = 168400 N \qquad \text{(A11)}$$

Shear failure

The shear capacity:

$$F_{v,j,k} = k_{v,cnctr}\ (n_{ef}/n) A_{v,j} f_{v,k} = 1.0(5.02/6) \cdot 42400 mm^2 \cdot 3.2 N/mm^2 = 113400 N \qquad \text{(A12)}$$

Interaction of tension and shear

The interaction of tension and shear stresses is taken into account similarly as for the inner parts [subscripts 1 => v, 2 => t and $F_{v,j,k} < F_{t,j,k}$].

$$F_{t+v,j,k} = F_{v,j,k}\left(1 - k_{interaction}\frac{F_{v,j,k}}{F_{t,j,k}}\right) = 113400 N/mm^2\left(1 - 0.3\frac{113400}{168400}\right) = 90500 N/mm^2 \qquad \text{(A13)}$$

Splitting failure

For consideration of the splitting of the outer parts, the effect of geometry for two different ways of splitting are considered:

– splitting originating at the dowel hole nearest to the end of the timber
– splitting originating at the end of the timber.

$$s_{\mathrm{t90,hole}} = \max\left(1\,,\, 0.65\, a_3 / a_4\right) = 1 \qquad \text{(A14,15)}$$
$$s_{\mathrm{t90,end}} = 2.7 / \cosh\left(a_3 / a_4 - 1.4\right) = 2.69$$

The splitting capacities are:

$$F_{\mathrm{splhole,j,k}} = k_{t90,cnctr}\, n_{\mathrm{ef}}\, 10\, f_{\mathrm{t,90,k}}\, t_{red}\, a_3 / s_{\mathrm{t90,hole}} = \qquad \text{(A16,17)}$$
$$0.7 \cdot 5.02 \cdot 10 \cdot 0.45 N/mm^2\, 62mm \cdot 114mm / 1 = 111700N$$

$$F_{\mathrm{splend,j,k}} = k_{t90,cnctr}\, n_{\mathrm{ef}}\, 10\, f_{\mathrm{t,90,k}}\, t_{red}\, a_3 / s_{\mathrm{t90,end}} =$$
$$0.7 \cdot 5.02 \cdot 10 \cdot 0.45 N/mm^2\, 62mm \cdot 114mm / 2.69 = 41600N$$

Interaction of shear and splitting at the dowel hole

The shear stress and splitting stress interaction effect on capacity

$$F_{\mathrm{v+splhole,j,k}} = F_{\mathrm{splhole,j,k}} \left(1 - k_{\mathrm{interaction}} \frac{F_{\mathrm{splhole,j,k}}}{F_{\mathrm{v,j,k}}}\right) = \qquad \text{(A18)}$$
$$111700N/mm^2 \left(1 - 0.3 \frac{113400}{111700}\right) = 78700N/mm^2$$

Capacity of the outer part

The capacity of the outer parts (j = 0.4) is obtained as the smallest capacity:

$$F_{\mathrm{j,k}} = \min\left(F_{\mathrm{h,j,k}}\,, F_{\mathrm{t+v,j,k}}\,, F_{\mathrm{v+splhole,j,k}}\,, F_{\mathrm{splend,j,k}}\right) = 41600N \qquad \text{(A19)}$$

Capacity of whole connection against timber failure

Finally, the capacity of the connection against timber failure is obtained in case of double shear connections as the sum:

$$F_{\mathrm{TFMk}} = \sum_{\mathrm{j}} F_{\mathrm{j,k}} = 276600N \tag{A20}$$

Appendix B: Calculation example, Kerto-S

Example of calculation (KS_TST_d12_6x4 series)

As an example of the calculation method, the capacity against timber failure mechnamisms of series KS_TST_d12_6x4 is shown below. The connection parameters are listed in Table 1. The material is KertoS with ρ_k = 480 kg/m^3, $f_{t,k}$ = 35 MPa, $f_{v,k}$ = 4.1 MPa, f_{t90k} = 0.8 MPa. (The capacities according to current design methods can be seen in Table 8.)

Table B1. The listed connection parameters.

nxm	d	t1	B	ts	a1	a2	a3	a4
	mm	mm	mm	mm	mm	mm	mm	mm
6x4	12	39	204	12	105	38	105	45

Division of connection area to parts

As a first step, the connection area is divided into parts j = 0…4 according to the possible failure surfaces as shown in Fig. B1.

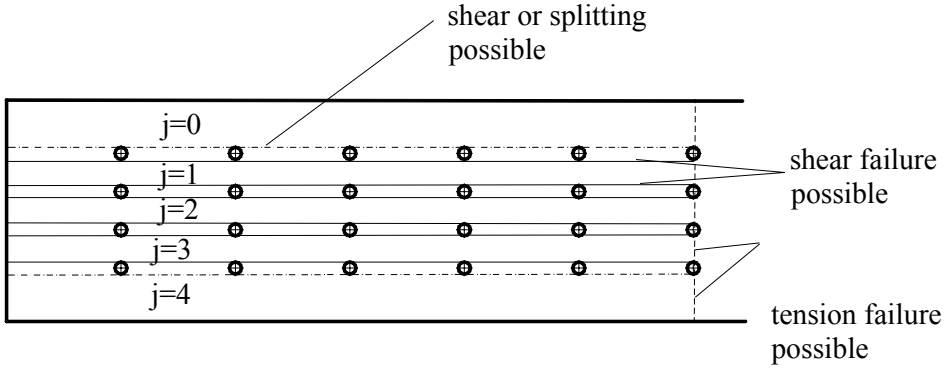

Figure B1. Division of connection area to parts.

Effect of load distribution between dowels

Effect of load distribution between dowels is taken into account by n_{ef}.

$$n_{ef} = n^{0.9} = 6^{0.9} = 5{,}02 \tag{B1}$$

The reduction is applied to all brittle failure modes: tension, shear and splitting, but *not* to embedment failure.

Effect of dowel deformations (slenderness)

The slenderness of the dowels is taken into account by reducing the timber thickness, but only when considering shear and splitting, not parallel-to-grain tension. d_{gr} is calculated first and then t_{red}. (It is the limit, above which the dowel is rigid according to the Johansen theory.) When calculating d_{gr}, the mean embedment strength $f_{h,k}$ should be taken as 1.5 times the characteristic value $f_{h,k}$ and the mean yield strength of $f_{y,m}$ of dowels as the nominal yield strength (here: $f_{h,m}$ = 1.5 · 34.6 MPa = 52.0 MPa and $f_{y,m}$ = 0.8 · 800 MPa = 640 MPa for dowel strength class 8.8).

$$d_{gr,1} = 2.45\sqrt{\frac{f_{h,m}}{f_{y,m}}}\,t_1 = 2.45\sqrt{\frac{1.5 f_{h,k}}{f_{y,nominal}}}\,t_1 = 2.45\sqrt{\frac{52.0\ \text{MPa}}{640\ \text{MPa}}}\,39\ \text{mm} = 27.2\ \text{mm} \tag{B2, 3, 4}$$

$$t_{1,red} = \min\left(1, \frac{d}{0.6\, d_{gr,1}}\right) t_1 = \min\left(1, \frac{12\ \text{mm}}{0.6\ \ 27.2\ \text{mm}}\right) 39\text{mm} = 28.7\text{mm}$$

$$t_{red} = 2t_1 = 57.3\text{mm}, \quad \text{(two side members)}$$

Calculation of capacity of inner parts

When calculating the capacity of the inner parts (in the example case j = 1…m-1 = 1…3), the following areas are calculated first:

– embedment failure area $A_{h,j} = n\ d\ t$ =6 · 12 mm · 78 mm = 5616 mm^2.

– tension failure area $A_{t,j} = (a_2 - d)\, t$ = (38mm–12 mm) · 78 mm = 2028 mm^2

– shear failure area $A_{v,j} = 2\,[(n-1)a_1 + a_3]\, t_{red}$ = 2 · [(6–1) 105mm +105 mm] · 57.3 mm = 72200 mm^2.

Embedment failure

The embedment capacity of the inner parts:

$$F_{h,j,k} = A_{h,j} f_{h,k} = 5616\ mm^2\ 34.6\ N/mm^2 = 194500\ N \qquad \text{(B5)}$$

Tension failure

The tension capacity:

$$F_{t,j,k} = k_{t,cnctr}\,(n_{ef}/n) A_{t,i} f_{t,0,k} = 1.7(5.02/6)\ 2028\ mm \cdot 35 N/mm^2 = 118700 N \qquad \text{(B6)}$$

Shear failure

The shear capacity:

$$F_{v,j,k} = k_{v,cnctr}\,(n_{ef}/n) A_{v,j} f_{v,k} = 0.7(5.02/6) \cdot 72200 mm^2 \cdot 4.1 N/mm^2 = 247500 N \qquad \text{(B7)}$$

Interaction of tension and shear

The tension stresses and shear stresses are assumed to have an interaction effect on capacity, which is taken into account by [subscripts 1 => t, 2 => v and $F_{t,j,k} < F_{v,j,k}$].

$$F_{t+v,jk} = F_{t,j,k}\left(1 - k_{interaction}\frac{F_{t,j,k}}{F_{v,j,k}}\right) = 118700 N/mm^2\left(1 - 0.3\frac{118700}{247500}\right) = 101600 N/mm^2 \qquad \text{(B8)}$$

Capacity of the inner part

The capacity of all inner parts is obtained as the smaller of the embedment strength and the combined effect of tension and shear:

$$F_{\mathrm{j,k}} = \min\left(F_{\mathrm{h,j,k}}, F_{\mathrm{t+v,j,k}}\right) = 64500 N/mm^2 \qquad \text{(B9)}$$

Calculation of capacity of outer parts

When calculating the capacity of the outer parts (in the example case $j = 0$ and $j = m = 4$), the following areas are calculated first:

- embedment failure area $A_{\mathrm{h,j}} = n\ 0.5\ d\ t = 6 \cdot 0{,}5 \cdot 12\ \mathrm{mm} \cdot 2 \cdot 39\ \mathrm{mm} = 2808\ \mathrm{mm}^2$
- tension failure area $A_{\mathrm{t,j}} = (a_4 - d/2)\ t = (76\mathrm{mm} - 12/2\ \mathrm{mm}) \cdot 2 \cdot 39\ \mathrm{mm} = 3042\ \mathrm{mm}^2$
- shear failure area $A_{\mathrm{v,j}} = [(n-1)a_1 + a_3]\ t_{red} = [(6-1)\ 105\mathrm{mm} + 105\ \mathrm{mm}\ ] \cdot 57.3\ \mathrm{mm} = 36100\ \mathrm{mm}^2$.

Embedment failure

The embedment capacity of the outer parts:

$$F_{\mathrm{h,j,k}} = A_{\mathrm{h,j}} f_{\mathrm{h,k}} = 2808\ mm^2\ 34.6\ N/mm^2 = 97300\ N \qquad \text{(B10)}$$

Tension failure

The tension capacity is calculated (factor $k_{\mathrm{t,outer}} = 1/(1+A_{\mathrm{t,j}}/A_{\mathrm{v,j}}) = 0.92$):

$$F_{\mathrm{t,j,k}} = k_{t,cnctr}\, k_{t,outer}\, (n_{\mathrm{ef}}/n) A_{\mathrm{t,i}} f_{t,0,k} = 1.7 \cdot 0.92 \cdot (5.02/6)\ \ 3042\ mm \cdot 35 N/mm^2 = 164200 N \qquad \text{(B11)}$$

Shear failure

The shear capacity:

$$F_{\mathrm{v,j,k}} = k_{v,cnctr}\, (n_{\mathrm{ef}}/n) A_{\mathrm{v,j}} f_{\mathrm{v,k}} = 0.7 (5.02/6) \cdot 36100 mm^2 \cdot 4.1 N/mm^2 = 123700 N \qquad \text{(B12)}$$

Interaction of tension and shear

The interaction of tension and shear stresses are taken into account similarly as for the inner parts [subscripts 1 => v, 2 => t and $F_{v,j,k} < F_{t,j,k}$].

$$F_{t+v,j,k} = F_{v,j,k}\left(1 - k_{interaction}\frac{F_{v,j,k}}{F_{t,j,k}}\right) = 123700N/mm^2\left(1 - 0.3\frac{123700}{164200}\right) = 95800N/mm^2 \quad \text{(B13)}$$

Splitting failure

For consideration of the splitting of the outer parts, the effect of geometry for two different ways of splitting are considered:

- splitting originating at the dowel hole nearest to the end of the timber
- splitting originating at the end of the timber.

$$s_{t90,hole} = \max\left(1\,,\, 0.65\,a_3/a_4\right) = 1.52 \quad \text{(B14, 15)}$$
$$s_{t90,end} = 2.7/\cosh\left(a_3/a_4 - 1.4\right) = 1.84$$

The splitting capacities are:

$$F_{splhole,j,k} = k_{t90,cnctr}\, n_{ef}\, 10 f_{t,90,k}\, t_{red}\, a_3/s_{t90,hole} = \quad \text{(B16, 17)}$$
$$0.7 \cdot 5.02 \cdot 10 \cdot 0.8N/mm^2\, 57.3mm \cdot 105mm/1.52 = 111400N$$

$$F_{splend,j,k} = k_{t90,cnctr}\, n_{ef}\, 10 f_{t,90,k}\, t_{red}\, a_3/s_{t90,end} =$$
$$0.7 \cdot 5.02 \cdot 10 \cdot 0.8N/mm^2\, 57.3mm \cdot 105mm/1.84 = 91900N$$

Interaction of shear and splitting at the dowel hole

The shear stress and splitting stress interaction effect on capacity

$$F_{v+splhole,j,k} = F_{splhole,j,k}\left(1 - k_{interaction}\frac{F_{splhole,j,k}}{F_{v,j,k}}\right) = \quad \text{(B18)}$$
$$111400N/mm^2\left(1 - 0.3\frac{111400}{123700}\right) = 81300N/mm^2$$

Capacity of the outer part

The capacity of the outer part (j = 0, m) is obtained as the smallest capacity:

$$F_{j,k} = \min\left(F_{h,j,k}, F_{t+v,j,k}, F_{v+splhole,j,k}, F_{splend,j,k}\right) = 81300N \quad \text{(B19)}$$

Capacity of whole connection against timber failure

Finally, the capacity of the connection against timber failure is obtained in case of double shear connections as the sum:

$$F_{TFMk} = \sum_{j} F_{j,k} = 467400N \quad \text{(B20)}$$

Appendix C: Load-displacement curves

Double shear glulam series with dowel diameter 12 mm

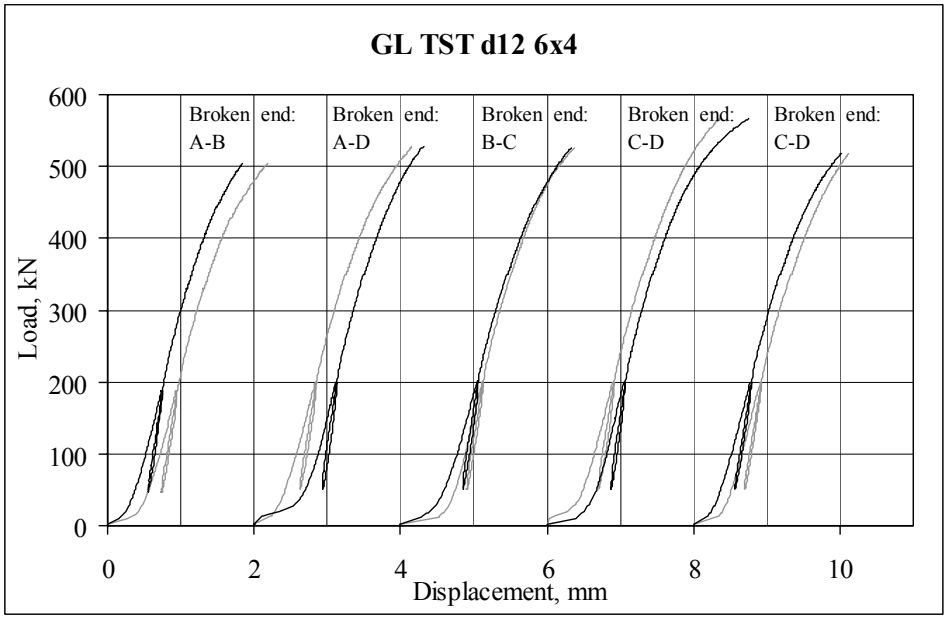

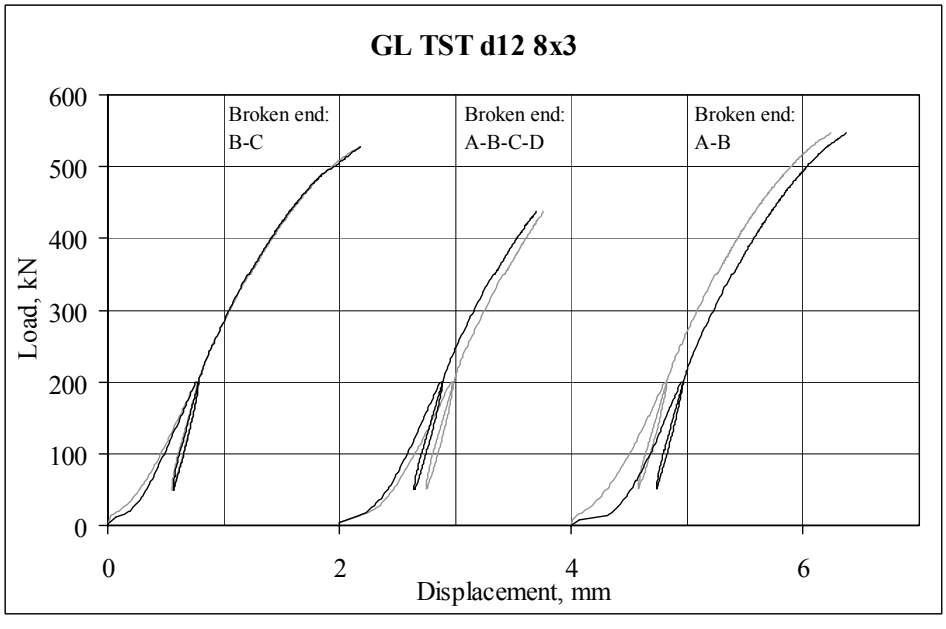

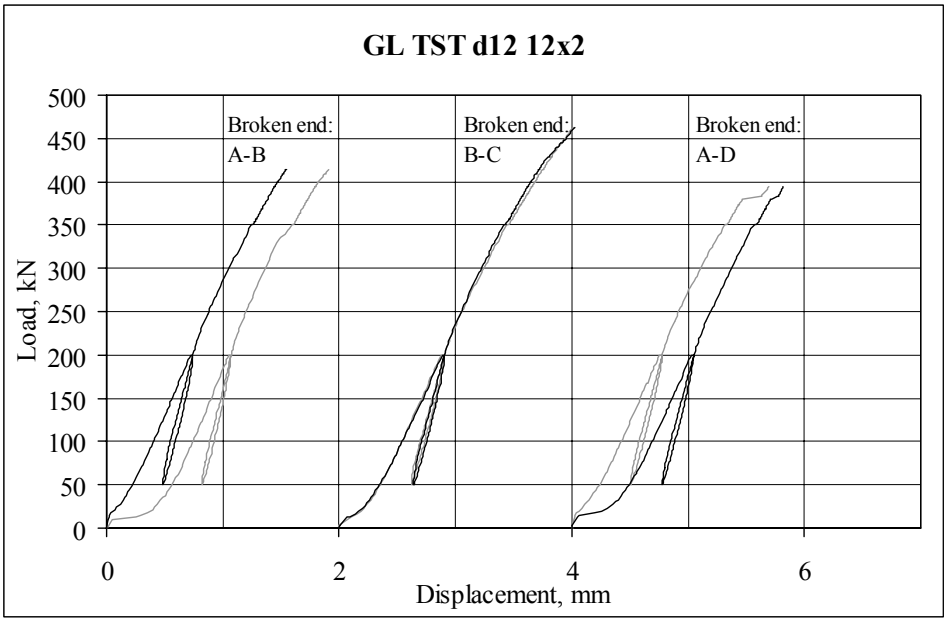
GL TST d12 12x2
Broken end:
A-B
Broken end:
B-C
Broken end:
A-D
Load, kN
Displacement, mm
0
50
100
150
200
250
300
350
400
450
500
0
2
4
6

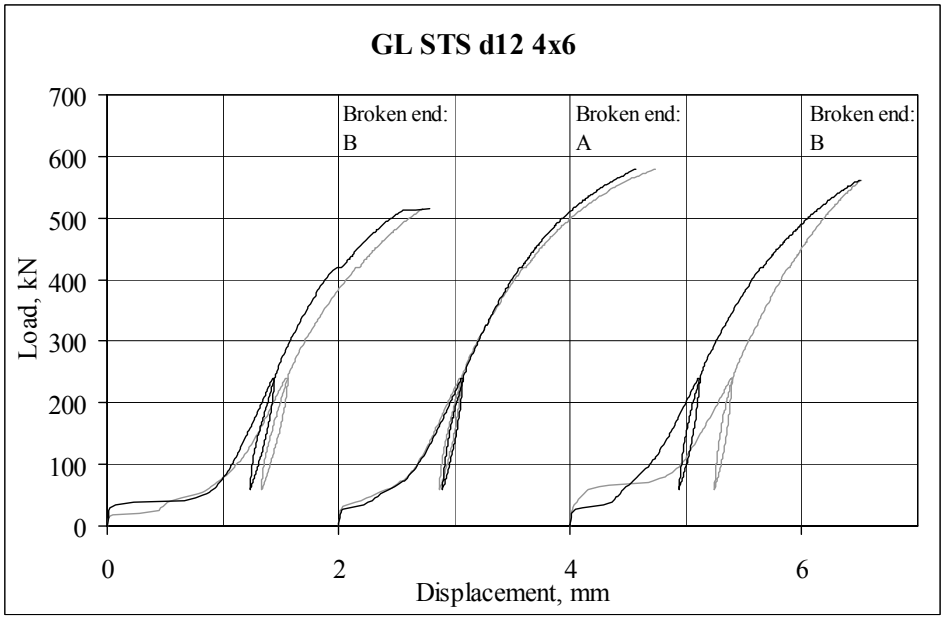
GL STS d12 4x6
Broken end:
B
Broken end:
A
Broken end:
B
Load, kN
Displacement, mm
0
100
200
300
400
500
600
700
0
2
4
6

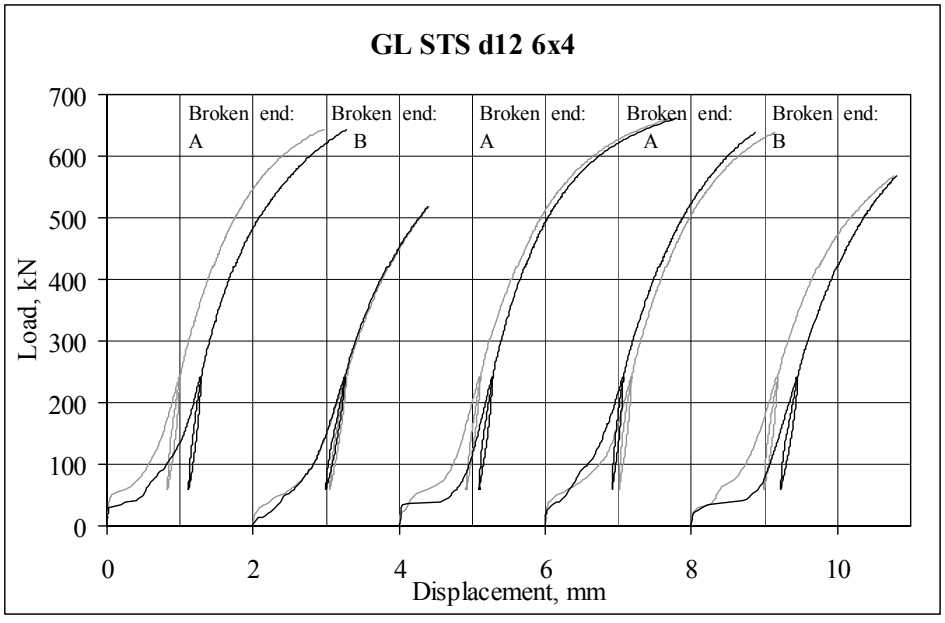
GL STS d12 6x4
Broken end: A
Broken end: B
Broken end: A
Broken end: A
Broken end: B
Load, kN
Displacement, mm
0
100
200
300
400
500
600
700
0
2
4
6
8
10

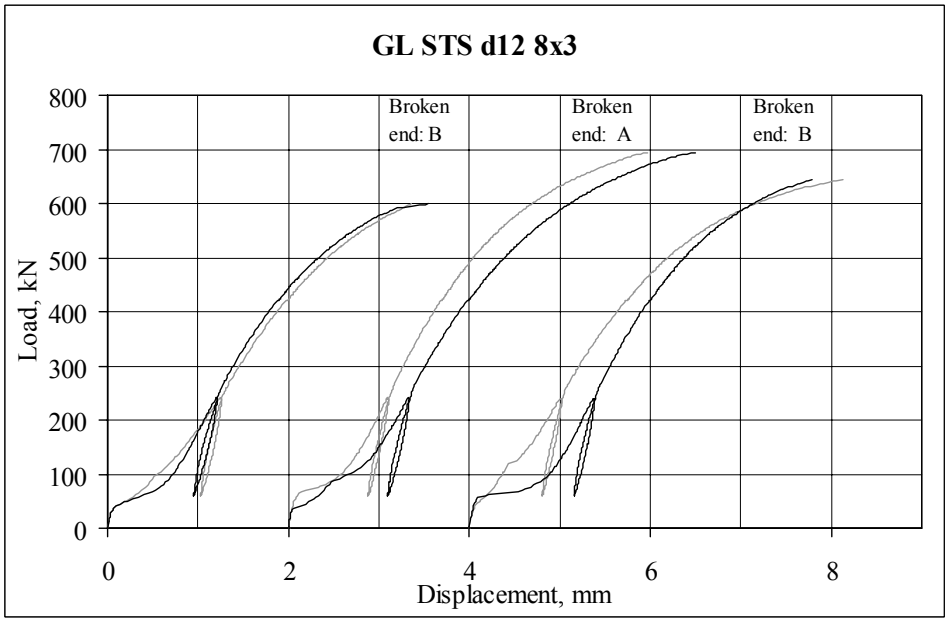
GL STS d12 8x3
Broken end: B
Broken end: A
Broken end: B
Load, kN
Displacement, mm
0
100
200
300
400
500
600
700
800
0
2
4
6
8

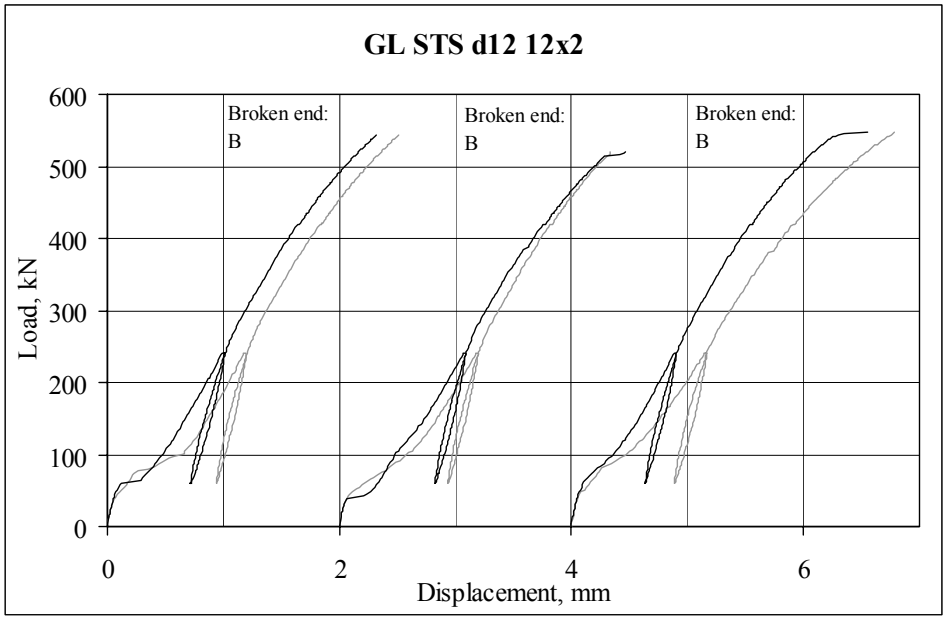
GL STS d12 12x2
Broken end:
B
Broken end:
B
Broken end:
B
600
500
400
300
200
100
0
Load, kN
0
2
4
6
Displacement, mm

Double shear glulam series with dowel diameter 8 mm

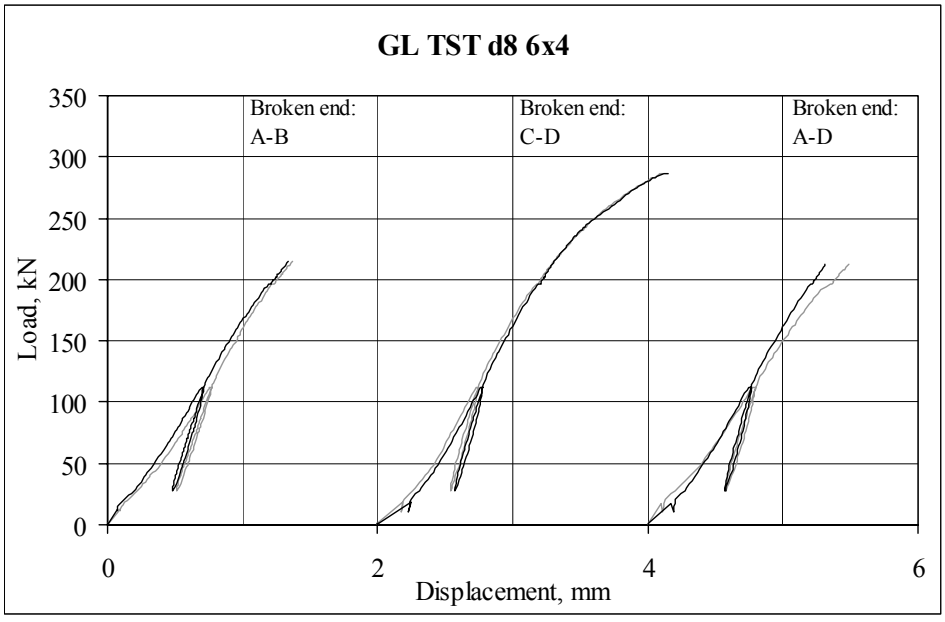

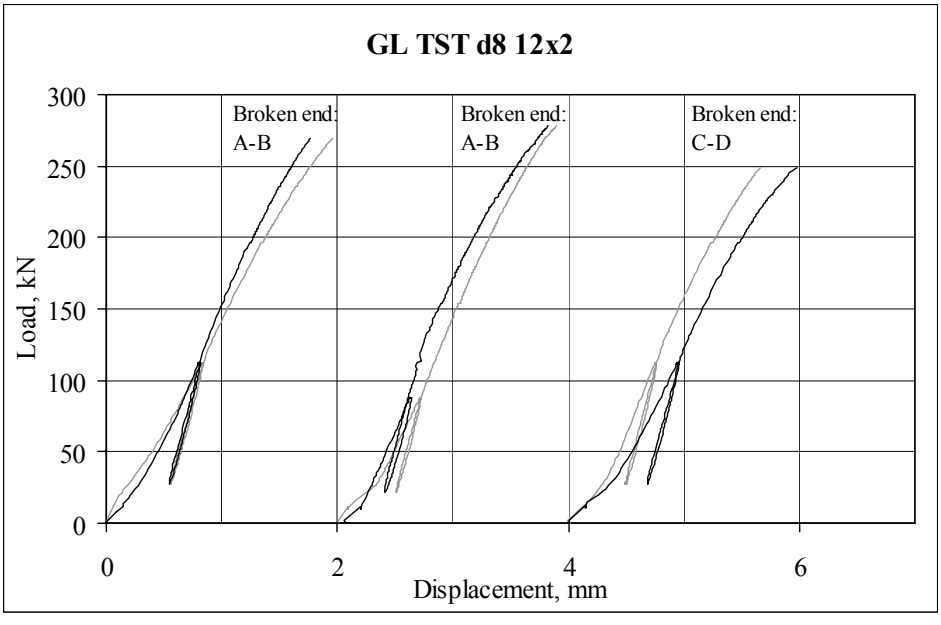

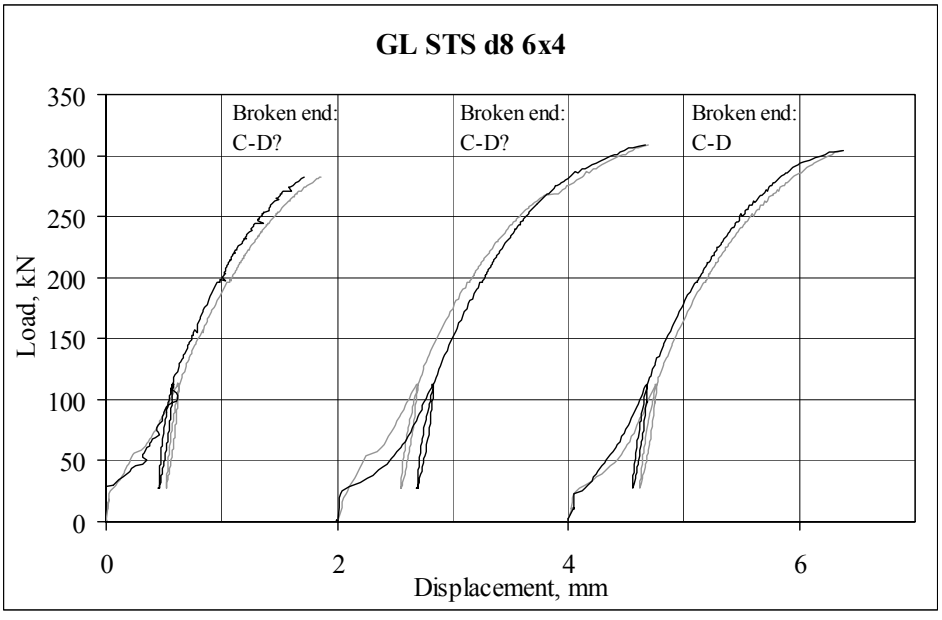
GL STS d8 6x4
Broken end:
C-D?
Broken end:
C-D?
Broken end:
C-D
Load, kN
Displacement, mm
0
50
100
150
200
250
300
350
0
2
4
6

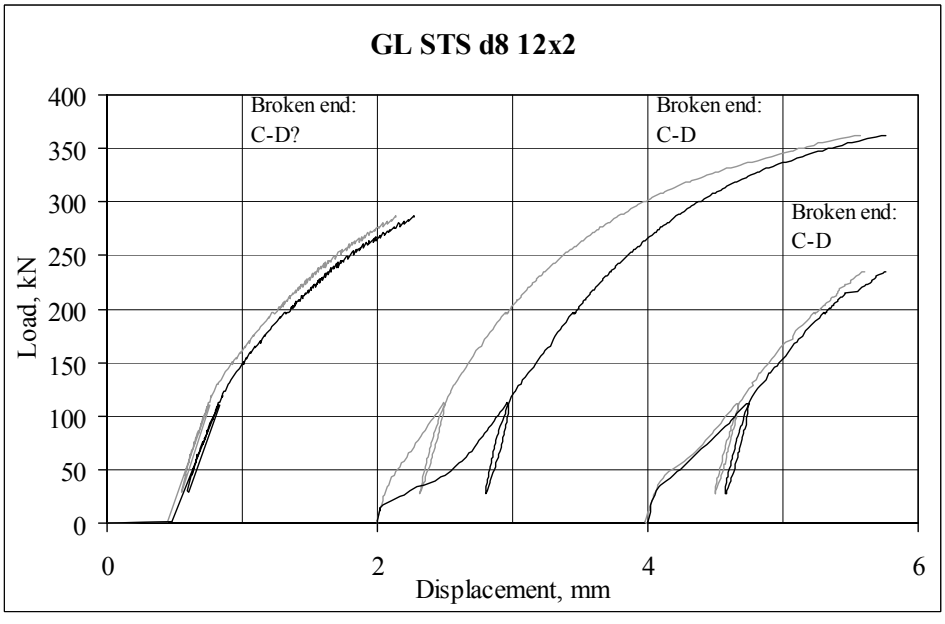
GL STS d8 12x2
Broken end:
C-D?
Broken end:
C-D
Broken end:
C-D
Load, kN
Displacement, mm
0
50
100
150
200
250
300
350
400
0
2
4
6

Double shear Kerto series with dowel diameter 12 mm

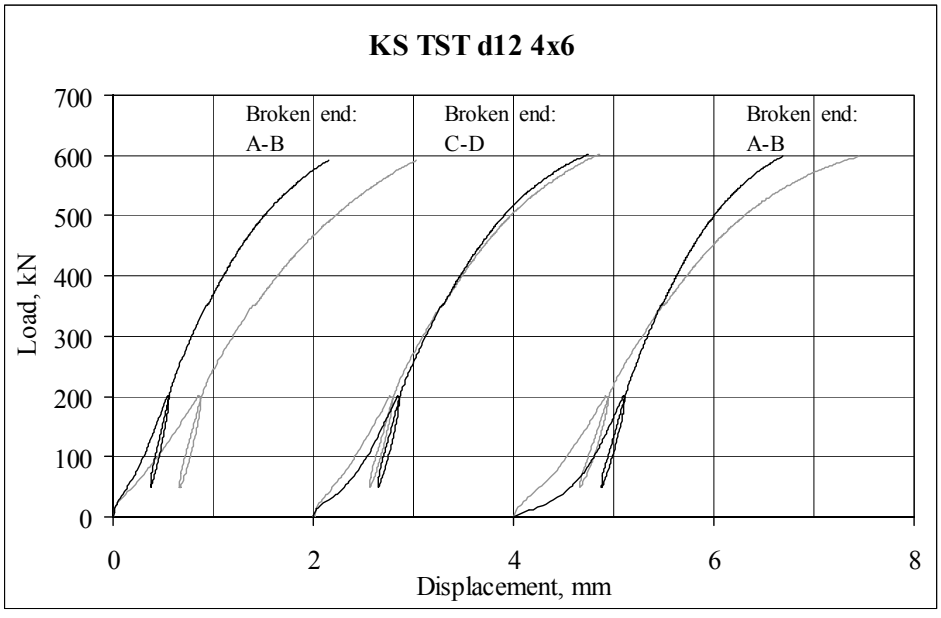

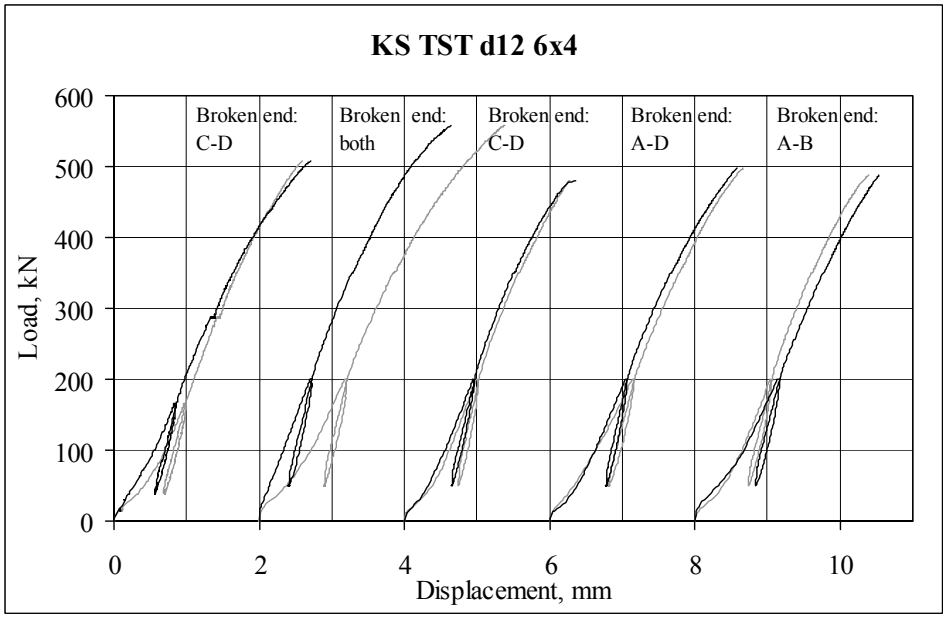

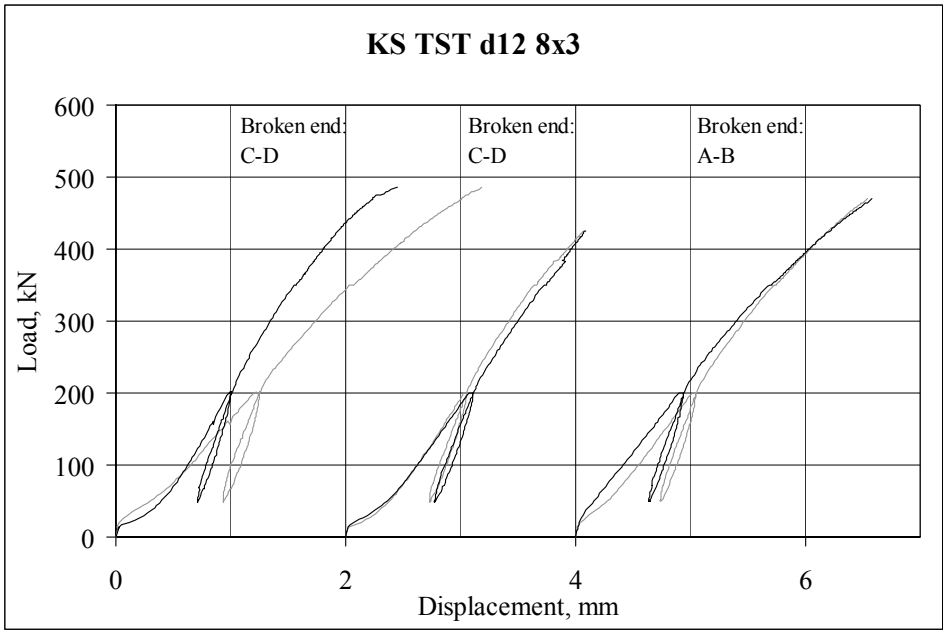
KS TST d12 8x3
Broken end:
C-D
Broken end:
C-D
Broken end:
A-B
Load, kN
600
500
400
300
200
100
0
0
2
4
6
Displacement, mm

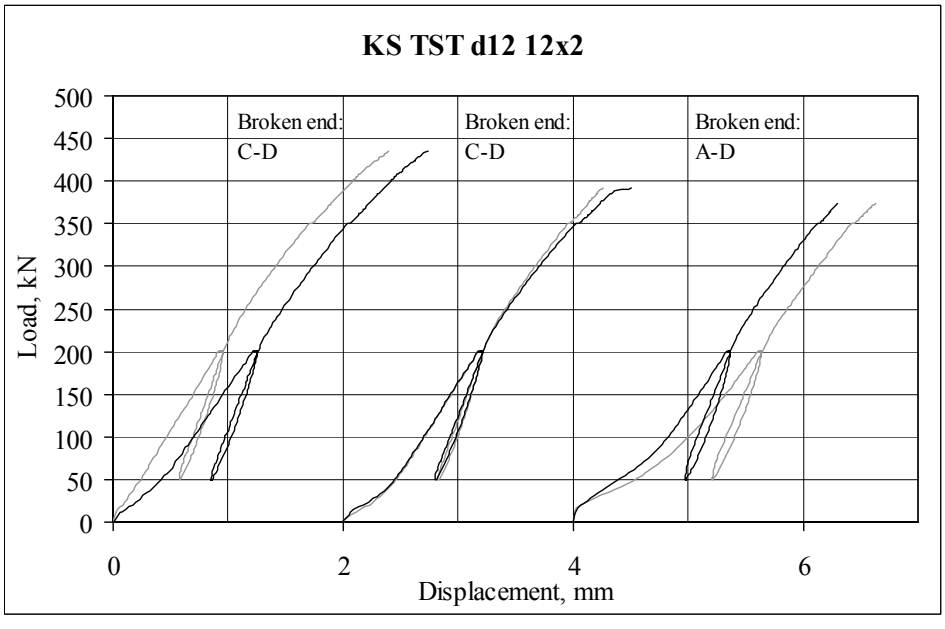
KS TST d12 12x2
Broken end:
C-D
Broken end:
C-D
Broken end:
A-D
Load, kN
500
450
400
350
300
250
200
150
100
50
0
0
2
4
6
Displacement, mm

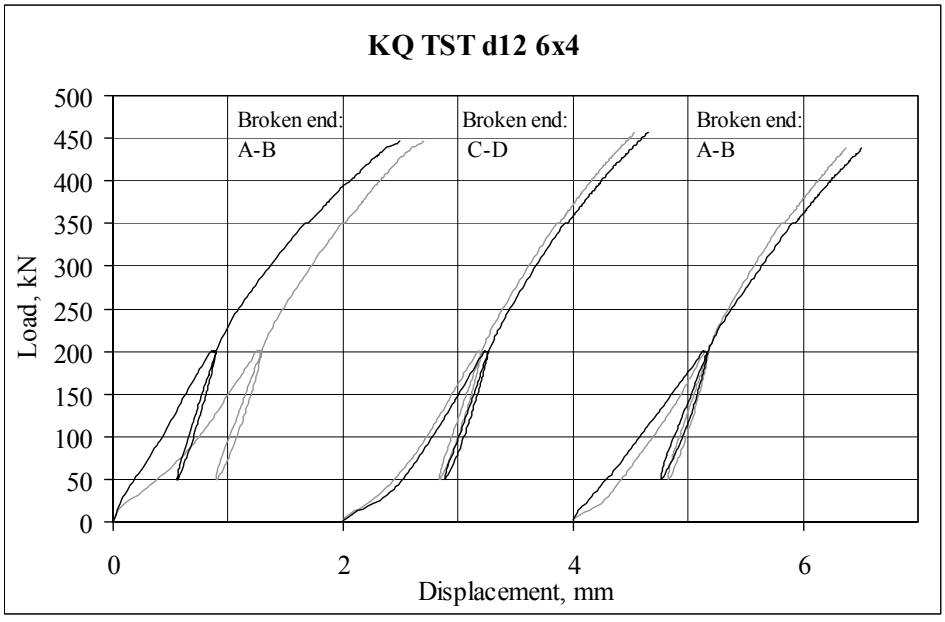
KQ TST d12 6x4
Broken end:
A-B
Broken end:
C-D
Broken end:
A-B
Load, kN
500
450
400
350
300
250
200
150
100
50
0
0
2
4
6
Displacement, mm

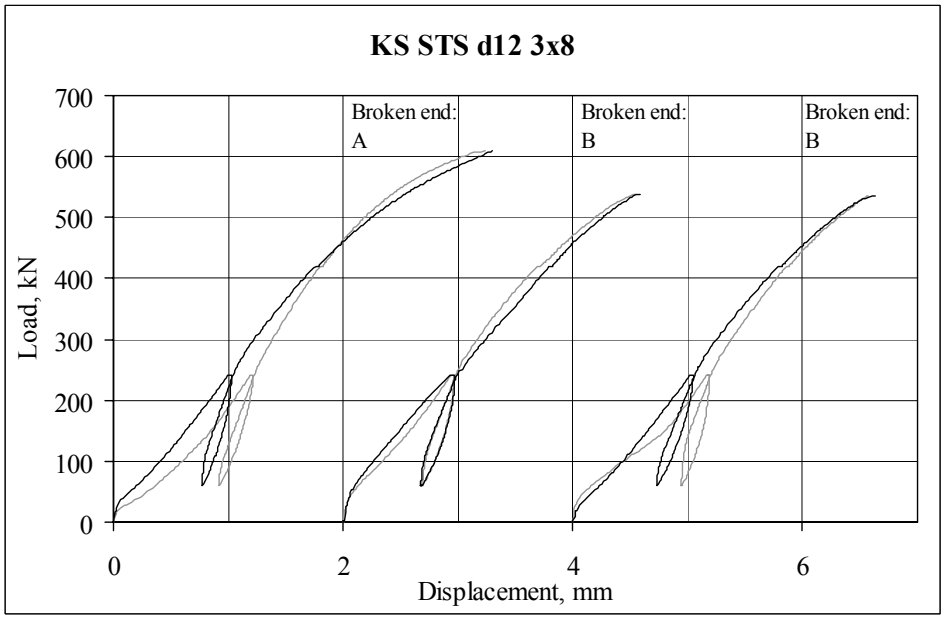
KS STS d12 3x8
Broken end:
A
Broken end:
B
Broken end:
B
Load, kN
700
600
500
400
300
200
100
0
0
2
4
6
Displacement, mm

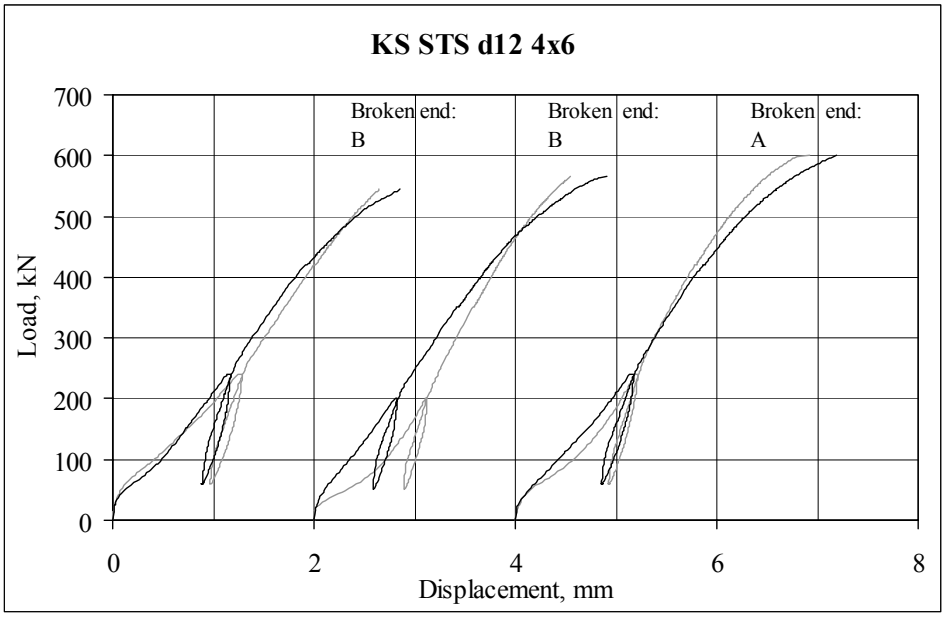
KS STS d12 4x6
Broken end: B
Broken end: B
Broken end: A
Load, kN
Displacement, mm
0
100
200
300
400
500
600
700
0
2
4
6
8

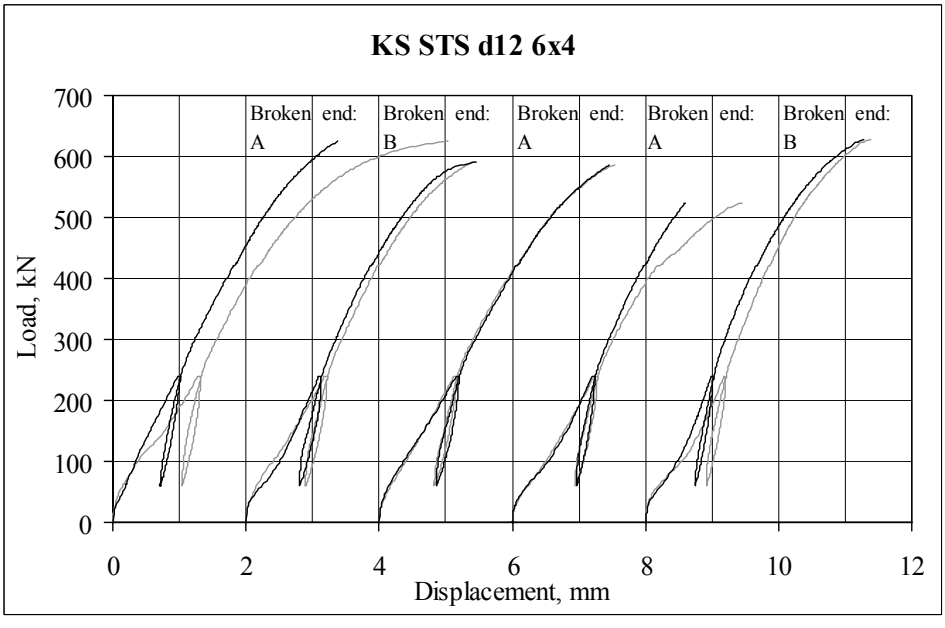
KS STS d12 6x4
Broken end: A
Broken end: B
Broken end: A
Broken end: A
Broken end: B
Load, kN
Displacement, mm
0
100
200
300
400
500
600
700
0
2
4
6
8
10
12

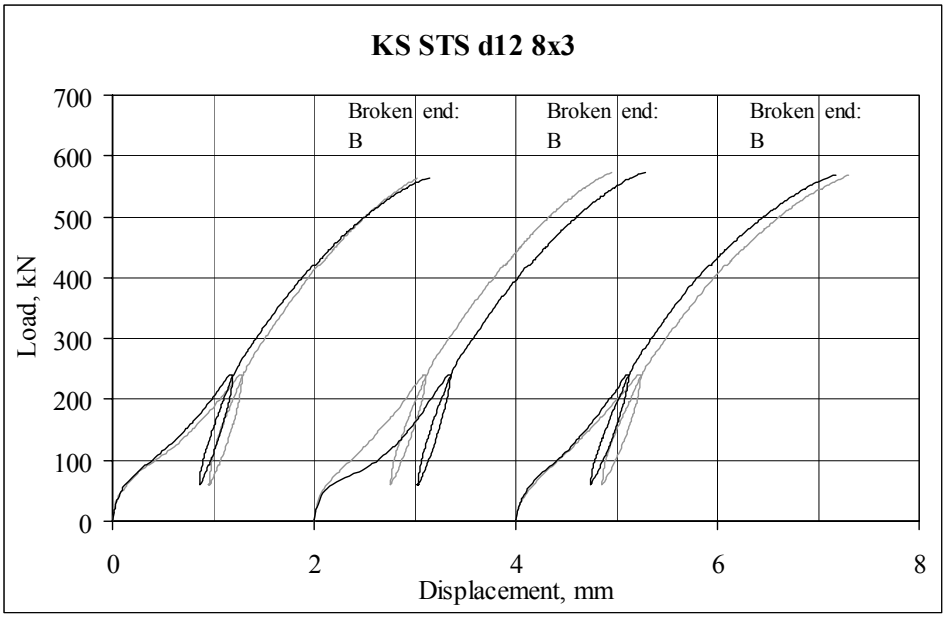
KS STS d12 8x3
Broken end: B
Broken end: B
Broken end: B
Load, kN
Displacement, mm
0
100
200
300
400
500
600
700
0
2
4
6
8

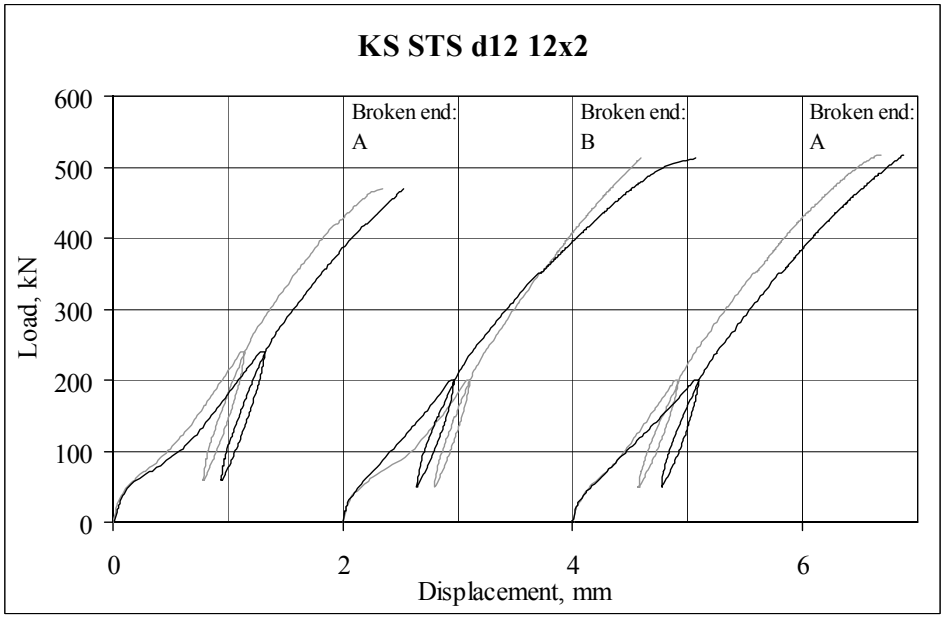
KS STS d12 12x2
Broken end: A
Broken end: B
Broken end: A
Load, kN
Displacement, mm
0
100
200
300
400
500
600
0
2
4
6

Double shear Kerto series with dowel diameter 8 mm

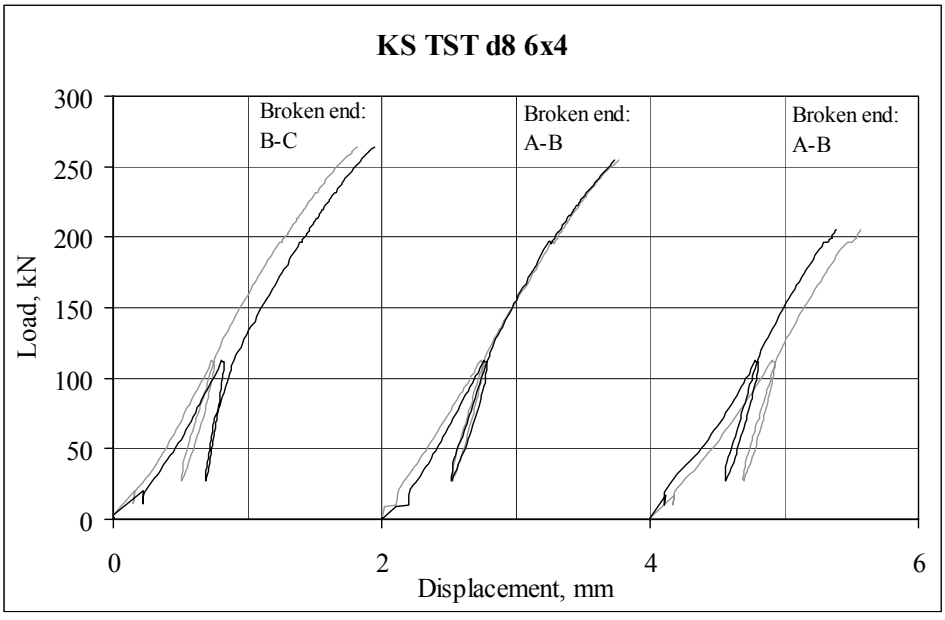

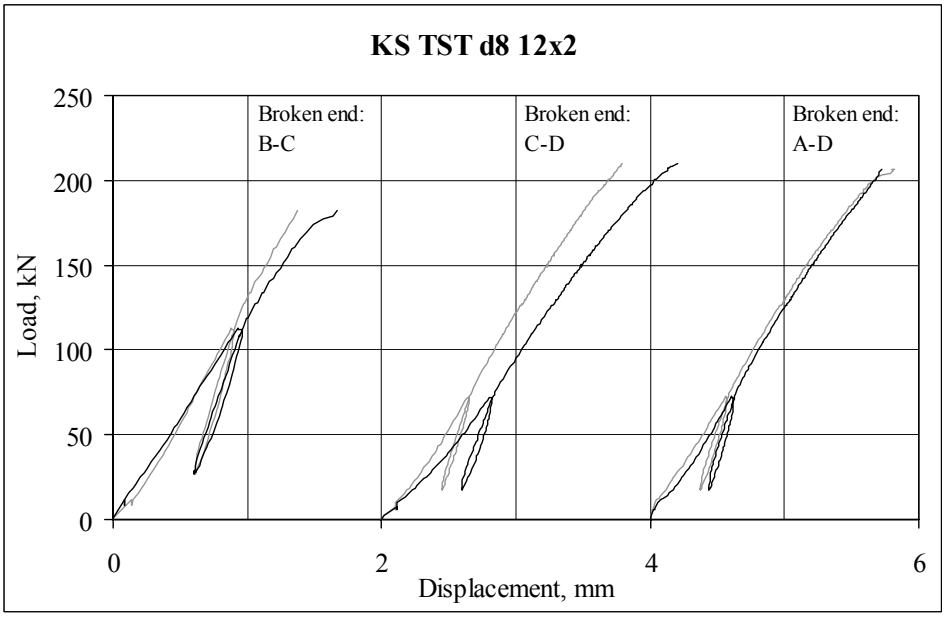

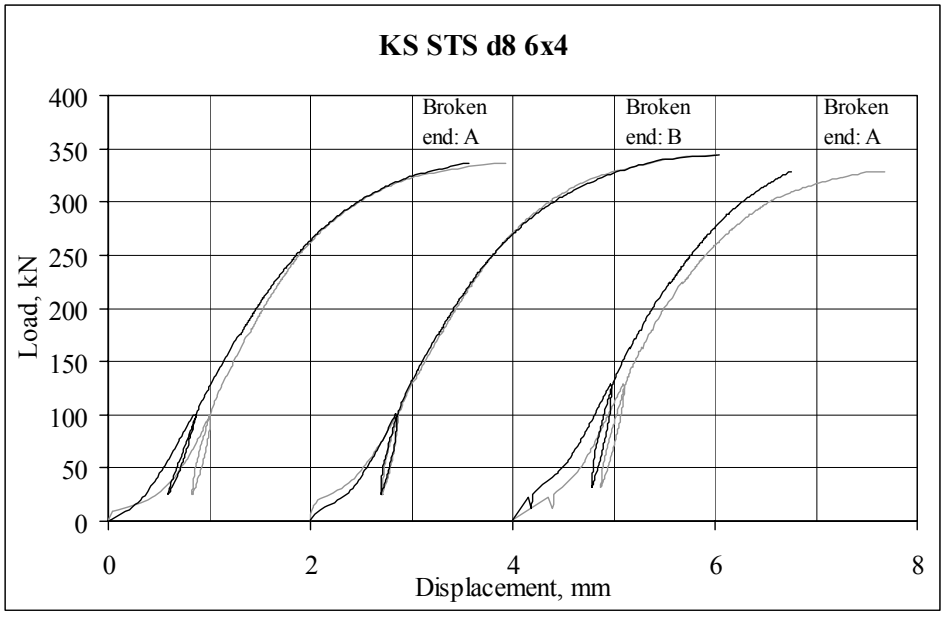
KS STS d8 6x4
Broken end: A
Broken end: B
Broken end: A
Load, kN
Displacement, mm
0
50
100
150
200
250
300
350
400
0
2
4
6
8

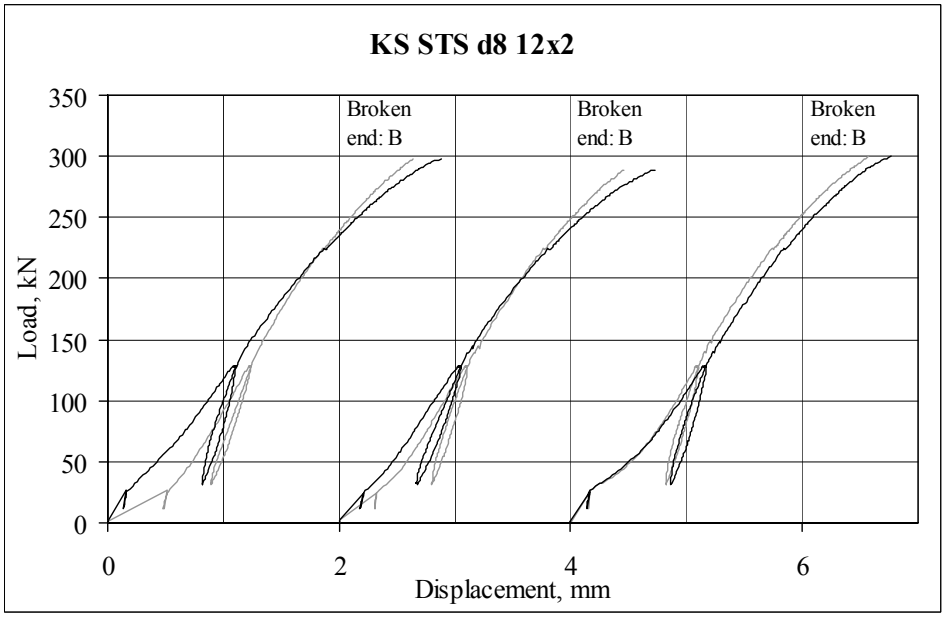
KS STS d8 12x2
Broken end: B
Broken end: B
Broken end: B
Load, kN
Displacement, mm
0
50
100
150
200
250
300
350
0
2
4
6

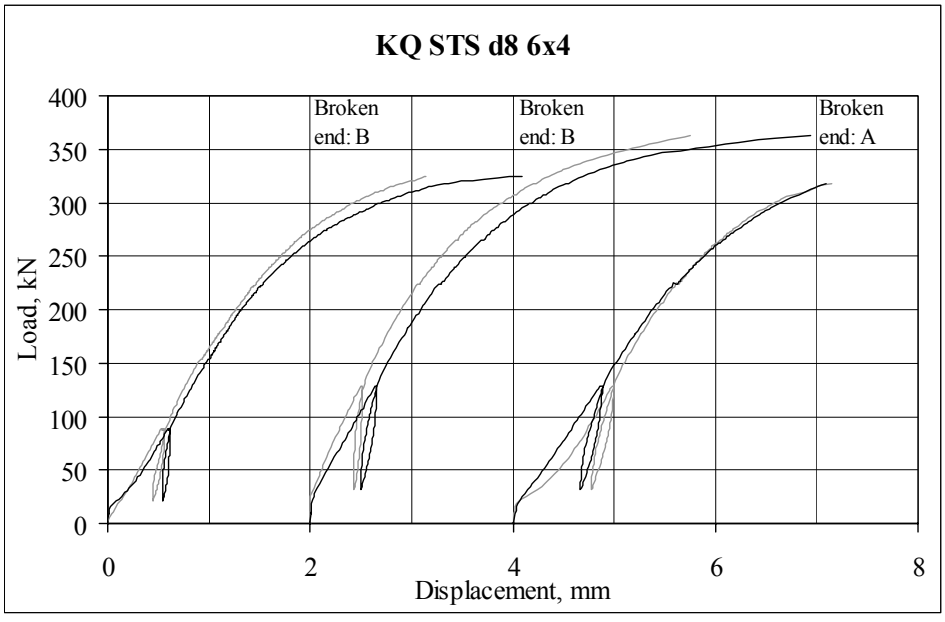
KQ STS d8 6x4
Broken end: B
Broken end: B
Broken end: A
Load, kN
Displacement, mm
0
50
100
150
200
250
300
350
400
0
2
4
6
8

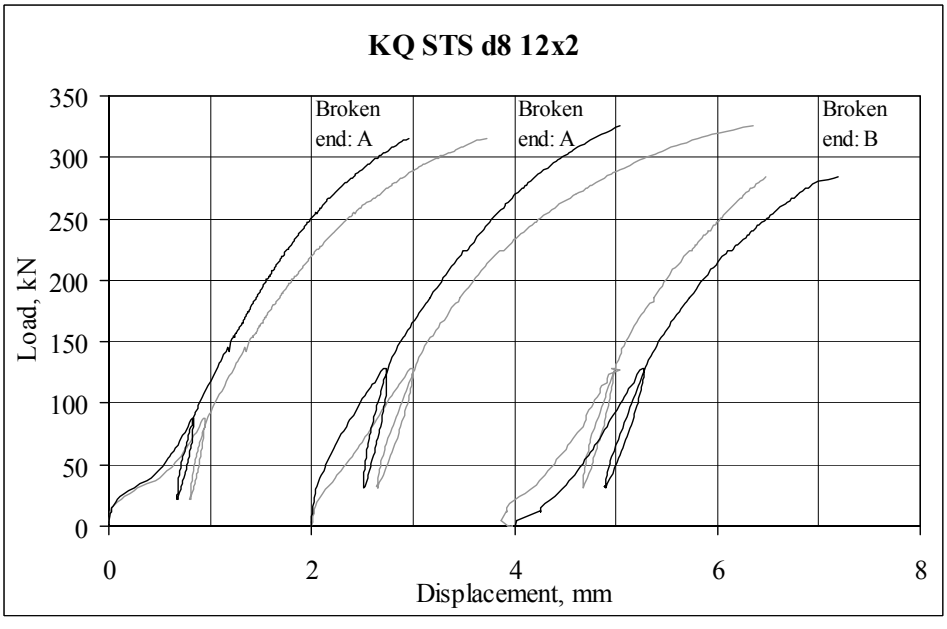
KQ STS d8 12x2
Broken end: A
Broken end: A
Broken end: B
Load, kN
Displacement, mm
0
50
100
150
200
250
300
350
0
2
4
6
8

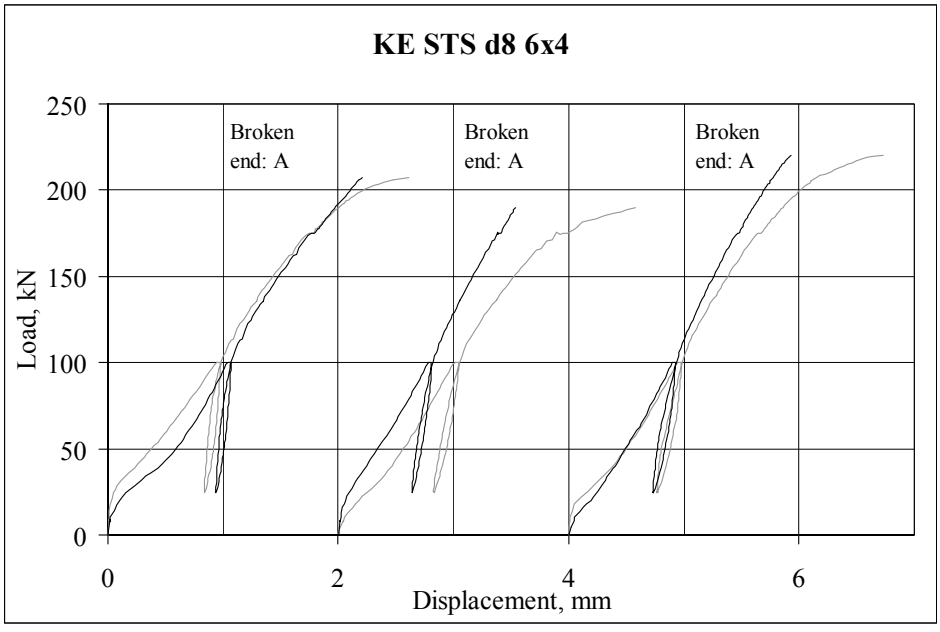
KE STS d8 6x4
Broken end: A
Broken end: A
Broken end: A
Load, kN
250
200
150
100
50
0
0
2
4
6
Displacement, mm

Multiple shear Glulam series

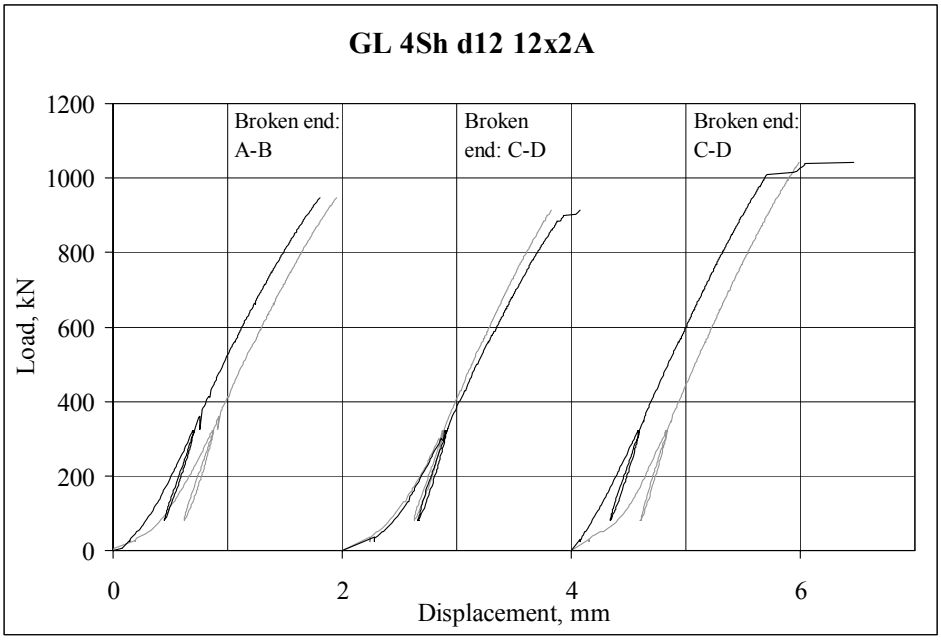

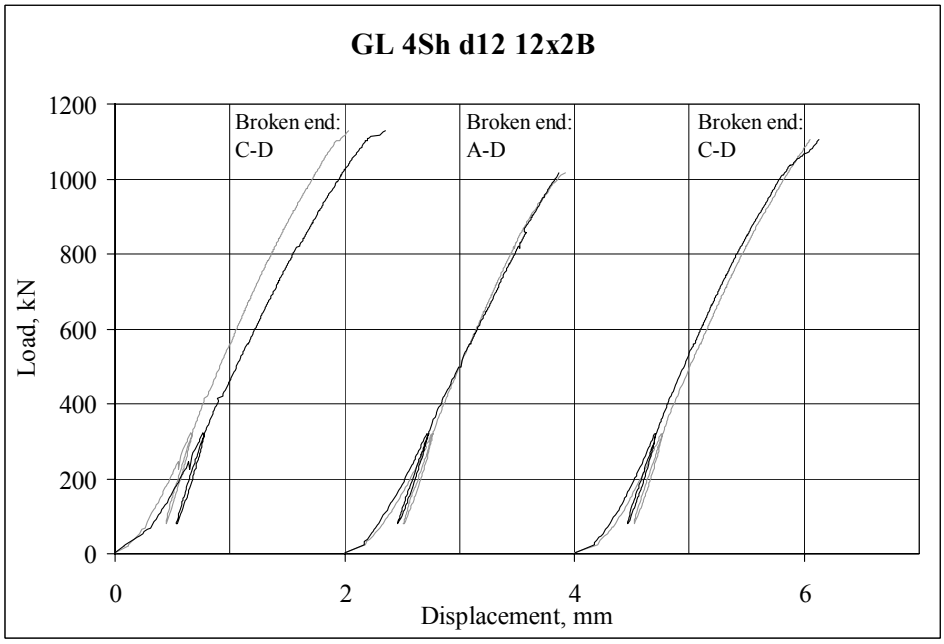

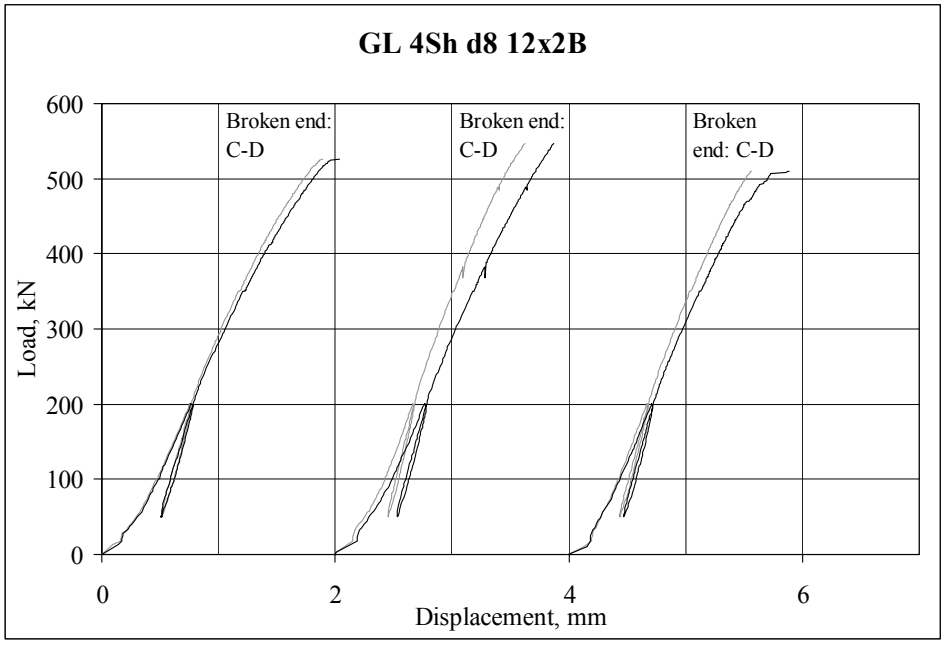
GL 4Sh d8 12x2B
Broken end: C-D
Broken end: C-D
Broken end: C-D
Load, kN
Displacement, mm
0
100
200
300
400
500
600
0
2
4
6

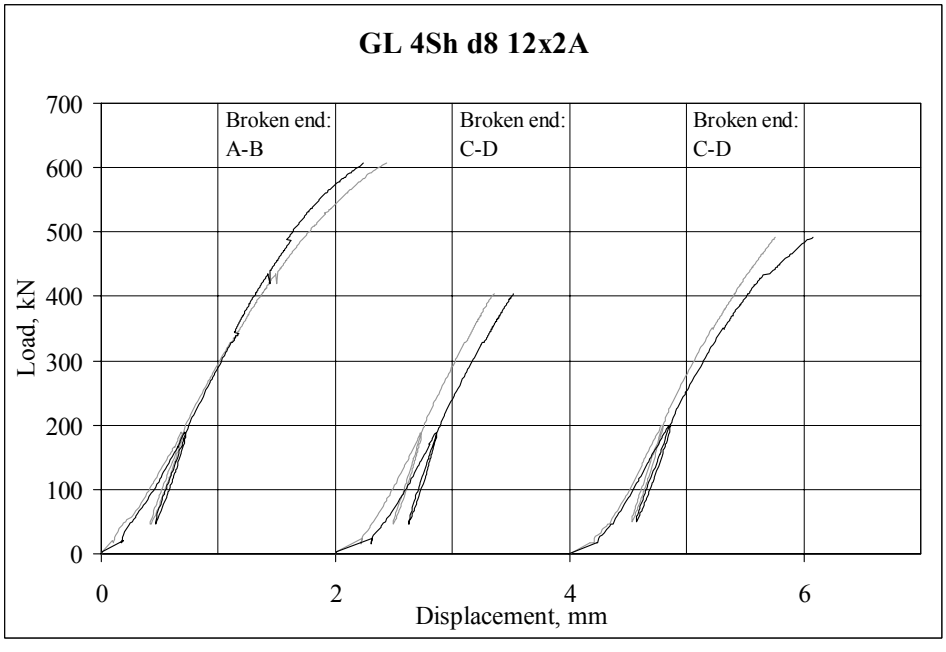
GL 4Sh d8 12x2A
Broken end: A-B
Broken end: C-D
Broken end: C-D
Load, kN
Displacement, mm
0
100
200
300
400
500
600
700
0
2
4
6

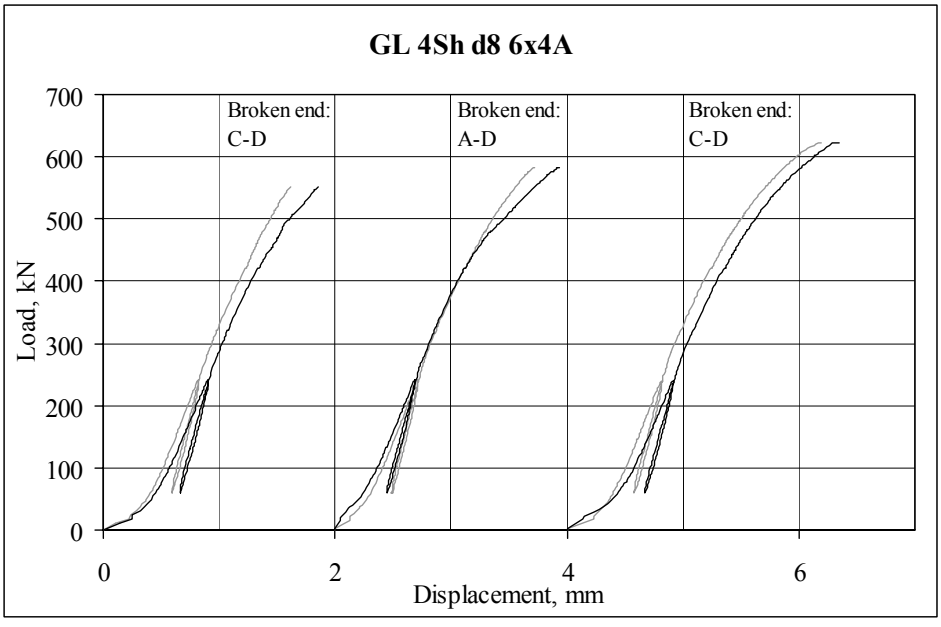
GL 4Sh d8 6x4A
Broken end:
C-D
Broken end:
A-D
Broken end:
C-D
Load, kN
700
600
500
400
300
200
100
0
0
2
4
6
Displacement, mm

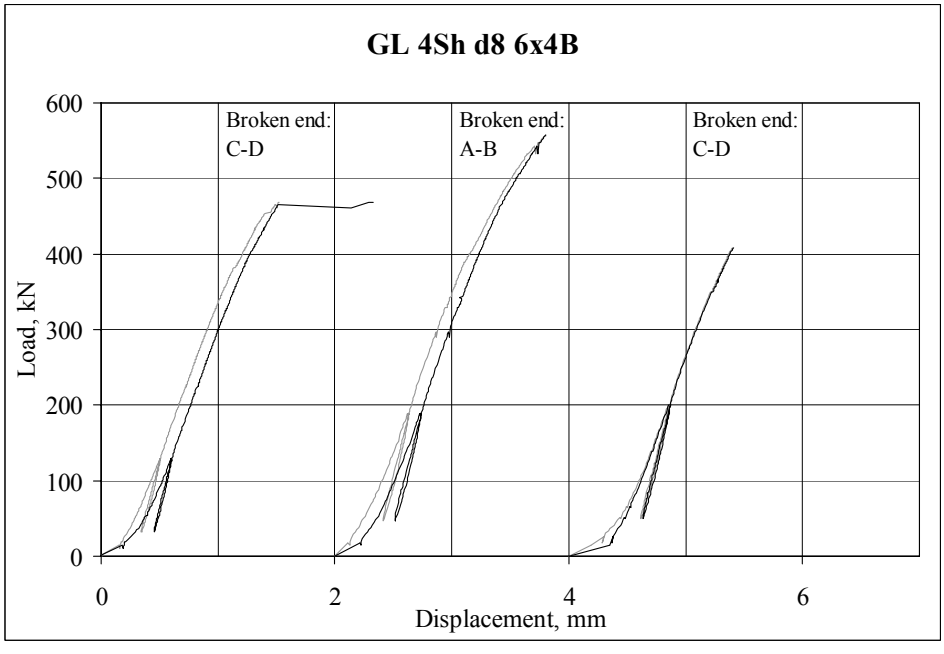
GL 4Sh d8 6x4B
Broken end:
C-D
Broken end:
A-B
Broken end:
C-D
Load, kN
600
500
400
300
200
100
0
0
2
4
6
Displacement, mm

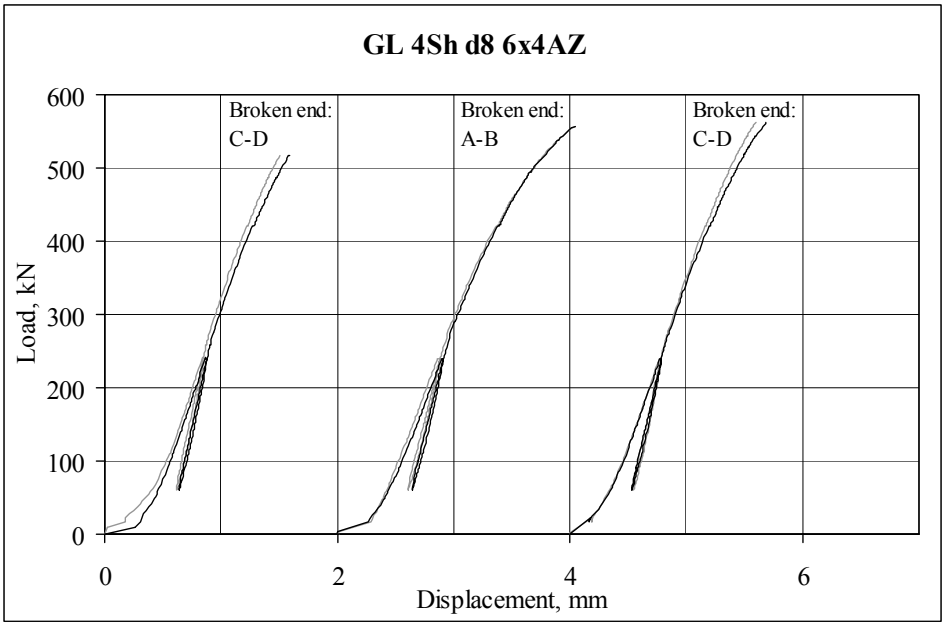
GL 4Sh d8 6x4AZ
Broken end:
C-D
Broken end:
A-B
Broken end:
C-D
Load, kN
600
500
400
300
200
100
0
0
2
4
6
Displacement, mm

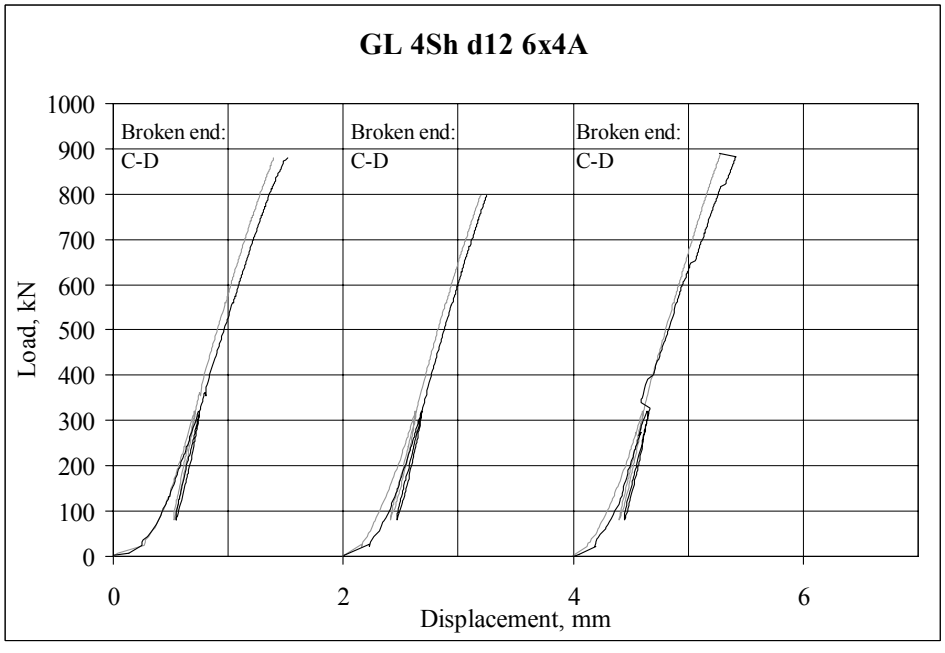
GL 4Sh d12 6x4A
Broken end:
C-D
Broken end:
C-D
Broken end:
C-D
Load, kN
1000
900
800
700
600
500
400
300
200
100
0
0
2
4
6
Displacement, mm

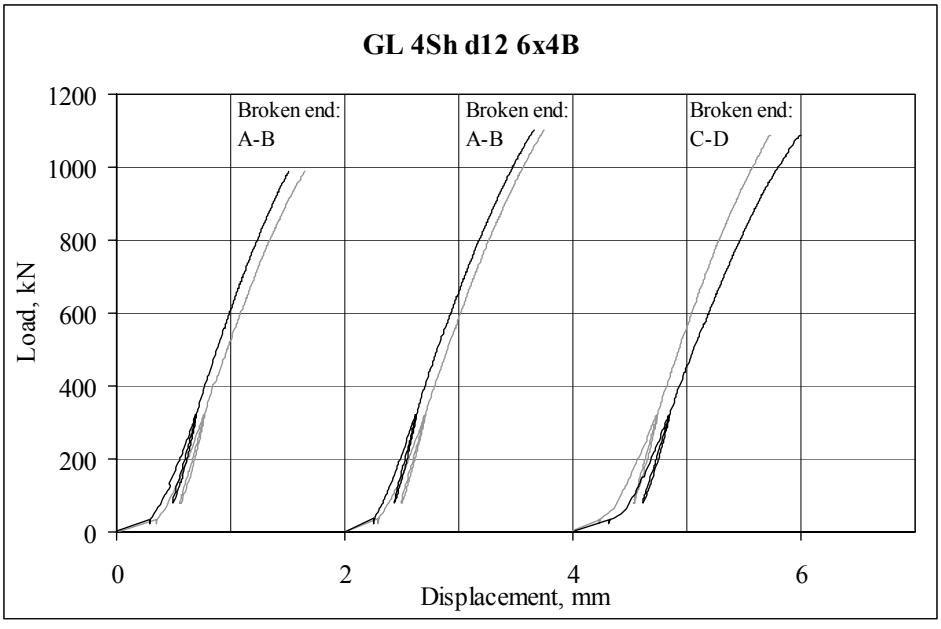
GL 4Sh d12 6x4B
Broken end:
A-B
Broken end:
A-B
Broken end:
C-D
Load, kN
1200
1000
800
600
400
200
0
0
2
4
6
Displacement, mm

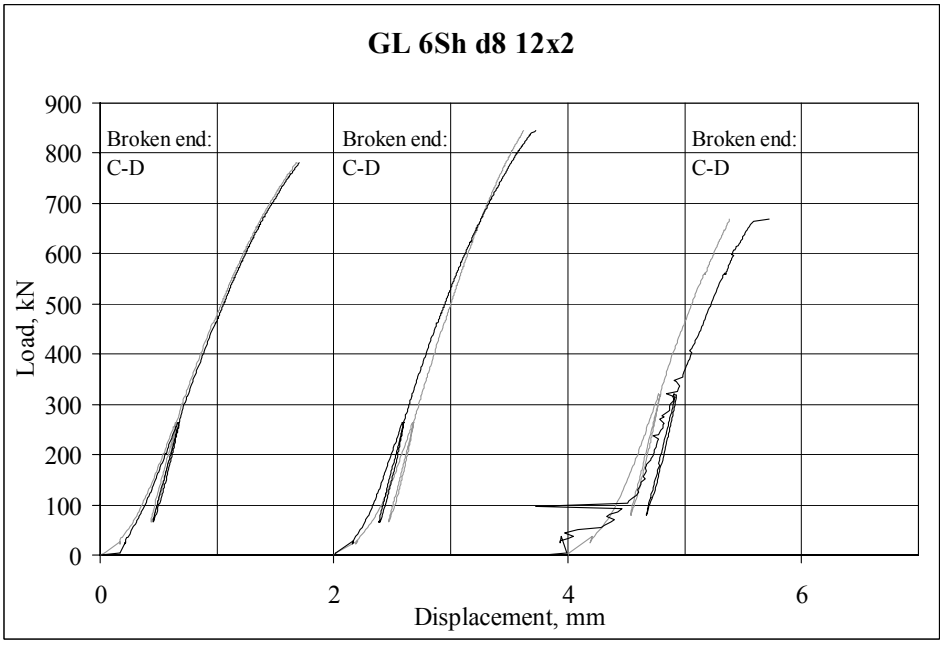
GL 6Sh d8 12x2
Broken end:
C-D
Broken end:
C-D
Broken end:
C-D
Load, kN
900
800
700
600
500
400
300
200
100
0
0
2
4
6
Displacement, mm

Multiple shear Kerto series

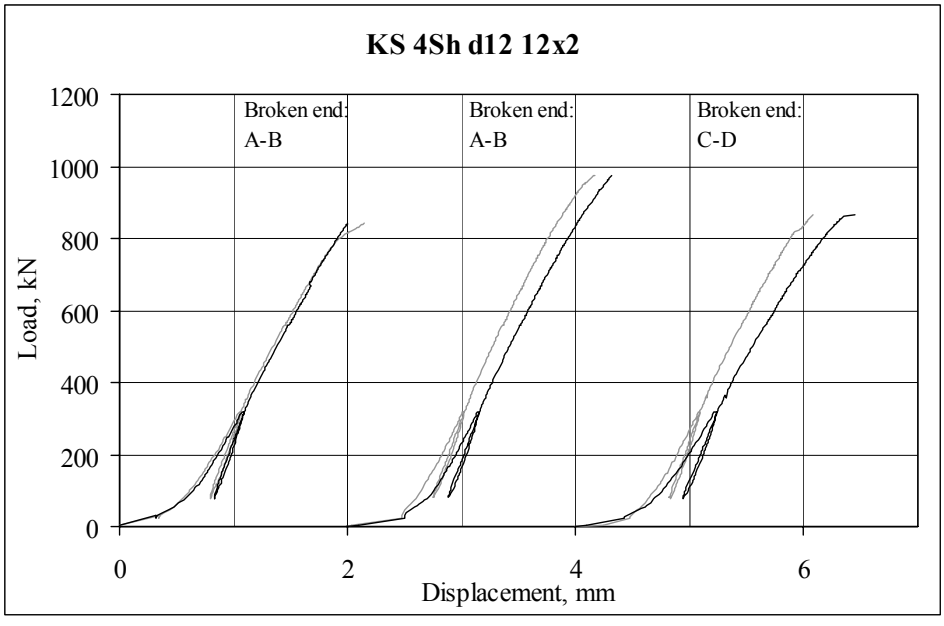

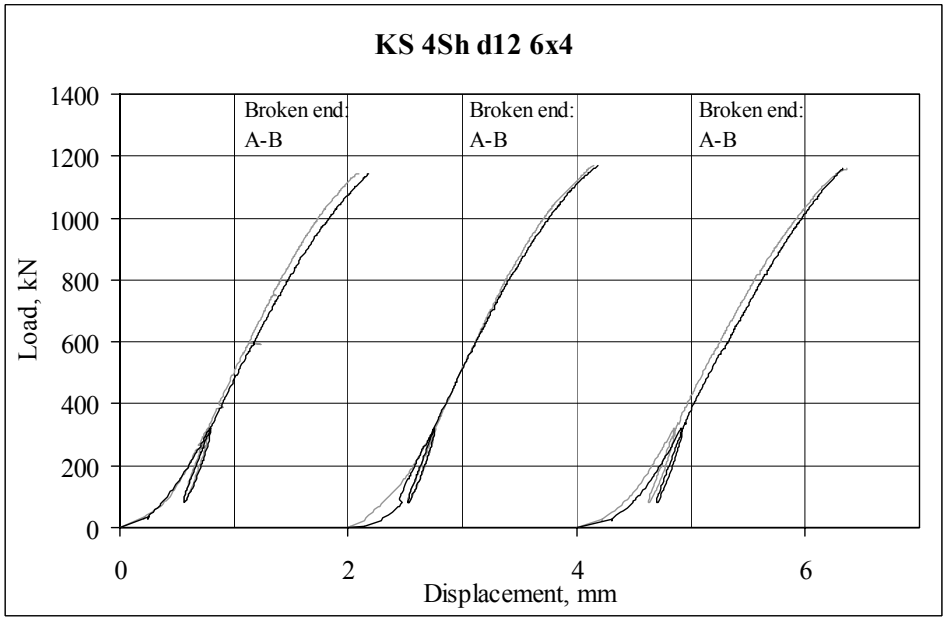

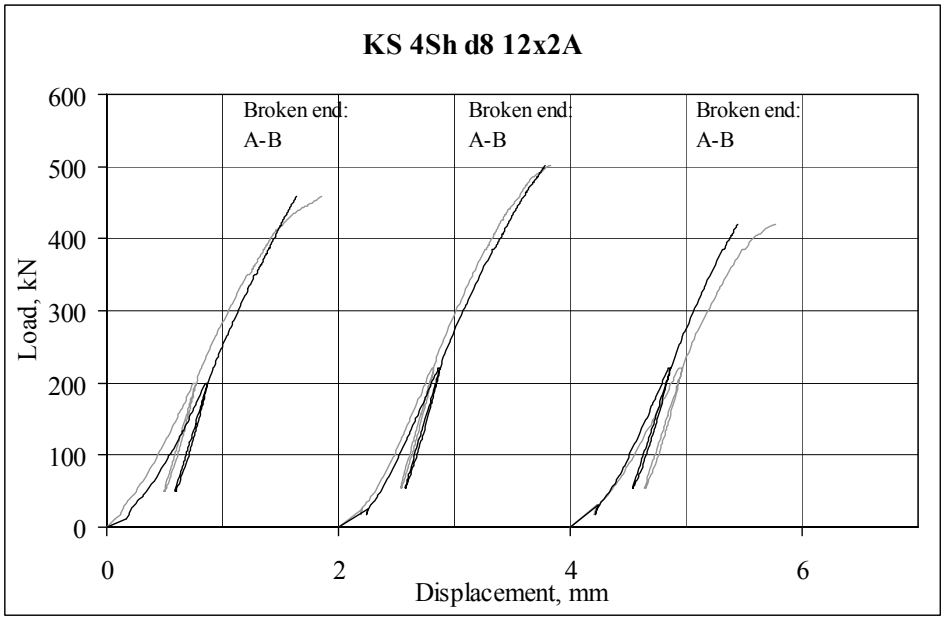
KS 4Sh d8 12x2A
Broken end:
A-B
Broken end:
A-B
Broken end:
A-B
Load, kN
600
500
400
300
200
100
0
0
2
4
6
Displacement, mm

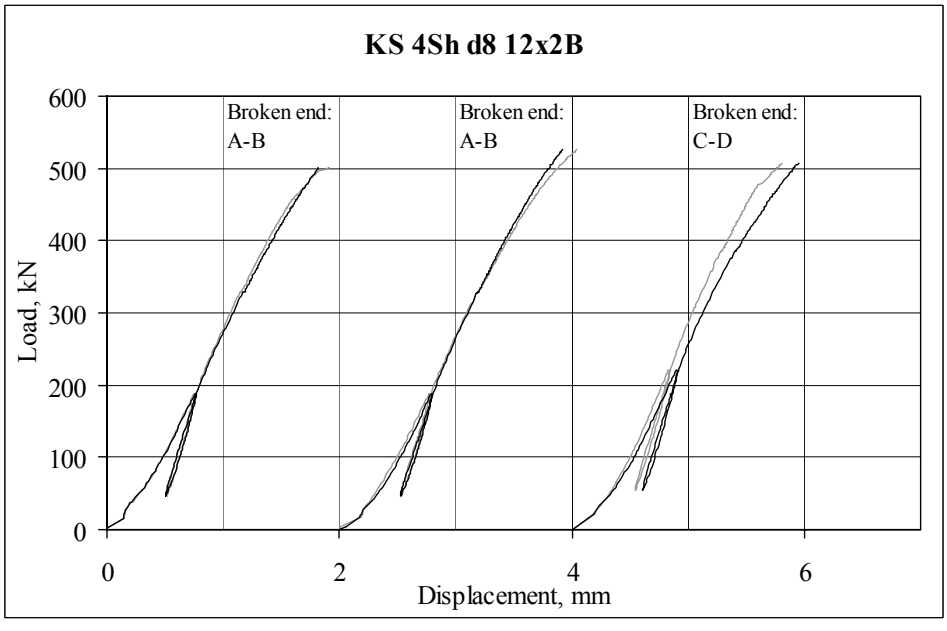
KS 4Sh d8 12x2B
Broken end:
A-B
Broken end:
A-B
Broken end:
C-D
Load, kN
600
500
400
300
200
100
0
0
2
4
6
Displacement, mm

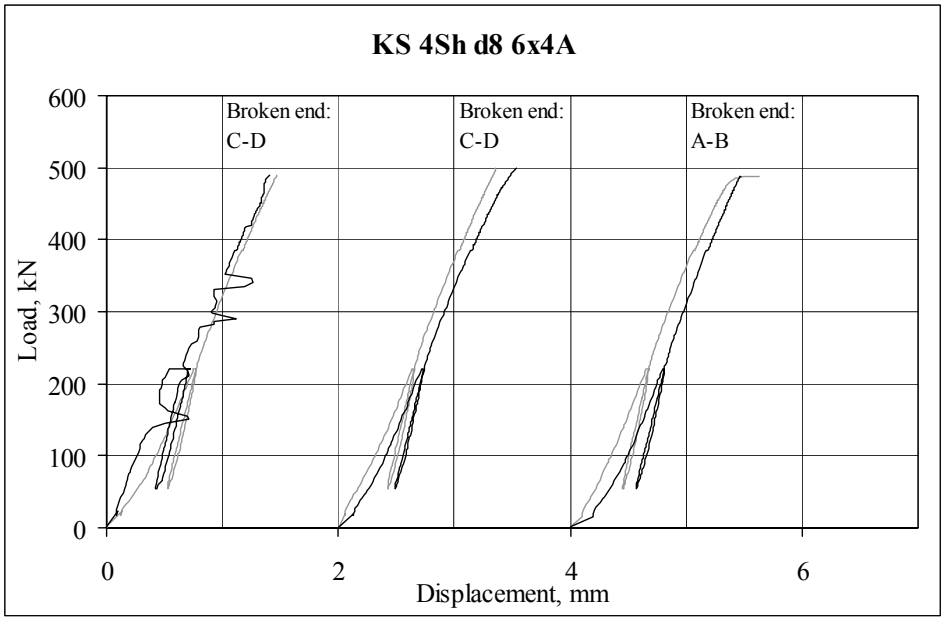
KS 4Sh d8 6x4A
Broken end:
C-D
Broken end:
C-D
Broken end:
A-B
Load, kN
600
500
400
300
200
100
0
0
2
4
6
Displacement, mm

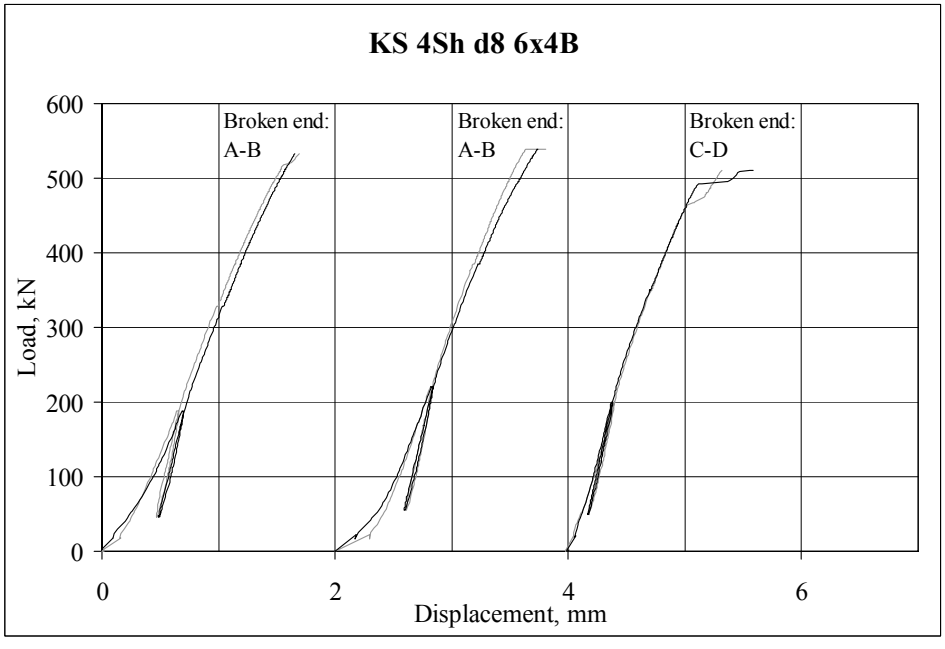
KS 4Sh d8 6x4B
Broken end:
A-B
Broken end:
A-B
Broken end:
C-D
Load, kN
600
500
400
300
200
100
0
0
2
4
6
Displacement, mm

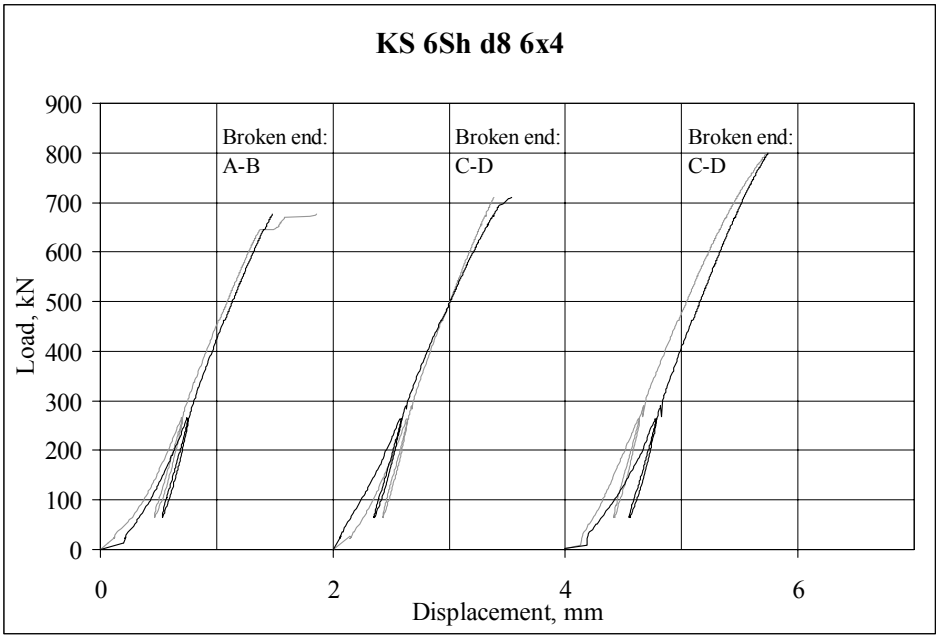
KS 6Sh d8 6x4
Broken end:
A-B
Broken end:
C-D
Broken end:
C-D
Load, kN
Displacement, mm
0
100
200
300
400
500
600
700
800
900
0
2
4
6

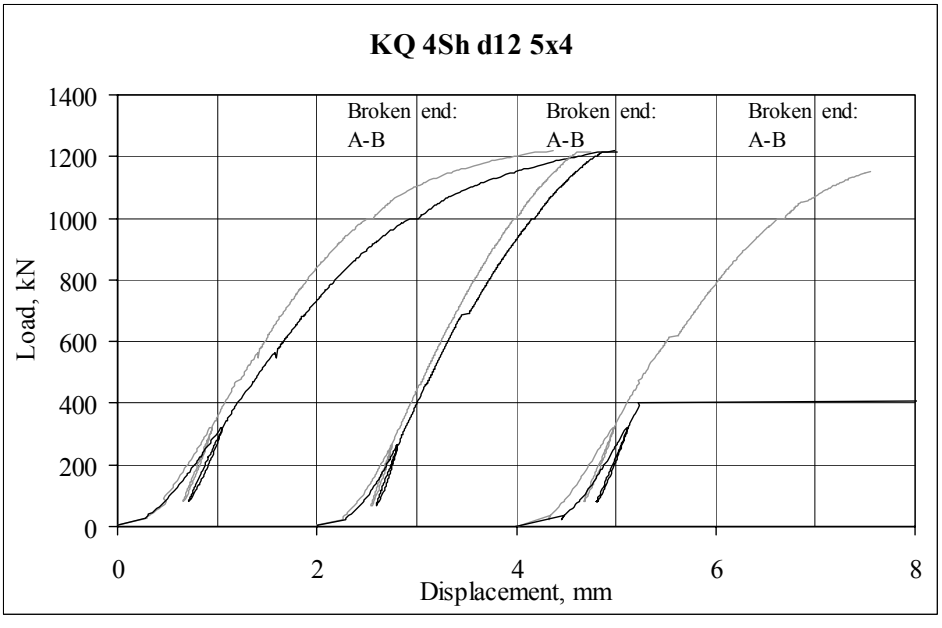
KQ 4Sh d12 5x4
Broken end:
A-B
Broken end:
A-B
Broken end:
A-B
Load, kN
Displacement, mm
0
200
400
600
800
1000
1200
1400
0
2
4
6
8

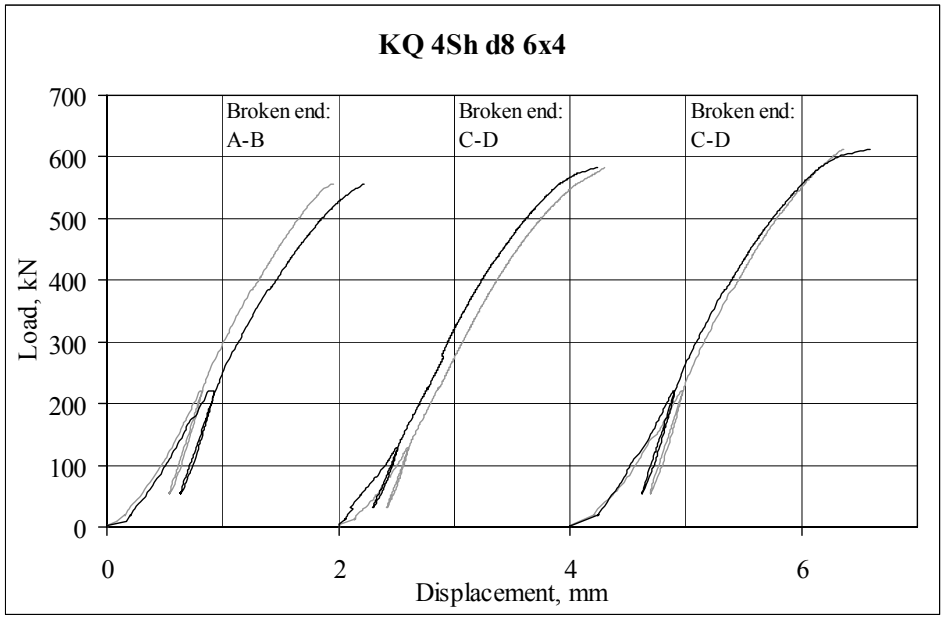
KQ 4Sh d8 6x4
Broken end:
A-B
Broken end:
C-D
Broken end:
C-D
Load, kN
700
600
500
400
300
200
100
0
0
2
4
6
Displacement, mm

Series title, number and report code of publication

VTT Publications 677
VTT-PUBS-677

Author(s)
Hanhijärvi, Antti & Kevarinmäki, Ari

Title

Timber failure mechanisms in high-capacity dowelled connections of timber to steel
Experimental results and design

Abstract

The timber failure mechanisms at the connection area (block shear, plug shear, row shear, tension at the joint area) of high capacity dowelled steel-to-timber connections were explored by arranging a large experimental program to investigate the strength of both double shear and multiple shear connections. All tested connections were steel-to-timber connections using large diameter and consequently fairly rigid dowels. The experiments consisted altogether of more than 150 tension tests by which different and versatile dowel configurations were tested. Based on the experimental results, a new design method against timber failure mechanisms at the connection area was developed. The new method is suitable especially for high capacity steel-to-timber connections.

ISBN
978-951-38-7090-4 (URL: http://www.vtt.fi/publications/index.jsp)

Series title and ISSN	Project number
VTT Publications 677 1455-0849 (URL: http://www.vtt.fi/publications/index.jsp)	25418

Date	Language	Pages
April 2008	English, finnish abstr.	53 p. + app. 37 p.

Name of project	Commissioned by
SUURLIITOS	Tekes, Exel Oyj, Finnforest, Late-Rakenteet Oy, SPU Systems Oy, Versowood Oyj

Keywords	Publisher
timber, gluelam, LVL, dowelled connections, high capacity, design methods, steel-to-timber connections, block shear, plug shear, row shear	VTT Technical Research Centre of Finland P.O. Box 1000, FI-02044 VTT, Finland Phone internat. +358 20 722 4520 Fax +358 20 722 4374

Julkaisun sarja, numero ja raporttikoodi

VTT Publications 677
VTT-PUBS-677

Tekijä(t)
Hanhijärvi, Antti & Kevarinmäki, Ari

Nimeke

Puurakenteiden tappivaarnaliitosten murtomekanismit

Tiivistelmä

Suuren kapasiteetin omaavien tappivaarnaliitosten puustamurtomekanismeja (lohkeamismurtotavat: läpilohkeaminen, palalohkeaminen, rivilohkeaminen ja vetomurto liitosalueella) tutkittiin laajalla koeohjelmalla. Kokeissa tutkittiin sekä kaksileikkeisiä että monileikkeisiä liitoksia vedossa. Kaikki testatut liitokset olivat teräs-puuliitoksia, joissa käytettiin halkaisijaltaan melko suuria tappeja, jotka ovat siten myös jäykkiä. Koeohjelmaan kuului järjestää yli 150 vetokoetta, joissa käytettiin erilaisia ja monipuolisia tappiasetelmia. Koetuloksiin perustuen kehitettiin uusi mitoitusmenetelmä puustamurtomekanismikapasiteetin laskemiseen nimenomaan korkean kapasiteetin teräs-puuliitoksille.

ISBN
978-951-38-7090-4 (URL: http://www.vtt.fi/publications/index.jsp)

Avainnimeke ja ISSN	Projektinumero
VTT Publications 1455-0849 (URL: http://www.vtt.fi/publications/index.jsp)	25418

Julkaisuaika	Kieli	Sivuja
Huhtikuu 2008	Englanti, suom. tiiv.	53 s. + liitt. 37 s.

Projektin nimi	Toimeksiantaja(t)
SUURLIITOS	Tekes, Exel Oyj, Finnforest, Late-Rakenteet Oy, SPU Systems Oy, Versowood Oyj

Avainsanat	Julkaisija
timber, gluelam, LVL, dowelled connections, high capacity, design methods, steel-to-timber connections, block shear, plug shear, row shear	VTT PL 1000, 02044 VTT Puh. 020 722 4404 Faksi 020 722 4374

This publication reports the performance of dowelled timber connections and the timber failure mechanisms involved. The experiments consisted altogether of more than 150 tension tests by which different and versatile dowel configurations were tested. Based on the experimental results, a new design method against timber failure mechanisms at the connection area was developed.

VTT
PL 1000
02044 VTT
Puh. 020 722 4520
http://www.vtt.fi

VTT
PB 1000
02044 VTT
Tel. 020 722 4520
http://www.vtt.fi

VTT
P.O. Box 1000
FI-02044 VTT, Finland
Phone internat. + 358 20 722 4520
http://www.vtt.fi

ISBN 978-951-38-7090-4 (URL: http://www.vtt.fi/publications/index.jsp)
ISSN 1455-0849 (URL: http://www.vtt.fi/publications/index.jsp)